Атомная
энергия

Volume 2, Number 5, 1957

The Soviet Journal of

ATOMIC ENERGY

IN ENGLISH TRANSLATION

CONSULTANTS BUREAU, INC.

227 WEST 17TH STREET, NEW YORK 11, N. Y.

ATOMNAYA ENERGIYA

Academy of Sciences of the USSR

Volume 2, Number 5, 1957

The Soviet Journal

of

ATOMIC ENERGY

IN ENGLISH TRANSLATION

CONSULTANTS BUREAU, INC.
227 West 17th Street
New York 11, N. Y.

Printed in the United States

Annual Subscription $75.00
Single Issue 20.00

SIGNIFICANCE OF ABBREVIATIONS MOST FREQUENTLY ENCOUNTERED IN SOVIET PHYSICS PERIODICALS

AN SSSR	*Academy of Sciences, USSR*
FIAN	*Physics Institute, Academy of Sciences USSR*
GITI	*State Scientific and Technical Press*
GITTL	*State Press for Technical and Theoretical Literature*
GOI	*State Optical Institute*
GONTI	*State United Scientific and Technical Press*
Gosenergoizdat	*State Power Press*
Gosfizkhimizdat	*State Physical Chemistry Press*
Gozkhimizdat	*State Chemistry Press*
GOST	*All-Union State Standard*
Goztekhizdat	*State Technical Press*
GTTI	*State Technical and Theoretical Press*
GUPIAE	*State Office for Utilization of Atomic Energy*
IF KhI	*Institute of Physical Chemistry Research*
IFP	*Institute of Physical Problems*
IL	*Foreign Literature Press*
IPF	*Institute of Applied Physics*
IPM	*Institute of Applied Mathematics*
IREA	*Institute of Chemical Reagents*
ISN (Izd. Sov. Nauk)	*Soviet Science Press*
I YaP	*Institute of Nuclear Studies*
Izd	*Press (publishing house)*
KISO	*Solar Research Commission*
LETI	*Leningrad Electrotechnical Institute*
LFTI	*Leningrad Institute of Physics and Technology*
LIM	*Leningrad Institute of Metals*
LITMiO	*Leningrad Institute of Precision Instruments and Optics*
Mashgiz	*State Scientific-Technical Press for Machine Construction Literature*
MATI	*Moscow Aviation Technology Institute*
MGU	*Moscow State University*
Metallurgizdat	*Metallurgy Press*
MOPI	*Moscow Regional Institute of Physics*
NIAFIZ	*Scientific Research Association for Physics*
NIFI	*Scientific Research Institute of Physics*
NIIMM	*Scientific Research Institute of Mathematics and Mechanics*
NII ZVUKSZAPIOI	*Scientific Research Institute of Sound Recording*
NIKFI	*Scientific Institute of Motion Picture Photography*
OIYaI	*Joint Institute of Nuclear Studies*
ONTI	*United Scientific and Technical Press*
OTI	*Division of Technical Information*
OTN	*Division of Technical Science*
RIAN	*Radium Institute, Academy of Sciences of the USSR*
SPB	*All-Union Special Planning Office*
Stroiizdat	*Construction Press*
URALFTI	*Ural Institute of Physics and Technology*

NOTE: Abbreviations not on this list and not explained in the translation have been transliterated, no further information about their significance being available to us.—*Publisher.*

THE MEASUREMENT OF THE RESONANCE ABSORPTION OF NEUTRONS IN AN ATOMIC POWER STATION REACTOR

Z.I. Gromova, B.G. Dubovsky, A.V. Kamaev and V.V. Orlov

One of the most important quantities determining the possibility of the development of a nuclear chain reaction in the system uranium-moderator is $1-\varphi$ – the probability of the resonance absorption of neutrons by U^{238} in the process of their slowing down from the fission to thermal energies. Up to the present time the calculation of $1-\varphi$ for heterogeneous reactors is not sufficiently accurate; there arises, in this connection, the necessity for an experimental determination of $1-\varphi$ directly in the reactor lattice. In this paper the experimental methods for the determination of the resonance absorption are discussed. Various corrections are considered, taking into account the neutron loss, the fission of the uranium and the neutron capture in the resonance region. For an atomic power station reactor employing enriched uranium (5% U^{235}) these corrections are found to be significant. Three methods are used to calculate φ – the resonance escape probability – for an atomic power station reactor. φ was found to be equal to 0.900 ± 0.015.

The Method of Measurement

The basis for experimentally measuring the probability φ for avoiding the resonance absorption of neutrons consists in measuring the ratio R/T, where R is the number of resonance neutrons present and T is the number of thermal neutrons absorbed per second by U^{238} in the working element of the reactor [1].

By measuring R/T and some other reactor characteristics, φ can be calculated by three methods.

1. If in one cubic centimeter of the reactor cell Q fast neutrons are born per second through fission, then the slowing-down density at an energy E will be equal to the product $Q\Phi(E)\varphi(E)$, where $\Phi(E)$ is the probability that a fast neutron, in slowing down to an energy E, avoids leakage from the reactor and escapes absorption by the U^{235} and by the constructional materials. Taking into account that $\Phi(E)$ is a slowly varying function, while the U^{238} absorption takes place mainly in a narrow energy interval of 6-200 ev, then

$$R \approx Q\Phi(\bar{E})(1-\varphi), \tag{1}$$

where $\Phi(\bar{E})$ determines the fraction of the total number of neutrons born, Q, which are slowed down to the effective energy of the U^{238} resonance absorption (Figure 1).

The U^{238} activation by the thermal neutrons can be written in the form

$$T \approx \int_0^{0,4\,\text{ev}} (nv)_U \, \Sigma_{a238}(E)\, dE, \tag{2}$$

where $(nv)_U$ is the thermal neutron flux in the uranium and $\Sigma_{a238}(E)$ the macroscopic cross section for absorption of neutrons by U^{238}. From this

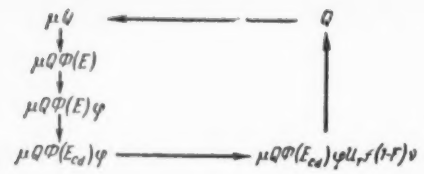

Fig. 1. Neutron balance in the reactor. U_T is the thermal neutron leakage; other symbols are given in the text.

$$\frac{R}{T} = \frac{Q\Phi(\bar{E})(1-\varphi)}{\int_0^{0.4\,ev} (nv)_U \Sigma_{a238}(E)\,dE}. \qquad (3)$$

The number of fast neutrons born per second is related to the thermal neutron flux by the equation

$$Q = \left\{\mu\nu \int (nv)_U \Sigma_{f235}(E)\,dE\right\}\left[1 + \left(\frac{R}{T}\right)_f\right], \qquad (4)$$

where μ is the multiplication factor for fast neutrons, ν the number of neutrons produced in one act of fission, $\Sigma_{f235}(E)$ the macroscopic cross section for U^{235} fission, and $(R/T)_f$ is the experimentally determined U^{235} fission fraction for energies above the "cadmium" region. This expression for Q describes the fact that, in reactors using enriched uranium, a significant fraction of the fission occurs at energies greater than 0.4 ev (10-20%).

In this way we obtain:

$$\varphi = 1 - \frac{R}{T}\cdot\frac{\bar{\Sigma}_{a238}}{\nu\mu\bar{\Sigma}_{f235}\left[1+\left(\frac{R}{T}\right)_f\right]\Phi(\bar{E})}, \qquad (5)$$

where $\bar{\Sigma}_{a238}$ and $\bar{\Sigma}_{f235}$ are the macroscopic cross sections for U^{238} absorption and U^{235} fission, averaged over the spectrum of neutrons for energies below the "cadmium" region, at a given temperature and taking into account the departure of the cross sections from the 1/v law.

2. The expression for φ can be obtained in another way, having determined the flux $(nv)_U$ with the help of Q. The number of neutrons slowed down per second to an energy $E < E_{Cd}$, is obviously equal to $Q\varphi\Phi(E_{Cd})$, where $E_{Cd} = 0.4$ ev is the limit for the absorption of neutrons by cadmium. The absorption of thermal neutrons by U^{238} is expressed with the help of the slowing-down flux in the following way:

$$\int_0^{0.4ev} (nv)_U \Sigma_{a238}(E)\,dE = Q\varphi\Phi(E_{Cd})\,P_{Cd}\,f\,F, \qquad (6)$$

where P_{Cd} is the probability for the neutrons to escape leakage from the cell in the thermal region, f the thermal neutron utilization coefficient, and F is the fraction of U^{238} absorptions in the uranium absorption of thermal neutrons. The magnitudes of f and F are determined from the following equations:

$$f = \frac{\int_0^{0.4ev} (nv)_U \Sigma_{aU}(E)\,dE}{\int_0^{0.4ev} (nv)_U \Sigma_{a\ \mathrm{total}}(E)\,dE};$$

$$F = \frac{\int_0^{0.4ev} (nv)_U \Sigma_{a238}(E)\,dE}{\int_0^{0.4ev} (nv)_U \Sigma_{aU}(E)\,dE},$$

where $\Sigma_{aU}(E)$ is the macroscopic cross section for the neutron absorption by uranium, and $\Sigma_{a\,total}(E)$ the macroscopic cross section for neutron absorption by the uranium and the constructional materials.

Substituting (6) in (3), we get:

$$\varphi = \frac{\frac{T}{R}}{\frac{T}{R} + fF\frac{\Phi(E_{Cd})P_{Cd}}{\Phi(\bar{E})}}. \qquad (7)$$

This method for determining φ is used in Reference [2]. The additional multiplier $\Phi(E_{Cd})P_{Cd}/\Phi(E)$ determines the loss of neutrons through absorption and leakage in the region from an energy $\bar{E}$, at which the main part of the resonance absorption occurs, to thermal energy.

The quantity $\Phi(\bar{E})$ can be expressed in the form $\Phi(\bar{E}) = P(\bar{E})\chi(\bar{E})$, where $P(\bar{E})$ is the probability for escaping leakage and $\chi(\bar{E})$ the probability for escaping absorption by U^{235} and the constructional materials during the slowing-down process to the U^{238} resonance energy. $\chi(\bar{E})$ can be evaluated using the known cross sections and resonance integrals.

3. φ can be obtained by comparing the value of R/T for uranium with that for a resonance indicator with a known absorption cross section in the thermal region and a known resonance absorption integral.

For a resonance indicator we can write

$$\left(\frac{R}{T}\right)_r = \frac{Q\Phi(E_r)\varphi(E_r)\frac{1}{\xi\Sigma_s}\int\limits_{0.4\,ev}^{\infty}\sigma_{ar}(E)\frac{dE}{E}}{\int\limits_{0}^{0.4\,ev} nv\,\sigma_{ar}(E)\,dE}, \qquad (8)$$

where E_r is the indicator resonance energy; ξ the average logarithmic energy loss per collision; Σ_s the macroscopic cross section for scattering in the moderator; $\int\limits_{0.4\,ev}^{\infty}\sigma_{ar}(E)\frac{dE}{E}$ the resonance absorption integral for the indicator; $\sigma_{ar}(E)$ the energy-dependent absorption cross section for the indicator and $\underline{nv}$ the thermal-neutron flux. For uranium

$$\left(\frac{R}{T}\right)_{238} = \frac{Q\Phi(\bar{E})(1-\varphi)}{\int\limits_{0}^{0.4\,ev}(nv)_U N_{238}\sigma_{a238}(E)\,dE}, \qquad (9)$$

where N_{238} is the number of U^{238} nuclei per cm^3 and $\sigma_{a238}(E)$ the U^{238} energy-dependent absorption cross section.

From Equations (8) and (9) we find:

$$\frac{1-\varphi}{\varphi(E_r)} = \frac{\left(\frac{R}{T}\right)_{238}}{\left(\frac{R}{T}\right)_r}\cdot\frac{\int\limits_{0}^{0,4\,ev}(nv)_U N_{238}\sigma_{a238}(E)\,dE}{\int\limits_{0}^{0.4\,ev} nv\,\sigma_{ar}(E)\,dE} \times \qquad (10)$$

$$\times\frac{\int\limits_{0.4\,ev}^{\infty}\sigma_{ar}\frac{dE}{E}}{\xi\Sigma_s}\cdot\frac{\Phi(E_r)}{\Phi(\bar{E})}.$$

Measurements

The β-activity of U^{239}, produced by neutron capture according to the reaction

$$U^{238} + n \rightarrow U^{239} \xrightarrow[\beta,\gamma]{23.5\ min} Np^{239} \xrightarrow[\beta,\gamma]{2.3\,day} Pu^{239}.$$

was used as a measure of the number of neutrons absorbed by the U^{238}. The ratio R/T was determined from the activities of a cadmium-clad and a bare uranium sample. The thickness of the cadmium sheath, equal to 0.25 mm, determined the upper limit of the absorption – 0.4 ev. To carry out the measurements a special experimental channel was constructed, similar to the working channel of the atomic power station reactor. The samples studied were pieces of the heat-producing uranium elements used in the reactor. The arrangement was such that the uranium sample and the element studied imitated completely a working channel (Figure 2). This enabled φ to be measured for the actual uranium-graphite lattice of the reactor.

Determination of R. The cadmium-clad sample was introduced into the experimental channel of the reactor. Simultaneously with the experimental channel, iodine and indium indicators were placed in the reactor to serve as monitors used to determine the activation integral for the irradiation period.

After the reactor was loaded the power output was raised to 1 kw. The sample was irradiated for 10 min. After irradiation the sample was chemically treated to separate the fission products and products of natural decay. The sample was dissolved in concentrated nitric acid; ether extraction was performed twice. It is known that uranyl nitrate, $UO_2(NO_3)_2$, dissolves well in ether. The method of purification was based on this (ether extraction), consisting of the extraction with ether of the uranium nitrates from an aqueous solution.

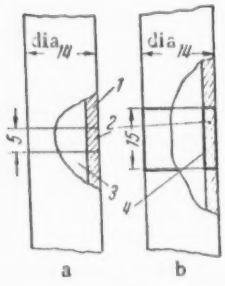

Fig. 2. The activation of uranium samples in the reactor experimental channel: a) without a cadmium sheath; b) with a cadmium sheath; 1) uranium; 2) uranium sample to be studied; 3) water; 4) cadmium sheath. Dimensions are given in mm.

The activity of the purified uranyl nitrate solution, characterized by the β decay of U^{239}, was measured using standard geometry and a cylindrical β counter.

The measurements were carried out for 3-4 periods so as to determine the quality of the chemical purification. Usually, the quality of the purification was completely adequate, the half life obtained being equal to 23.5 min, which corresponds to the half life of U^{239}.

Determination of R + T. The sample was placed in the experimental channel without a cadmium sheath. The procedures for irradiation, treatment and measurement was the same as for measuring R. By measuring the activities of the solutions we obtain quantities proportional to R + T and R. After making corrections for the activation integral and for the quantity of uranium in each solution the ratio R/T was determined.

As a result of 10 measurements, carried out in the central cell of the reactor, the magnitude of R/T was found equal to 1.67 ± 0.03 (mean-square error).

Control measurements. The influence of the thickness of the cadmium sheath on the value of φ was determined experimentally. Experiment showed that for thicknesses of the cadmium sheath used, in the conditions of the reactor lattice investigated, this effect can be neglected.

Control measurements at the boundary between the active zone and the reflector showed that R/T = 1.2. The ratio was found to be smaller, as expected, because the reflector enriches the spectrum with thermal neutrons.

Measurements carried out in the cell, at a position situated between two boron compensating rods, gave R/T = 1.9. These control experiments showed that for measurement it is necessary to choose a region in which the neutron spectrum reaches equilibrium. Such a region, for our measurements, was the central reactor cell, which was sufficiently far removed from absorbing rods.

Results

The results of the calculation of φ by the three methods considered are given below.

1. To calculate φ using the first method [Equation (5)] the following values have been adopted for the constants:

$$\frac{\bar{\Sigma}_{a239}}{\bar{\Sigma}_{f235}} = \frac{\bar{\sigma}_{a238}}{\sigma_{f235}} \cdot \frac{N_{238}}{N_{235}},$$

where $\bar{\sigma}_{a238}/\bar{\sigma}_{f235} = 1.93$ barn/362 barn is the ratio of the cross sections averaged over the Maxwellian distribution of neutrons at a temperature of 500°K*; $N_{238}/N_{235} = 22.6$ is the ratio of the numbers of U^{238} and U^{235} nuclei per cm^3; $\nu = 2.46$; $\mu = 1$; $\Phi(\bar{E}) = P(\bar{E})\chi(E) = 0.8$, where $P(\bar{E})$, the probability to escape leakage, is calculated from the equation $P(\bar{E}) = \exp[-\kappa^2\tau(\bar{E})]$; $\chi(\bar{E})$ was evaluated from the cadmium ratio for fission and from the resonance integrals for the absorbers present in the cell. The ratio $(R/T)_f$ was obtained by measuring in the central cell the cadmium ratio, which was found to be equal to 12, for U^{235} foil. $\varphi = 0.906$, calculated from Equation (5). The error in φ is determined mainly by the inaccuracies of the values taken for the constants, as also by the uncertainties in the cross sections and leakage. According to our estimates it is 1.5%.

2. In calculating φ using the second method [Equation (7)] the following values have been adopted for the constants:

$$P_{Cd} = 0.955; \quad \frac{\Phi(E_{Cd})}{\Phi(\bar{E})} = 0.905;$$

$$f = 0.74; \quad F = 0.108.$$

$\varphi = 0.90$, calculated from Equation (7).

The good agreement in the values of φ calculated from Equations (5) and (7) shows that the "leakage" and "absorption", which appear in these equations, have been correctly evaluated.

3. To calculate φ using the third method [Equation (10)] we use the cadmium ratio for a thin gold indicator. The resonance energy for gold is equal to 4.91 ev, i.e., the resonance is situated lower than the first resonance for U^{238} (6.7 ev). This enables us to consider that φ (4.91 ev) = φ (0.4 ev), i.e., in Equation (10) $\varphi(E_r) = \varphi$.

The ratio $(R/T)_{238} = 1.67$ was obtained for a real uranium reactor element, i.e., the measured R/T is an effective one and takes into account the geometry of the uranium element. The ratio $(R/T)_r = (R/T)_{Au} = 2$ was measured using a thin (10 mg/cm^2) gold indicator, which does not distort the thermal neutron flux.

The mean neutron flux in the uranium element is 85% of the flux in the moderator where $(R/T)_r$ was measured. Hence, provided that the U_{238} and Au cross sections in the thermal region follow the 1/v law, the ratio

$$\frac{\int_0^{0.4\,ev} (nv)_U N_{238}\sigma_{a238}(E)\,dE}{\int_0^{0.4\,ev} nv\,\sigma_{a}(E)\,dE},$$

appearing in Equation (10), will be equal to $0.85\sigma_{a238}N_{238}/\sigma_{Au}$. Since $E_r \approx \bar{E}$, then $\Phi(\bar{E}) \approx \Phi(E_r)$, and Equation (10) can be written in the form

$$\frac{1-\varphi}{\varphi} = \frac{\left(\frac{R}{T}\right)_{238}}{\left(\frac{R}{T}\right)_{Au}} \cdot \frac{0.85\,\sigma_{a238}\cdot N_{238}}{\sigma_{Au}\xi\Sigma_s} \int_{0.4\,ev}^{\infty} \sigma_{a\,Au}(E)\frac{dE}{E}. \qquad (11)$$

In the calculation the following values have been adopted for the constants:

$$\int_{0.4\,ev}^{\infty} \sigma_{a\,Au}\frac{dE}{E} = 1300 \text{ barn}; \quad \sigma_{Au} = 95 \text{ barn};$$

$$\sigma_{a238} = 2.8 \text{ barn}; \quad \frac{\xi\Sigma_s}{N_{238}} = \xi\sigma_s = 216 \text{ barn},$$

* The neutron gas temperature was measured by E.F. Makarov.

where σ_s is the moderator scattering cross section per atom of U^{238}.

$\varphi = 0.89 \pm 0.02$, calculated from Equation (11).

The agreement between the three calculated values indicates that the methods considered for calculating the resonance escape probability are correct. The mean value of φ for the atomic power station reactor is equal to 0.900 ± 0.015.

SUMMARY

The measurement of φ in an atomic power station reactor was made difficult by a number of circumstances, among them being the comparatively large neutron leakage from the reactor, the high enrichment of the uranium, and the presence of a large number of absorbing constructional elements in the active zone.

These circumstances magnified the error and made it difficult to determine the value of 4 to better than 1.5%.

The assessment of these factors and the introduction of corrections into the experimental results can also be of interest in the case of other measurements in similar conditions.

The experimental results obtained in the present work are in satisfactory agreement with calculations, using equations given in References [1] and [3], taking into account the complicated geometry of an uranium element.

The authors consider it necessary to express their gratitude to Dr. A.K. Krasin for the continual interest in the work, for valuable advice and help, to M.E. Minashin for valuable comments, and also to the collective of the atomic power station associates, who created the necessary conditions for the work.

LITERATURE CITED

[1] M.B. Egiazarov, V.S. Dikarev and V.G. Madeev, Session of the Academy of Sciences, USSR on the peaceful uses of atomic energy (Meeting of the physico-mathematical section), USSR Academy of Sciences Press, 1955, p. 53.

[2] S. Krasik and A. Radkovsky, Atomic Power Engineering (Reports of foreign scientists at the International Conference on the peaceful uses of atomic energy), State Power Eng. Press, 1956, p. 375.

[3] I.I. Gurevich and I.Y. Pomeranchuk, The Construction and Theory of Reactors (Reports of the Soviet delegation at the International Conference on the peaceful uses of atomic energy) USSR Academy of Sciences Press, 1955, p. 220.

Received November 2, 1956

THE INFLUENCE OF CAVITIES ON THE CRITICAL MASS OF A "BASIN-TYPE" REACTOR

B.P. Rastogi

(Indian Center for Atomic Research, Bombay)

It is shown that the influence of cavities, formed in the reactor active zone after the removal of regulating and emergency rods, on the critical mass of a "basin-type" reactor cannot always be neglected. For example, after the removal of four special assemblies representing a combination of regulating rods and heat-producing elements, the reactor critical mass can increase by 20-30%, depending on the position of the rods and the size of the cavities in the active zone.

The evaluation of the influence of the cavities was made with the help of the two-group method, for a reactor consisting of a number of zones. The first zone was taken to be the central cavity, which behaves as a reflector, the second taken to be the active zone. The external reflector was considered to be the third zone.

It was found that the change in the distribution of the thermal neutron flux, caused by the presence of the central cavity, extends to a distance of 8 cm from the center of a cavity of radius ~3.2 cm. Therefore, if the regulating rods in a "basin-type" reactor are separated by a distance of 15-20 cm, as is the case in practice, then it can be expected that the influence of one cavity on another will be small and that reasonably good results can be obtained if the effects produced by the individual cavities are simply added.

INTRODUCTION

A "basin-type" reactor is usually provided with two emergency and two regulating rods, which are placed in four special heat-producing elements. In the cases where the emergency and regulating rods have a relatively large cross section, the cavities, left in the lattice after the rods are removed, are also relatively large. This paper is devoted to this question and it is shown that the critical mass of the reactor from which the regulating and emergency rods are removed is considerably larger than that of a reactor in which the cavities formed are filled by heat-producing elements.

To evaluate the influence of the cavities on the reactor critical mass, let us assume that the presence of the cavity in the center of the active zone does not affect the vertical distribution of the neutron flux. The effective height of the active zone will be the same as that for a lattice without a central cavity [1].

For a cylindrical active zone, the evaluation of the influence of a cavity in the reactor center was carried out using the two-group method; in addition the reactor was considered to consist of two zones, the central cavity, acting as a reflector, was taken as the first zone and the active zone, as the second. The external reflector was taken to be the same as that in the case without a central cavity. More detailed calculations were also carried out in which the external reflector was considered as the third zone. As expected, the results of these calculations are in agreement [2].

After a quantitative evaluation of the effect of a central cavity on the reactor critical mass was made, the influence of peripheral cavities was evaluated using perturbation theory.

Theory

The calculations were made in the usual homogeneous approximation, which is used for such reactors. The central cavity was considered as Reflector No. 1, while the external reflector, as Reflector No. 2.

Denoting the effective height of the cylindrical active zone by H (whose value is obtained for the uniform reactor), the radial diffusion equation for the reflectors and the active zone can be written in the following form:

$$\text{Reflector № 1}\quad \begin{cases} \nabla_r^2\Phi_{1r_1} - \chi_{1r}^2\Phi_{1r_1} = 0, \\ \nabla_r^2\Phi_{2r_1} - \chi_{2r}^2\Phi_{2r_1} + \dfrac{\Sigma_{1r}}{D_{2r}}\Phi_{1r_1} = 0; \end{cases}$$

$$\text{Active zone}\quad \begin{cases} D_{1c}\nabla_r^2\Phi_{1c} - \Sigma_{1c}\Phi_{1c} + \dfrac{k}{p}\Sigma_{2c}\Phi_{2c} = 0, \\ D_{2c}\nabla_r^2\Phi_{2c} - \Sigma_{2c}\Phi_{2c} + p\Sigma_{1c}\Phi_{1c} = 0; \end{cases}$$

$$\text{Reflector № 2}\quad \begin{cases} \nabla_r^2\Phi_{1r_2} - \chi_{1r}^2\Phi_{1r_2} = 0, \\ \nabla_r^2\Phi_{2r_2} - \chi_{2r}^2\Phi_{2r_2} + \dfrac{\Sigma_{1r}}{D_{2r}}\Phi_{1r_2} = 0. \end{cases}$$

In these equations the indices 1 and 2 refer to the fast and slow neutron fluxes, correspondingly, r_1 and r_2 to reflectors No. 1 and No. 2, and c to the active zone. The expression

$$\chi_{1r}^2 = \frac{1}{\tau_r} + \left(\frac{\pi}{H}\right)^2, \quad \chi_{2r}^2 = \frac{1}{L_{2r}^2} + \left(\frac{\pi}{H}\right)^2$$

and other symbols have their usual meaning.

These equations can be easily solved, and the solutions have the form

$$\begin{aligned} \Phi_{1r_1} &= FI_0(\chi_{1r}r), \\ \Phi_{2r_1} &= GI_0(\chi_{2r}r) + S_3FI_0(\chi_{1r}r), \\ \Phi_{1c} &= AJ_0(\mu r) + BY_0(\mu r) + CI_0(\nu r) + EK_0(\nu r), \\ \Phi_{2c} &= S_1[AJ_0(\mu r) + BY_0(\mu r)] + \\ &\quad + S_2[CI_0(\nu r) + EK_0(\nu r)]. \\ \Phi_{1r_2} &= NK_0(\chi_{1r}r), \\ \Phi_{2r_2} &= LK_0(\chi_{2r}r) + S_3NK_0(\chi_{1r}r), \end{aligned}$$

where

$$\tau_r = \frac{D_{1r}}{\Sigma_{1r}};$$

$$S_1 = \frac{D_{1c}}{\tau_c D_{2c}} \frac{1}{\frac{1}{L_{2c}^2} + \mu'^2};$$

$$S_2 = \frac{D_{1c}}{\tau_c D_{2c}} \frac{1}{\frac{1}{L_{2c}^2} - \nu'^2};$$

$$S_3 = \frac{\Sigma_{1r}}{D_{2r}} \frac{1}{(\chi_{2r}^2 - \chi_{1r}^2)};$$

$$\mu'^2 = \frac{1}{2}\left[-\left(\frac{1}{\tau_c} + \frac{1}{L_{2c}^2}\right) + \sqrt{\left(\frac{1}{\tau_c} + \frac{1}{L_{2c}^2}\right)^2 + \frac{4(k_\infty - 1)}{\tau_c L_{2c}^2}} \right];$$

$$-\nu'^2 = \frac{1}{2}\left[-\left(\frac{1}{\tau_c} + \frac{1}{L_{2c}^2}\right) - \sqrt{\left(\frac{1}{\tau_c} + \frac{1}{L_{2c}^2}\right)^2 + \frac{4(k_\infty - 1)}{\tau_c L_{2c}^2}} \right];$$

$$\mu^2 = \mu'^2 - \left(\frac{\pi}{H}\right)^2$$

and

$$\nu^2 = \nu'^2 + \left(\frac{\pi}{H}\right)^2$$

(F, G, A, B, C, E, N and L are arbitrary constants).

To obtain the critical radius of the reactor, the usual conditions were used: a) the continuity of the fast and slow neutron fluxes and b) the continuity of the derivatives of the fast and slow neutron fluxes at the active zone internal and external boundaries, here denoted by a and R respectively. The use of these eight boundary conditions gives eight equations with eight unknowns. For a nontrivial solution, the determinant of the system (see below) must be equal to zero. ($\Delta = 0$ is the condition for criticality). The value of the radius R, for which the determinant becomes zero, is obtained by a numerical solution of the equations. Knowing R, the unknown constants can be determined and the neutron fluxes obtained.

Knowing the critical radius in the presence of a central cavity, the critical mass can be obtained and compared to the reactor critical mass in the absence of the cavity.

$$\Delta = \begin{vmatrix}
I_0(\chi_{1r}a) & 0 & -J_0(\mu a) & -Y_0(\mu a) & -I_0(\nu a) & -K_0(\nu a) & 0 & 0 \\
S_2 I_0(\chi_{1r}a) & I_0(\chi_{2r}a) & -S_1 J_0(\mu a) & -S_1 Y_0(\mu a) & -S_2 I_0(\nu a) & -S_2 K_0(\nu a) & 0 & 0 \\
0 & 0 & J_0(\mu R) & Y_0(\mu R) & I_0(\nu R) & K_0(\nu R) & -K_0(\chi_{1r}R) & 0 \\
0 & 0 & S_1 J_0(\mu R) & S_1 Y_0(\mu R) & S_2 I_0(\nu R) & S_2 K_0(\nu R) & -S_2 K_0(\chi_{1r}R) & -K_0(\chi_{2r}R) \\
D_{1r}\chi_{1r} I_1(\chi_{1r}a) & 0 & D_{1c}\mu J_1(\mu a) & D_1 \mu Y_1(\mu a) & -D_{1c}\nu I_1(\nu a) & D_{1c}\nu K_1(\nu a) & 0 & 0 \\
D_{2r}S_2\chi_{1r} I_1(\chi_{1r}a) & D_{2r}\chi_{2r} I_1(\chi_{2r}a) & D_{2c}S_1\mu J_1(\mu a) & D_{2c}S_1\mu Y_1(\mu a) & -D_{2c}S_2\nu I_1(\nu a) & D_{2c}S_2\nu K_1(\nu a) & 0 & 0 \\
0 & 0 & -D_{1c}\mu J_1(\mu R) & -D_{1c}\mu Y_1(\mu R) & D_{1c}\nu I_1(\nu R) & -D_{1c}\nu K_1(\nu R) & D_{1r}\chi_{1r} K_1(\chi_{1r}R) & 0 \\
0 & 0 & -D_{2c}S_1\mu J_1(\mu R) & -D_{2c}S_1\mu Y_1(\mu R) & D_{2c}S_2\nu I_1(\nu R) & -D_{2c}S_2\nu K_1(\nu R) & D_{2r}S_2\chi_{1r}K_1(\chi_{1r}R) & D_{2r}\chi_{2r}K_1(\chi_{2r}R)
\end{vmatrix}$$

Results

The system of equations was solved with respect to R using the data given in the table (R = 20.65 cm). Calculations made for the same multiplying medium without a central cavity give R = 19.65 cm. The critical masses in these two cases, for the cylindrical active zone taken, are equal to 2.6 and 2.4 kg, respectively, i.e., they are different by approximately 8%.

The various constants in the equations for the fluxes were then determined. The graphs of the fast and slow neutron fluxes are given in Figure 1. The fast neutron flux is normalized so that it coincides with the slow neutron flux in the region where both fluxes are described by the function $J_0(\mu r)$. The dashed curve is the graph of the function $J_0(\mu r)$, which coincides with the fluxes in this region. This curve is a good approximation to the flux distribution in the active zone up to a distance of a few centimeters from the cavityless reactor boundary.

The perturbation theory was used to evaluate the effect of the cavity on the peripheral regions of the active zone. The two-group equation for a small perturbation, arising in the lattice, is given in S. Glasstone and M. Edlund [3]. The relative importance of the various terms in the above-mentioned equation was evaluated. It was found that terms referring to the diffusion are negligibly small compared to terms referring to the absorption and slowing-down properties of the medium. If we assume that the average group velocity of fast neutrons is considerably greater than that of slow neutrons, then the equation mentioned reduces to the expression

$$\frac{\delta k}{k}\frac{\text{eff}}{\text{eff}} \sim \left[\int \delta(\Sigma_1)\Phi_1^+\Phi_1\, dv + \int \delta(k\Sigma_2)\Phi_1^+\Phi_2\, dv \right]$$

Reflector	Active zone
$\tau_r = 33\ см^2$ $L_{2r}^2 = 6.30\ см^2$ $D_{1r} = 0.9\ см$ $D_{2r} = 0.1350\ см$ $S_3 = 1.5763$ $R_{equiv}^{*}) = 3,265\ см$	$\tau_c = 63\ см^2$ $L_{2c}^2 = 2.722\ см^2$ $D_{1c} = 1.2414\ см^2$ $D_{2c} = 0.2056\ см$ $S_1 = 0.255042$ $S_2 = -3.95375$ $H_{eff} = 82\ см$ $H_{actual} = 63.5\ см$ $k = 1.562$ $p \sim 1$

*) R_{equiv} – equivalent radius of the internal reflector or cavity.

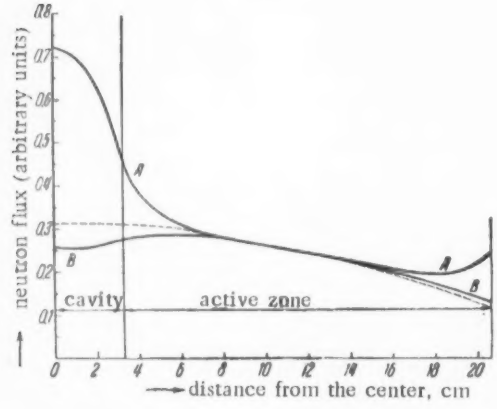

Fig. 1. The neutron fluxes in arbitrary units as a function of the distance from the center of the active zone: Curve A) slow neutron flux; Curve B) fast neutron flux divided by 3.16. Dashed curve) the function $J_0(\mu r)/3.16$.

where Φ_1 and Φ_2 are the fast and slow neutron fluxes and Φ_1^+ and Φ_2^+ are their adjoint functions.

It must be noted that Φ_1 and Φ_2, as also their adjoints, are given in terms of the function $J_0(\mu r)$ for a region not too near the boundary of the active zone. Therefore,

$$\frac{\delta k_{eff}}{k_{eff}} \sim J_0^2(\mu r).$$

Figure 2 gives the function $J_0^2(\mu r)$ normalized to one at the reactor center. This curve gives the value of $\delta k_{eff}/k_{eff}$ for different positions of a cavity on the periphery of the active zone. Since $\delta M \sim \sim \delta k_{eff}$, where δM is the change in the critical mass determined by the presence of a peripheral cavity in the active zone, at a distance r from its center, then

$$(\delta M)_r = (\delta M)_{r=0} \frac{J_0^2(\mu r)}{J_0^2(0)}. \qquad (1)$$

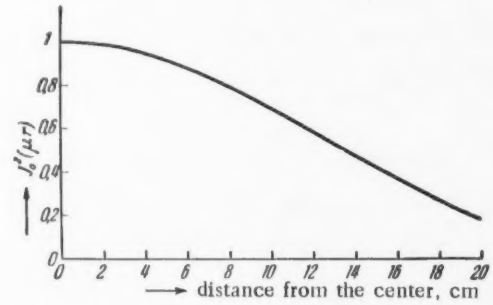

Fig. 2. Graph of $J_0^2(\mu r)$ as a function of the distance of the cavity from the center of the active zone.

SUMMARY

As mentioned above, the evaluation of the influence of the cavity was carried out for a two-zone reactor. Calculations for two-zone and three-zone reactors showed that the results are in agreement with each other, thus also verifying the applicability of this method for calculating the effect of regulating rods.

Curve B of Figure 1 shows that the main characteristics of the fast neutron flux remains the same, the only difference being a reduction of the flux in the cavity. Curve A has a sharp hump inside the cavity, the flux outside the cavity remains more or less normal. The appearance of the hump is explained by the production of slow neutrons within the cavity.

The calculation of the flux distribution in a reactor with several cavities will be made considerably more complicated by the presence of interference between the perturbations produced by each cavity. The presence of regulating rods in any of the cavities will also considerably change the distribution of the slow neutron flux.

From Figure 2 it can be seen that the change δM (1), in the region we are interested in, is 5-7%. In practice, three or four regulating rods are usually used; therefore, the change in the critical mass, determined by the presence of cavities for these rods, can reach 20-30%. Figure 1 shows that the disturbance of the neutron flux distribution, caused by the presence of one cavity extends to a distance of about 8 cm from its center. Therefore,

if the individual regulating rods are at distances of ~15-20 cm from one another, as occurs in practice, it can be expected that the influence of one cavity on another will be small and that good results can be obtained by simply adding the magnitudes of the effects of the individual cavities.

The author expresses his gratitude to Dr. K.S. Syngve and Mes. Udgaonkar and Kotari for discussion and advice during the work, and, also, for permission to use results of their calculations.

LITERATURE CITED

[1] L.S. Kothari and B.M. Udgaonkar (1955), (unpublished data).

[2] R.L. Murray and J.W. Niestlie, Nucleonics 13, 2, 18 (1955).

[3] S. Glasstone and M.C. Edlund, The Elements of Nuclear Reactor Theory, D. Van.Nostrand Company, N.Y., 1952 [Russian translation].

Received December 12, 1957.

A TURBOGENERATOR DESIGNED FOR ATOMIC ELECTRO-STATIONS

M.M. Kogan

The basic type of atomic electrogenerating station should be the heat and power central station, since it allows good fuel economy, utilizing the fuel not only for generation of electricity but for heating of buildings and supply of hot water. This is very important in areas that are short of fuels. The existing type of heat extraction turbogenerator with adjustable steam extraction and condensation, does not provide constant loading of the reactor, and therefore its use in an atomic central station is not justifiable. In view of this, a new type of heat extraction turbogenerator for these stations is proposed, incorporating constant steam flow through the high pressure cylinder. The quantity of steam flowing to the low pressure cylinder of the turbine varies with the demand for steam. When there is no demand for heat the steam flow through the two cylinders is equal. The proposed turbogenerator has variable power output, which with no steam extracted, increases 38 to 69% over the output of existing types, depending on the initial steam conditions. This turbogenerator insures a constant load on the reactors.

Atomic electro-stations can utilize either a condensing cycle or a mixed flow cycle that provides for simultaneous output of electricity and heat.

Condensing electro-stations incur considerable heat losses in the cooling water, and their efficiencies, even with high initial steam parameters and high system ratings, do not exceed 35 to 40%. In mixed flow electro-stations the heat of the exhaust steam is used, and because of this the system efficiency reaches 80%.

To decide the proper choice of system design for an atomic electro-station it is necessary to compare performance figures of condensing electro-stations and heat-power central stations when operating on conventional fuels and on nuclear fuel.

Increasing the power rating of atomic electro-stations is more profitable than increasing the rating of conventional stations. Thanks to advances in transmission of electrical energy it is feasible to build condensing electro-stations of very large power ratings. The transmission of heat, however, requires larger capital investments and incurs larger operating costs than the transmission of electricity; therefore the limits of power of condensing stations are greater than those of heat-power central stations.

Furthermore, because of the high cost of atomic electro-stations and the relatively low cost of nuclear fuel it follows that atomic electro-stations should run at full power the greatest possible number of hours during a year. Thanks to this, conventional heat-power stations that deliver to the same energy supply system, can operate less time at installed power.

Ordinarily, condensing electro-stations operate at full power a greater number of hours than heat-power centrals that supply the community and household heat requirements of cities. This applies particularly to the heat generators. It is shown here that with a certain type of heat extraction turbogenerator, the time at full power of a heat-power central station, can be made even greater than the time of a condensing electro-station.

It is practical to build atomic electro-stations for simultaneous generation of electricity and heat, and the generation of electricity through condensing cycles should be concentrated in very large condensing electro-stations that are located close to sources of fuel. This is conditional to the following assumptions:

1) The removal of coal burning electro-stations from sources of fuel incurs the reduction of transmission distance of heat when these stations are used as heat-power centrals, and is not economical since the transmission of electricity is considerably cheaper than the rail delivery of fuel.

2) Atomic electro-stations should be built in regions that lack local fuel, that is, in regions where supplies of fuel for household and community needs are lacking. It is well known that in the USSR about 20% of the coal produced is used to generate electricity, 10% for heating of city buildings, and all the rest is used up by industry, transport, etc. In regions that do not have local fuel, the relative use of fuel for heating is much greater than the average for the Union, and this determines the importance of replacing conventional fuel with nuclear fuel not only for generation of electricity but for household needs as well.

Of basic significance for making the choice of type of conventional or atomic station is the possible degree of proximity to the city. As is known, the construction of Moscow's suburban coal burning heat-power centrals is planned for a distance of 20-30 km from the city line. The delivery of fuel to these sites, its storage, the removal of ash, etc., incurs great difficulties and additional capital outlays.

The reactor safeguards committee [1] of the Atomic Energy Commission of the USA recommends the following formula for choice of distance of an atomic power station from a city.

$$R = 0.016 \quad N,$$

where R is the distance in km; $N = N_{st}/\eta_{st}$ is the delivered thermal power in kw. For instance, when $N_{st} = 200{,}000$ kw and $\eta_{st} = 0.2$, $R = 16$ km.

Thus the distances from a city to a heat-power central on conventional fuel and one on nuclear fuel are about equal. A heat-power central working on gaseous fuel can be located within the city limits, and in this respect has an advantage over an atomic central. Erection of atomic electro-stations is therefore restricted to areas that do not receive gas.

The above mentioned considerations are evidence that some atomic electro-stations must be devoted to the simultaneous generation of electricity and heat.

The economics of atomic electro-stations are basically different from the economics of conventional stations [2].

The capital investments in atomic electro-stations are relatively heavy, while the fuel costs in operation are no greater than 20-30%.(In coal burning stations they are 50-70%.)

The advisability of maximum power operation of reactors dictates the selection of special turbogenerator types, especially those working on a mixed flow cycle.

Improvement of turbine economy is achieved through elevation of the initial conditions of the steam, increase in the number of stages and decrease in the energy drop in each stage, and also through increase of vacuum. All this is associated with additional capital outlays, so that in view of the low atomic fuel cost it is possible to get by with only moderately economic refinements of turbines.

During the summer months when vacuum is decreased by 4-5%, condensing turbines use proportionately more steam. For equal loading of atomic condensing electro-stations in summer and winter it is desirable that the turbines and generators of the station operate during the winter months under an overload of about 5%, so that steam demand is maintained at a constant level in winter and summer. Condensing turbines and generators of conventional types allow such overloads, therefore atomic condensing electro-stations do not require special turbogenerators [3].

The selection of turbogenerator design for atomic heat-power central stations is more involved. The thermal power output of contemporary turbines in heat-power centrals that supply community household needs is usually half their thermal loading ($\alpha_{cs} = 0.5$). Any unfilled demand for heat is satisfied by live steam from the central station boilers or by steam from a special boiler plant. An increase of α_{cs} is associated with a decrease in the number of hours of electrical energy available from a central station working on a heat extraction cycle and incurs a corresponding increase in consumption of electricity generated by central stations working on condensing cycles, which produces excessive fuel consumption in the over-all system. The latter is subject to the

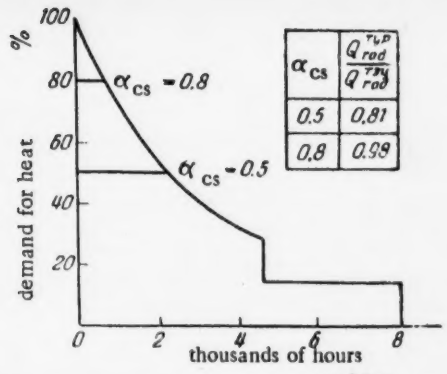

Fig. 1. Annual heat expenditure. $Q_{year}^{turbine}$ – quantity of heat delivered by turbine per year; $Q_{year}^{central}$ – quantity of heat delivered by the whole central station per year.

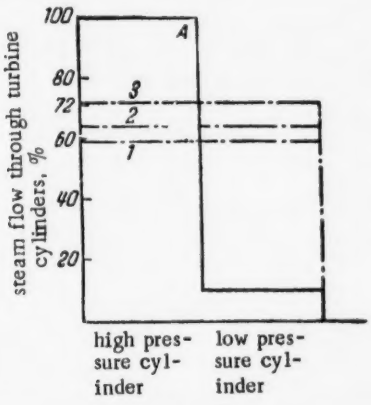

Fig. 2. Steam flow through the turbine cylinders. Initial steam parameters: 1) 15 atmospheres abs, 350°C; 2) 35 atmospheres abs, 435°C; 3) 90 atmospheres abs, 500°C; A) heat extracting operation, $E = E_{max}$; B) condensing operation, $E = 0$, $N = N_{max}$ (where E is the quantity of extracted steam, N is the turbine power).

fact that specific fuel consumption (in kg/kw-hr) in condensing electro-stations is usually lower than in heat-power central stations that generate electricity by a condensing cycle.

A lowering of α_{cs} produces a decrease in generation of electricity for any given heat extraction, that is, the effective thermal utilization is lowered. The choice of the optimum value of α_{cs} for a given heat-power central station depends on a series of factors, primarily on the operating data of the energy cycle. However, for most heat-power central stations the optimum value of α_{cs} is near 0.5 [4].

The optimum value of α_{cs} for atomic electro-stations must be greater, since an increase of α_{cs} produces an increase in nuclear fuel consumption and a corresponding decrease in conventional fuel consumption. However, even for atomic heat-power central stations α_{cs} must be less than unity, since at certain values of this coefficient, increasing it does not produce an increase in electrical energy output per given heat input because of the increase in stage idling in the turbine. For atomic heat-power central stations it is possible to predict that the best value of α_{cs} is near 0.8.

Figure 1 shows a common curve of annual heat expenditure for heating and hot water. The curve shows that when $\alpha_{cs} = 0.5$, the mixed flow supplies 81% of the required heat in the course of a year, and when $\alpha_{cs} = 0.8$, it supplies on the order of 98% of the requirement.

All of the following considerations of turbo-generator type for atomic heat-power centrals are based on $\alpha_{cs} = 0.8$; however, the conclusions reached are good for other values of heat extraction coefficient.

In heat-power central stations intended for supplying of urban heating needs, condensing turbines with adjustable steam extraction at 1.2 to 2.5 atmospheres abs are generally installed. Soviet heat extraction turbines are designed so that with shut off extraction they produce full electrical power rating. At full extraction, that is at maximum heat removal, the steam flow through the low pressure cylinder is 10% of the steam flow through the head section of the turbine, which is essential for ventilation of the tail section of the turbine.

The question of best steam parameters for atomic electro-stations has not yet been conclusively answered, therefore the following discussion is carried out for various initial steam parameters:

1) low – 15 atmospheres abs, 350°C
2) medium – 35 atmospheres abs, 435°C
3) high – 90 atmospheres abs, 500°C.

The table shows calculated figures of heat drops in the turbine cylinders and the relative quantities of steam passing through the low pressure cylinder under fully condensing operation (steam extraction equal to zero) for various initial steam parameters.

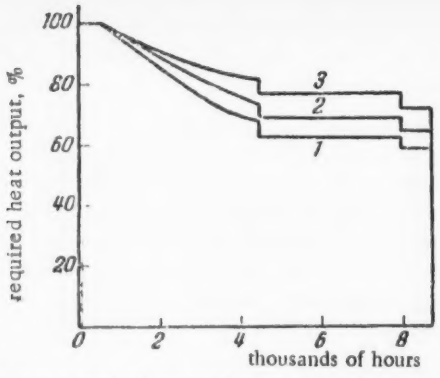

Fig. 3. Required annual heat output of reactors. Initial steam parameters: 1) −15 atmospheres abs, 350°C, $Q_{yr}^{ra} = 0.74Q_{max}$; 2) −35 atmospheres abs, 435°C, $Q_{yr}^{ra} = 0.77\ Q_{max}$; 3) −90 atmospheres abs, 500°C, $Q_{yr}^{ra} = 0.82Q_{max}$ (where Q_{yr}^{ra} is the average annual loading of the reactor).

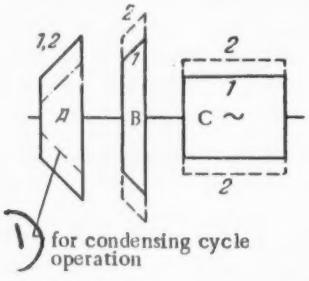

Fig. 4. Schematic representation of turbogenerators with (1) constant and (2) variable electrical power output: A) cylinder for high pressure; B) low pressure cylinder; C) generator.

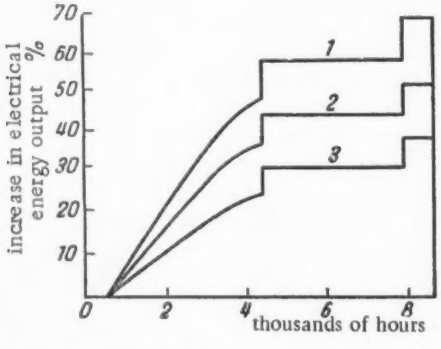

Fig. 5. Increase in electrical energy output obtainable from changeover to turbines with constant steam flow. Initial steam parameters: 1) −15 atmospheres abs, 350°C, $\Delta E = 43\%$; 2) 35 atmospheres abs, 435°C, $\Delta E = 32\%$; 3) 90 atmospheres abs, 500°C, $\Delta E = 24\%$.

The heat content of the steam and its adiabatic drop are determined from a chart, and the relationship of steam quantities for condensing and extracting modes of operation, by the formula

$$G_{cond}/G_{extracting} = (0.9\ h'/h + 0.1)\ 100,$$

where h' and h are adiabatic).

The data given for steam flow in the table (as well as the following discussion) does not consider steam utilization for regeneration.

In Figure 2, based on data in the table, are given curves of steam flow through the high pressure and low pressure cylinders under conditions of full electrical energy output for various initial steam parameters.

Figure 2 and the table show that under condensing operation the turbine uses 59-72% of the steam quantity that is used under extracting operation and full electrical power output. An increase in steam used by the turbine under condensing operation is prevented by the capacity of the low pressure cylinder of the turbine and by the capacity of the generator.

The sources of steam, that is, the reactors must also produce in compatibility with the steam flow through the turbine.

In Figure 3 are shown curves of relative heat expenditure by the turbine working on a condensing cycle with steam extraction at a pressure of 1.2 atmospheres abs, for various initial steam parameters and $\alpha_{cs} = 0.8$ and full electrical power output.

It is evident from these curves that the reactors work under full load only 600 hours per year, and that the average annual loading of the reactors with low initial steam parameters is equal to 74%, and with high steam parameters − 82%. Thus the use of heat extracting turbines of existing types results in 18 to 26% of installed reactor capacity being unused during the year, and consequently the cost of heat and electricity from the atomic central station increases proportionately.

For a heat-power central station operating on conventional fuels, such unused boiler capacity is entirely allowable. Usually powerful condensing electro-stations have the largest possible load factors, and central stations for heat and power generate electricity on a condensing cycle only during peaks of electrical loading. In this latter case the unused boiler capacity in a heat-power central increases still more, but for the over-all system this is allowable.

The same problem is approached altogether

Heat Drops in the Turbine and Relative Steam Flows Under Condensing Operation

Parameter	Units	Initial steam parameters, atmospheres abs/°C		
		15/350	35/435	90/500
Initial heat content of steam, i_H	kcal/kg	751	789	811
Adiabatic heat content drop to 1.2 atmospheres abs, h'	kcal/kg	131	179	229
Adiabatic heat content drop to 0.04 atmospheres abs, h	kcal/kg	241	289	332
Ratio of steam quantity flowing through the turbine under condensing operation to steam quantity under heat extraction operation (under full electric power generation) $G_{cond}/G_{extracting}$	%	59	66	72

differently for atomic heat-power centrals, in which the basic component of cost of the generated electricity is the amortization charge. In this case it is essential to achieve maximum load factor for the installed equipment, particularly the reactors.

This is fully met by the proposed type of turbine in which the maximum steam flow through the high and low pressure cylinders is equal, that is, the turbine works with constant steam utilization independent of the amount of extraction for heat output and with variable electrical output.

In turbines with constant steam flow, the flow through the low pressure cylinder can be the same as the flow through the high pressure cylinder; the power capacity of the generator is selected for this case. Schemes of turbogenerators with steam extraction and condensing operation, with constant and variable electrical power output, are shown in Figure 4.

Under maximum steam extraction the power of both types is equal, however as the steam extraction is decreased the turbogenerator with constant output maintains that output while the turbogenerator with variable output increases that output as the additional steam quantity, compared to common turbines, becomes available.

The increase in power output of the turbine with constant steam flow as compared with a common heat extraction turbine, can be determined from the formula

$$\Delta N = \left(\frac{1}{0.9 \frac{h'}{h} + 0.1} - 1 \right) 100.$$

where h' and h are adiabatic.

With initial steam at 15 atmospheres and 350°C the increase in power output of a turbine with constant steam flow as compared to one with constant output is 69%, and for turbines with high initial steam parameters – 38%.

The curves of Figure 5 show the increase in electrical power output during the course of a year, of turbines with constant steam flow as compared with common heat extracting turbines. As the curves indicate, this increase reaches the following values under the given initial steam parameters:

15 atmospheres abs, 350°C – 43%
35 atmospheres abs, 435°C – 32%
90 atmospheres abs, 500°C – 24%.

It is obvious that such a considerable increase of electrical energy output of atomic heat-power centrals obtainable from the adoption of heat extraction turbines of the proposed type, is very important.

The change to heat extraction turbines with constant steam flow incurs insignificant increases in the capital investment costs of the heat-power central when compared with the total cost of the station, and incurs low increases in costs of the low pressure cylinder, the generator, condenser and water supply system. The costs of the maintenance labor remain the same as the costs for central stations with conventional turbines.

When working in the same supply system, turbines with constant steam flow for atomic heat-power centrals, compare very well with turbines with back pressure.

Work of the Academy of Community Management of the RSFSR has proven the superiority of these turbines in a heating system for cities [5]. However these turbines have an inherent fault – their power depends on the heat loading.

Turbines with constant steam flow have a reverse characteristic and in the summer would develop high power output. Therefore combined use of both types of turbines provides the best overall summation of power from an atomic heat-power central and a conventional heat-power central equipped with back pressure turbines.

Savings in capital investment realized in installing turbines with back pressure over conventional heat extraction turbines with steam extraction and condensation, are compensated by greater costs incurred by turbines with constant steam flow for atomic centrals, as compared to costs of heat extraction turbines with constant electrical power output.

Therefore it is best to build atomic electro-stations as heat-power central stations, and to equip them with turbogenerators that condense steam and extract steam with varying power output but constant steam flow through the high pressure cylinder and variable (depending on quantity of steam extracted) steam flow through the low pressure cylinder.

LITERATURE CITED

[1] Nucleonics 12, No. 4, 78 (1954).

[2] A.I. Alikhanov, V.V. Vladimirovsky, P.A. Petrov and P.A. Khristenko, Atomic Energy 1, 5 (1956)*

[3] I.I. Kirillov and S.A. Kantor, Theory and Design of Steam Turbines (Machine Government Publishing House, 1947).

[4] L.A. Melentyev, Heating, Publication of Acad. of Sci. USSR (Part I) 1944; (Part II) 1948.

[5] M.M. Kogan, Heating of Small and Medium Cities (Publication of the Ministry of Community Management, RSFSR, 1956).

Received October 20, 1956

*Original Russian pagination. See C.B. Translation pagination.

THE PRINCIPLE OF COHERENT ACCELERATION OF CHARGED PARTICLES

V.I. Veksler

A description is given of a new principle for accelerating charged particles. The conditions are given under which the interaction between geometrically small clusters of charged particles and a stream of fast electrons or between a cluster at rest and a relativistic cluster of high-mass particles can be effectively utilized to transmit high energies to the particles at rest. It is shown that the interaction of electromagnetic waves with charged or even quasineutral clusters of charged particles may also lead to effective acceleration of the particles. Common to the cases here considered is the coherence of the interaction between the beam of accelerated particles and the electromagnetic field or particle cluster causing the acceleration.

In all the existing charged particle accelerators, the electric field which accelerates the particles is created by some external source. In the first approximation, the strength of this field is independent of the number of particles being accelerated. Therefore the motion of each particle is completely determined by this external field and is independent of the other particles.

We present below a new principle for particle acceleration. A characteristic property of this new principle is that the electric field accelerating the particles is not an external field, but arises as a result of the interaction of a geometrically small group of accelerated particles with another group of charges or a plasma, or with an electromagnetic wave. Such a method of acceleration has many important properties. In the first place, it turns out that the magnitude of the accelerating field arising from such an interaction and acting on each charged particle depends on the number of particles accelerated, being , in particular, proportional to this number. Therefore at least in principle, this method can be used to obtain a very high gradient of the accelerating electric field. Secondly, this method of acceleration does not require artificial maintenance of the synchronism between the motion of the accelerated particles and the electric field. Thirdly, it is possible to establish a situation in which a high field strength is produced only in a region containing accelerated particles, and finally, it is possible to obtain acceleration of quasineutral groups of particles.

The new method of acceleration may be called "coherent," since the magnitude of the accelerating field acting on each individual particle is proportional to the number of particles being accelerated. Although the methods of practically achieving the concepts presented below are still far from clear in all their details, the author feels that with their aid one can attack the problem of designing accelerators with very high currents and ultrahigh energies of the order of 10^{12}ev and even higher.*

Below are presented three methods for achieving coherent scattering.

I. Acceleration of Charged Clusters by the Medium

Tamm [1] has shown that energy losses to Cerenkov radiation can be "reversed," or that a medium moving

*The theoretical investigation of the various aspects of the principle of coherent scattering was performed by M.S. Rabinovich, A.A. Kolomenskii, B.M. Bolotovskii, L.M. Kovrizhnyi and Ia.V. Yankovyi, as well as A.I. Akhiezer, Ia.B. Fainberg, and co-workers.

at high velocity relative to a charged particle can transfer energy to this particle. It is natural, of course, that no attention has yet been paid to the possibility of practically achieving particle acceleration in this way. Indeed, if a high-energy and high-density electron beam were to be used as an accelerating medium to attempt to accelerate, for instance, hydrogen ions, the effective electric field strength on each positive particle would be very small. It is known, however, that the magnitude of the Cerenkov and ionization losses (as well as losses to the excitation of plasma oscillations), and therefore also the magnitude of the reversed accelerating field, are proportional to the square of the accelerated charge. Therefore, if instead of single particles, geometrically small ion clusters containing N charges were to be accelerated, the force acting on each separate particle of the charge could be increased by a factor of N.

This situation, as is easy to show, is related to the fact that each of the individual charges of the cluster excites an oscillation in the electron beam, and that these oscillations are coherently superposed and result in the creation of an electric field whose magnitude is proportional to the number of ions in the cluster. It is easy to show that this effect will arise if the dimensions a of the cluster are much smaller than the wavelength of plasma oscillations.

In this case the accelerating field strength is

$$E = \frac{eN\omega_0^2}{v^2} F \ln \frac{v}{D\omega_0}, \tag{1}$$

where ω_0 is the frequency of plasma oscillations, v is the velocity of the electron plasma, N is the number of charges in the cluster being accelerated, F is a form factor, D is the Debye radius.

$$\omega_0^2 = \frac{4\pi\rho e^2}{m}, \tag{2}$$

where ρ is the electron density, and m and e are the electron mass and charge. The form factor F is almost unity if the dimensions of the cluster are small compared with the wavelength v/ω_0 of a plasma oscillation. It is clear that an electron beam accelerating a cluster of charges must be stabilized in the radial direction. It is interesting to note that if the electron beam is stabilized, for instance, by a longitudinal magnetic field, the acceleration of the particles is achieved by "reversal" of the Cerenkov losses.*

The field strength E for large values of N may in theory attain values of the order of many electron volts per centimeter. The practical achievement, however, of an effective accelerating field with a high gradient necessitates very high power, as is easily shown. This is due to the fact that high gradients can in principle be obtained in the coherent scattering method only with very large numbers of particles in the cluster, that is, for very high current pulses of accelerated particles. When the number of particles in the cluster is small, no effective acceleration takes place. Therefore the method being considered would seem applicable, at least at the present level of technical development, to obtain ions with energies that are not too high.

It should be emphasized that Equation (1) is derived by considering the plasma in the linear approximation, and is not, of course, applicable for high energy transfers; undoubtedly, however, the energy transfer coefficient may be made sufficiently large.

In the practical achievement of the method proposed, the problem of cluster stability is extremely important. Although transverse stabilization is easily achieved due to the space charge of the electron beam itself, the cluster is unstable in the longitudinal direction. The attainment of longitudinal stability necessitates an additional interaction such as, for instance, density modulation of the electron beam. A modulated beam focuses the particles in the longitudinal direction when they are in a high-density region, and defocuses them at the density nodes. As has been shown by M.S. Rabinovich, for certain definite relations between the electron beam density, the length of the modulation wave, and the number of particles in the accelerated cluster, the focusing which takes place is

*There exists, of course, also the inverse effect, which has not yet been noted. As has been pointed out by the author, a cluster of particles (or a single particle) moving through an electron plasma in a magnetic field will emit Cerenkov radiation. This would seem to play a role in radio emission in the upper layers of stellar atmospheres for stars characterized by strong magnetic fields. A similar theoretical description of this phenomena is given by A.A. Kolomenskii [2].

similar to that obtained in strong-focusing accelerators. It is also significant that for short acceleration times clusters may be used which are not absolutely stable. The particles of the cluster can be accelerated to high energies if during the time of the acceleration the cluster changes its dimensions by an amount small compared with the plasma wavelength.

II. Coherent Impact Acceleration

We have considered above the interaction of an electron beam with an ion cluster. It would seem reasonable to use this method for accelerating ions in order to obtain high currents at energies that are not extremely high. If, however, we wish to consider the problem of obtaining ions accelerated to extremely high energies, it would seem more reasonable, at least in principle, to use another interaction, namely coherent "impact," which is based on the behavior of relativistic particles.

Let us consider the collision of a fast relativistic particle of mass M_1 with a particle at rest whose mass M_2 is much less than M_1. It is well known that if the condition $M_1 \gg M_2\gamma$ is satisfied, a head-on collision will give the particle with mass M_2 a very high energy

$$W \approx Mc^2\gamma^2, \text{ where } \gamma = \frac{1}{\sqrt{1-v^2/c^2}}. \tag{3}$$

It would seem possible to attempt to realize this acceleration method in two ways. Let us assume, for instance, that the "primary" particle of mass M_1 which is moving at high velocity is actually a cluster of N_1 particles of mass m_1, and that the "secondary" rest particle is a cluster of N_2 particles of mass m_2. It can be shown that during the time of collision the internal degrees of freedom of such clusters cannot be excited to any high energy if the dimensions of the clusters are small, if the condition $N_1m_1 \gg N_2m_2\gamma$ is satisfied, and finally if the collision is "head-on." As is well known, for a head-on collision the collision parameter p must satisfy the inequality

$$p \ll b,$$

where $b = N_1N_2e^2/m_0c^2$, and $m_0 = m_1m_2N_1N_2\gamma/(m_1N_1 + m_2N_2\gamma)$ is the reduced mass.

Therefore if all the N_1 particles of mass m_1, which make up the "primary" particle moving with velocity $v \approx c$, and all the N_2 particles of mass m_2 which make up the "secondary" particle are concentrated in spherical volumes of radii $a < b$, then we may neglect energy transfer to the internal degrees of freedom and consider the collision of two such particles (one of which is at rest and the other of which has a velocity $v \approx c$) as the collision of classical relativistic particles. In such a collision each particle of mass m_2 of the rest cluster will be given a very high energy which can be found from Equation (3).

Let us assume, for instance, that the rest cluster consists of protons, and that the relativistic cluster consists of electrons with $\gamma = 10^2$. In this case each of the rest protons will be given the enormous energy

$$W \sim m_2c^2\gamma^2 \approx 10^{13} \text{ ev}$$

as a result of the collision. It would seem unnecessary to have a long-term stable hyperdense cluster of relativistic particles. It is necessary only that this cluster exist for a time much longer than the collision time. Of course the total number N_1 of particles concentrated, even if for only a short time, in the relativistic cluster must be extremely large. This situation is the primary difficulty involved in attaining this method of acceleration. One may consider also another method for attaining impulse acceleration: this method is based on the use not of a charged cluster for the primary relativistic particle, but a quasineutral plasma cluster* accelerated to a high velocity and polarized by some external field at the instant of collision. Finally, we may consider the case in which a relativistic quasineutral plasma cluster, within which currents are excited, collides with a plasma cluster at rest, within which currents are also excited. If the mass ratio satisfies $M_1 \gg \gamma M_2$, and the collision parameter in these last two cases is less than the "dimensions" of the clusters, the impulse acceleration mechanism will operate.

*See the third method of coherent scattering.

III. Radiative Acceleration of Quasineutral Particle Clusters

As the next type of coherent scattering, let us consider the acceleration of a particle cluster by an electromagnetic wave; this is somewhat similar to "impulse" acceleration.

One of the fundamental difficulties of coherent scattering of charged clusters is that the Coulomb repulsion of the charges hinders the formation of clusters containing sufficient numbers of particles. In the present type of coherent scattering, however, we may use quasineutral clusters containing about equal numbers of ions or positrons and electrons [3].

Let us consider qualitatively the mechanism by which a cluster is accelerated by a plane electromagnetic wave. As is well known, an electron in the field of a plane electromagnetic wave whose energy density is $W = \frac{E^2 + H^2}{8\pi}$, is acted on by a mean force F directed along the direction of propagation of the wave and equal to

$$F = \sigma_T \overline{W}, \tag{4}$$

where $\sigma_T = \frac{8\pi}{3} r_0^2$ is the Thomson scattering cross section, and r_0 is the classical electron radius.

The force F is very small. But if we are considering a cluster of electrons whose radius is a, then the force acting on the cluster is proportional to $N^2\sigma_T$, where N is the number of electrons in the cluster. It follows that the force on each electron increases by a factor of N. We are, of course, considering that the conditions

$$k_1 a < 1; \quad k_2 a < 1, \tag{5}$$

are fulfilled, where k_1 and k_2 are the wave numbers in the surrounding medium and the cluster, respectively. The question of cluster stability during the acceleration process is important to the practical achievement of this method of acceleration. At present it is still impossible to answer this question.

A constant magnetic field directed along the axis (that is along the direction of propagation of the wave) would seem to have significant effect on the stability as well as on the magnitude of the accelerating force.

All the above, is a qualitative description of the physical basis of a new principle of acceleration, and cannot, of course, be considered final, even in its fundamental aspects.

In addition to the methods described above, we are at present considering also other methods of coherent scattering.

In conclusion it is interesting to note that primary cosmic rays may be generated by one of the indicated mechanisms. A radial flux of high-velocity electrons can effectively transfer its energy to ion clusters formed in the plasma of the upper layers of hot stellar atmospheres. In this case, the energy given a nucleus is proportional to Z^2, rather than Z, which differs from all other acceleration methods.

LITERATURE CITED

[1] I.E. Tamm, J. Phys. 1, 439 (1939).

[2] A.A. Kolomenskii, Proc. Acad. Sci. USSR 106, No. 6 (1956).

[3] V.I. Veksler, The Utilization of Coherent Interaction of Neutral Clusters with Electromagnetic Waves, Physical Institute Acad. Sci. USSR, 1955 (not published).

Received February 4, 1957

SOME THEORETICAL QUESTIONS CONCERNING THE 10-Bev PROTON SYNCHROTRON OF THE ACADEMY OF SCIENCES USSR*

M.S. Rabinovich

A method is developed for calculating those basic phenomena in a weak-focusing proton synchrotron which depend on the choice of the parameters of the accelerator. Free oscillations, variations of the orbit, resonances of free and phase oscillations, and injection theory are considered. The theory is applied to the 10-Bev proton synchrotron of the Academy of Sciences, USSR.*

INTRODUCTION

At present the greatest energy which can be obtained in accelerating charged particles is obtained from proton synchrotrons.

This method is characterized by the use of the "self-phasing" principle discovered by V.I. Veksler for particles moving in an alternating magnetic field in a constant (or nearly constant) equilibrium orbit. The frequency of the accelerating voltage in this case is varied proportionally to the particle velocity.

A significant fact is the possibility of acceleration in systems which are composed of magnetic sectors divided by linear sections.

The construction of accelerators necessitates the creation of the detailed and exact theory which may serve as a fundamental basis for their design and development. Such a theory was created in the Physical Institute of the Academy of Sciences USSR in 1948-1952 [1]. It is the basis of the design for a proton synchrotron [2] which is calculated to give 10-Bev protons. The methods for calculating developed, however, have a much larger range of applicability. For instance, they can be used in part for the calculation of strong-focusing accelerators.

The present article reviews the theory of particle motion in a proton synchrotron on which was based the choice of parameters for the proton synchrotron of the Academy of Sciences USSR (A.S. USSR).

Particles in an accelerator of any type undergo motion in the following way. There exists some synchrotron (closed) orbit. Its position is determined by the ratio between the frequency of the accelerating field and the magnetic field strength H(t). There exists also a family of instantaneous orbits which oscillate about the equilibrium synchrotron orbit. These radial phase oscillations are due to variations of the particle phases, that is of the phase of the accelerating field at the instant the particle passes through the accelerating gap. As a rule, however, particles do not move along these orbits. The major portion of the particles undergo free vertical and radial oscillations about the instantaneous orbit.

These three types of motion take place on three time scales. Let us consider this for the example of the A.S. USSR proton synchrotron: 1) the position of the equilibrium orbit changes significantly in the time of a single acceleration, i.e., in 3,300,000 μsec; 2) a radial phase oscillation takes place in 800-1800 μsec; 3) a free radial or vertical oscillation takes place in 7-1 μsec. According to the theory all three types of motion may, as a rule, be considered separately. Important exceptions are resonance phenomena and transient states, but we shall discuss these later.

*At present the proton synchrotron belongs to the Joint Institute for Nuclear Study (Ed.).

It follows from the independence of these types of motion, among other things, that it is possible to consider free oscillations of the particles without dealing also with the acceleration process. Vice versa, one may also consider the acceleration process without the free oscillations.

The relation between these motions can be taken into account as a correction and is of importance, in particular, in the so-called gap oscillations.

Free Particle Oscillations

The particle motion may be considered in a coordinate system in which the coordinate lines are the instantaneous orbits and the normals to them. It can then be shown [6, 9] that the equations of motion can be written (the particle energy is considered constant)

$$\chi'' + \varkappa^2 g(\sigma)\chi = 0, \tag{1}$$

where the primes denote derivaties with respect to the length σ along the trajectory, χ is the displacement of the orbit,

$$\varkappa^2 = \begin{cases} 1 - n(\sigma) & \text{for radial oscillations,} \\ n(\sigma) & \text{for vertical oscillations,} \end{cases}$$

and $g(\sigma) = 1/R^2(\sigma)$, where R is the radius of curvature of the trajectory at the point σ, and

$$n(\sigma) = -\frac{R(\sigma)}{H}\frac{\partial H}{\partial R}. \tag{2}$$

In an "ideal" accelerator, one in which the field does not alter in the circular sectors and does not enter into the linear sections,

$$g(\sigma) = \left\{ \begin{array}{l} 1/R_0^2 \text{ in the sectors,} \\ 0 \text{ in the linear sections.} \end{array} \right\} \tag{3}$$

Let us first consider an "ideal" accelerator. Equation (1) is an equation with periodically varying coefficients. The period is $\sigma_0 = R_0\nu + l$, where ν is the angle subtended by the sector and l is the length of the linear section.

We shall start counting σ from zero for each periodic element separately. Then, as is well known, the solution to Equation (1) for m periodic elements can be written

$$\chi = De^{i\mu m}\psi(\sigma) + \text{ c.c. }^{*}), \tag{4}$$

where $\psi(\sigma)$ is the solution of Equation (1) satisfying the boundary conditions

$$\left(\frac{d\ln\psi}{d\sigma}\right)_{\sigma=0} = \left(\frac{d\ln\psi}{d\sigma}\right)_{\sigma=\sigma_0}, \tag{5}$$

$$e^{i\mu} = \frac{\psi(\sigma_0)}{\psi(0)}. \tag{6}$$

For an "ideal" accelerator with a segmented magnet

$$\psi(\sigma) = \left\{ \begin{array}{l} \sin\varkappa\frac{\sigma}{R_0} + d\cos\varkappa\frac{\sigma}{R_0} \text{ in the sectors} \\ \frac{\varkappa(\sigma - R_0\nu)}{R_0}(c - ds) + s + dc \\ \qquad \text{in the linear sections} \end{array} \right\} \tag{7}$$

*c.c. is the complex conjugate.

$$\left(d=\frac{c-e^{i\mu}}{s},\quad p=\frac{\varkappa l}{2R_0},\ \cos\mu=c-ps,\ s=\sin\varkappa\nu,\quad c=\cos\varkappa\nu\right).$$

Let us consider a particle injected into the accelerator at an angle $\gamma = d\chi/d\sigma$ to the orbit. Let us denote the distance from the injector along the azimuth σ_i to the orbit by χ_{init}. With these initial conditions, it is easy to find the value of D and therefore the displacement χ, namely

$$D=\frac{\chi_{init}-i\Phi(\sigma_i)R_0(\gamma-\gamma_{opt}}{2\psi(\sigma_i)}, \tag{8}$$

where

$$\Phi(\sigma_i)=-2i\frac{\psi(\sigma_i)\psi^*(\sigma_i)}{BR_0} \tag{9}$$

is a real function, B is the Wronskian of ψ and ψ^* at the point σ_i (in our case the Wronskian of σ), R_0 is a radius which in each case is chosen from considerations of convenience, and

$$\gamma_{opt}=\frac{\chi_{init}}{2}\left(\frac{d\ln\Phi(\sigma)}{d\sigma}\right)_{\sigma=\sigma_i}. \tag{10}$$

Inserting (8) into (4), we obtain

$$\chi=\sqrt{\frac{\Phi(\sigma)}{\Phi(\sigma_i)}[\chi^2_{init}+R_0^2\Phi^2(\sigma_i)(\gamma-\gamma_{opt})^2]}\times\cos[\mu m+\alpha(\sigma)], \tag{11}$$

where

$$\alpha(\sigma)=\arg[D\psi(\sigma)]. \tag{12}$$

Equation (11) is fundamental in considering the free oscillations of particles.

We see that the amplitude of the oscillations $F(\sigma)$ depends on the azimuth σ according to

$$F^2(\sigma)=\frac{\Phi(\sigma)}{\Phi(\sigma_i)}[\chi^2_{init}+R_0^2\Phi^2(\sigma_i)(\gamma-\gamma_{opt})^2]. \tag{13}$$

The minimum value of $F(\sigma_i)$ at the injector azimuth is χ_{init}. It is attained if $\gamma=\gamma_{opt}$, that is if the particles are injected at the optimum angle γ_{opt}.

For given values of (χ_{init}, γ), the maximum and minimum amplitudes $F(\sigma)$ are attained at azimuths where $\Phi(\sigma)$ is minimum and maximum.

If m is treated as a parameter, Equation (11) is the equation of a one-parameter family of curves $\chi=\chi(\sigma)$. If, in addition, m is a continuous variable, then $\chi=\pm F(\sigma)$ is the equation of the envelope of this family.

Actually m is a variable which takes on integral values divisible by N for each element of periodicity, where N is the total number of elements of periodicity.

In practice, if the motion is far from resonant, in each element of periodicity there will be a sufficient number of different curves to consider $\chi=\pm F(\sigma)$ the envelope.

The value of $\kappa\Phi(\sigma)$ is inversely proportional to the focusing, where unity is taken to be the focusing in a circular accelerator.

In the A.S. USSR proton synchrotron, $\kappa\Phi(\sigma)$ varies from 1.05 to 1.10 for radial motion and from 1.03 to 1.12 for vertical motion. Thus, the presence of the linear segments decreases the focusing by only 10% and it is therefore obvious that their length is not limited for this reason. As shall be shown later, the length of the linear segments is limited by the displacement of the fundamental resonances into the region of stability.

In circular accelerators $\gamma_{opt}=0$, and in accelerators with linear sections,

$$\gamma_{opt} = \begin{cases} -p\,\frac{\varkappa\chi_{init}}{R_0}\sin\frac{\varkappa}{R}(2\sigma - R_0\nu) \\ \text{in the sectors,} \\ \frac{\varkappa\chi_{init}}{R_0}\left(\frac{\sigma'\varkappa}{R_0} - p\right) \\ \text{in the linear sections} \end{cases} \qquad (14)$$

The length σ' is counted from the beginning of the linear sections. In the A.S. USSR proton synchrotron, γ_{opt} may be as large as 3'. This is not a very small angle, since the tolerance in the injection angle is of the order of 10-15'.

If γ_{opt} were very large, it would be impossible to maintain injection of an almost parallel beam for any length of time. This situation [9, 10] is observed in strong-focusing accelerators.

Thus, the envelope method [4] led us to a clear and simple answer to all problems related to the properties of particle oscillations and the influence of linear sections.

The Effect of Distortion of the Magnetic Field on Particle Motion

When the magnetic field is distorted, the equation of motion can be written in the first approximation by adding the term $q(\sigma)$ to the right side of Equation (1):

$$\chi'' + \varkappa^2 g(\sigma)\chi = q(\sigma). \qquad (15)$$

Let us assume that $\kappa^2 = \text{const}$, and $q(\sigma)$ is a periodic function with period $N\sigma_0$, where N is the number of elements of periodicity in the orbit ($N\sigma_0$ is equal to the orbit perimeter).

In order to find the particular solution of Equation (15), we vary the constant in Equation (4), arriving at

$$\frac{dD}{d\sigma} = -\frac{q(\sigma)\psi(\sigma)}{B}e^{i\mu m} = -\frac{q(\sigma)\varphi(\sigma)}{B}. \qquad (16)$$

In order to describe the effect of an arbitrary nonresonance perturbation, it is sufficient to find a closed orbit about which the oscillation takes place in the same way as it does about the calculated one. Therefore, if there is a distortion, we lose a small path in the operating region of the magnet in the coordinate system (composed of calculated orbits) in which the new distorted orbit is located (Figure 1).

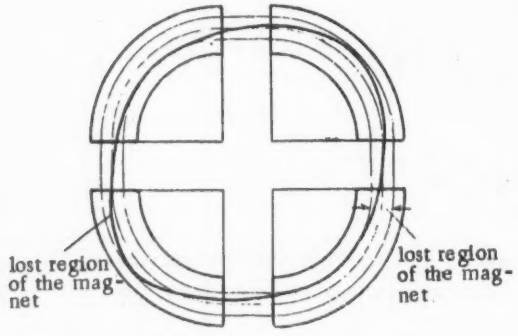

Fig. 1. A diagram indicating the operating region of the magnet which is unused due to distortion of the orbit.

Thus of all the solutions of Equation (15), we are interested only in those with period $N\sigma_0$:

$$\chi(\sigma) = -\frac{\varphi(\sigma)e^{i\mu N}}{B(1-e^{i\mu N})}\int_{\sigma}^{\sigma+N\sigma_0} q(\xi)\varphi(\xi)\,d\xi + \text{c.c.} \qquad (17)$$

Equation (17) is inconvenient for actual calculations, since it is difficult to use it to determine the danger of one or another kind of perturbation. Therefore (17) should be expanded either in a Fourier series or in a series of eigenfunctions of Equation (1). The advantage of the first of these expansions lies in the fact that we may use the developed methods of harmonic analysis, and the advantage of the second lies in the simplicity of the expressions obtained and in the direct relation to resonance theory. Since the eigenfunctions for the parameters of the A.S. USSR

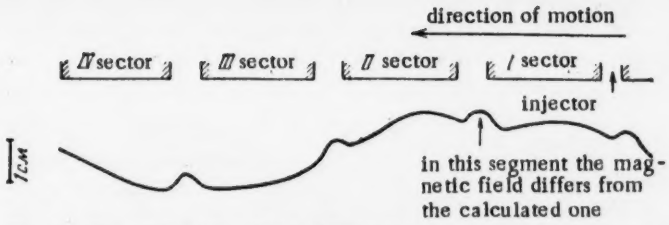

Fig. 2. The orbit with a field of 515 oersteds, calculated from magnetic measurements on the model of the A.S. USSR proton synchrotron.

proton synchrotron are not very different from harmonic functions, we may use either method.

We shall not present the calculated formulas here. It is more meaningful to perform a qualitative comparison of the result obtained with the result for a circular accelerator.

Let us expand the distortion of the magnetic field or of its median plane within the sectors in a Fourier series, and let us consider the first harmonic. In a circular accelerator the maximum distortion is proportional to the amplitude of the harmonic and to a resonance factor

$$\frac{1}{\varkappa^2_{res}-\varkappa^2}=\frac{1}{1-(1-n)}=\frac{1}{n} \quad \text{for vertical oscillations}$$

$$\frac{1}{\varkappa^2_{res}-\varkappa^2}=\frac{1}{1-n} \quad \text{for radial oscillations}$$

Since the rotational frequency is taken as unity, the first factor corresponds to resonance of radial oscillations with n = 0, and the second corresponds to resonance of vertical oscillations with n = 1.

In a circular accelerator these resonances happen to lie at the boundary of the stability region. In the case of linear sections, they move into the resonance region. For instance, in the A.S. USSR proton synchrotron, the resonance value for radial oscillations is $n_{res} = 0.16$, and that for vertical oscillations is $n_{res} = 0.84$. The resonance factors become

$$\frac{1}{0.84-(1-n)}=\frac{1}{n-0,16} \quad \text{for radial oscillations}$$

$$\frac{1}{0.84-n} \quad \text{for vertical oscillations}$$

In the operating part of the chamber

$$0.55<n<0.75.$$

Thus, in this proton synchrotron the effect of the first harmonic on distortion of the orbit due to linear sections is 30-40% greater than in the corresponding circular accelerator, and its influence on the distortion of the median plane is 2.8 times greater.

It is clear from this that it is unreasonable to choose linear sections greater than 8 m in length, since for a length of 12 m the magnitude of n_{res} is already of the order of 0.75. The effect of higher harmonics on the distortion of the orbit or the median plane decreases rapidly.

In Figure 2 we show the orbit of a particle in a 180 Mev model of the proton synchrotron, as calculated on the basis of magnetic measurements.

Resonance with Fast Oscillations

Resonance phenomena in accelerators with segmented magnets differ significantly from those in cyclic ac-

celerators. This difference can be noted first in the fact that certain resonance values of $\underline{n}$ are rather strongly displaced even for short linear sections. Figure 3 shows the dependence of the resonance value of $\underline{n}$ for ordinary resonance with vertical oscillations (discussed in the previous section) and for parametric resonance with radial oscillations on the length of the linear sections.*

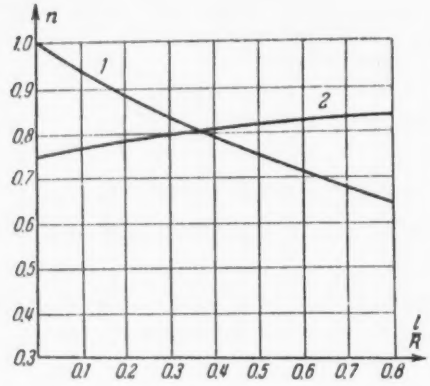

Fig. 3. The displacement of the resonance values of $\underline{n}$ as the length of the linear sections is increased: 1) n_{res} for vertical oscillations; 2) n_{res} for radial oscillations.

The second difference is the fact that in an accelerator with a segmented magnet, a whole set of harmonics in the Fourier expansion of the perturbation resonates simultaneously. This is explained by the fact that sine and cosine are no longer eigenfunctions of the problem.

A calculation of the resonances may be performed in the following way.

We shall write the equation of the oscillations in the form

$$\chi'' + \varkappa^2 [g(\sigma) + f(\sigma)]\chi = q(\sigma), \tag{18}$$

where the perturbations $q(\sigma)$ and $f(\sigma)$ are functions with period $N\sigma_0$ (q has period σ_0). Then instead of Equation (16), the constant D of Equation (4) is given by

$$\frac{dD_m}{d\sigma} = -[q - f\varkappa^2 (D_m e^{i\sum_0^m \mu_k} \psi(\sigma) + \text{c.c.})] \times \times \frac{\psi^*(\sigma)\, e^{-i\sum_0^m \mu_k}}{B}. \tag{19}$$

Let us integrate this equation over one element of periodicity σ_0, treating D_m as a constant on the right side. In order to simplify the notation, we shall provide the functions $\underline{q}$ and $\underline{f}$ with the index $\underline{m}$. Then q_m and f_m refer to the m-th element of periodicity, and we start counting σ from the beginning of this element:

$$D_{m+1} - D_m = = -\frac{e^{-i\sum_0^m \mu_k}}{B} \int_0^{\sigma_0} q_m \psi^* d\sigma + \frac{\varkappa^2 e^{-2i\sum_0^m \mu_k}}{B} D_m^* \times \times \int_0^{\sigma_0} f_m \psi^{*2} d\sigma + \frac{\varkappa^2}{B} D_m \int_0^{\sigma_0} f_m \psi\psi^* d\sigma = \frac{sI}{2i \sin \mu}; \tag{20}$$

Let us apply an averaging method to this difference equation. We then obtain the final equation of resonance theory (we have obtained more general equations [6, 8], taking into account damping of the oscillations, etc.):

$$D_{m+1} - D_m = \frac{sI_{av}}{2i \sin \mu}, \tag{21}$$

where the averaging is performed in the same way as in the method of averaging for differential equations.

For simplicity let us consider just one case.

*In the case of ordinary resonance we always have also parametric resonance.

Let the median plane (or the mean value of the magnetic field H) in different sectors be displaced by a distance Δz_m (or ΔH_m) and let n differ by Δn_m; then

$$f_m = \frac{\Delta n_m}{R_0^2 n}; \quad q_m = \frac{\pi^2 \Delta z_m}{R_0^2}; \quad \left(q_m = -\frac{\Delta H_m}{R_0 H}\right).$$

Example 1. If $\Delta z_1 = \Delta z_2 = a$; $\Delta z_3 = \Delta z_4 = -a$; $\mu_{k+1} - \mu_k = 2.5 \cdot 10^{-3}$, the amplitude F of vertical oscillations after passing through resonance (with $n = 0.84$) is almost 60 times greater than a.

Example 2. Let us take $q_m = 0$ ($f_m \neq 0$).

This case differs from the previous one in that here we have only parametric resonance. With $\mu = \pi/2$ ($n = 0.84$), there is resonance of the second harmonic of the field distortion with vertical oscillations, and with $\mu = \pi/4$ ($n = 0.79$), there is resonance of the first harmonic of the field distortion with radial oscillations.

In performing radial phase oscillations a particle may pass through a resonance region many times, and the point of maximum deviation may lie within the resonance region.

Let us consider some numerical results for resonance with $n = 0.79$ (and $\mu = \pi/4$).

If $\Delta n_1 = \Delta n_3 = h_0$; $\Delta n_2 = \Delta n_4 = -h_0$, then $D_m \leq D_0 e^{15h_0}$; since h_0 in the A.S. USSR proton synchrotron is no greater than 0.5%, while passing through resonance during injection D_m increases by 5-6%. Thus, if $\mu_{k+1} - \mu_k \approx 2.5 \cdot 10^{-3}$ or greater, the resonance being considered has practically no effect on the injection process.

This resonance plays an entirely different role during the acceleration period. If the amplitude of radial phase oscillations is so great that the instantaneous orbit falls into the resonance region, it is possible that oscillations will be gradually excited due to multiple transitions through resonance. In order to avoid such excitation, it is sufficient that the amplitude of oscillations decrease during one period of phase oscillations faster due to the increase of the magnetic field, than it increases while passing through resonance. If the pivot point for radial phase oscillations with amplitude $0.02\ R_0$ lies exactly in the resonance region, $R\frac{\partial n}{\partial R} \approx 100$, the particle energy $W_i = 10$ Mev, and the accelerating voltage is 6 kv, then $D_m \leq D_0 e^{32h_0}$.

In this case, the exponent is greater than in the previous one. This is as to be expected, since in our example the radial velocity at the resonance point changes direction. The particle orbit therefore remains in the resonance region for a relatively long time. If, however, we move 3 cm away from the resonance point, the exponent decreases by a factor of 16. Similar expressions are obtained also with $n = 0.84$ for parametric resonance between the second harmonic of the distortion of n and vertical oscillations.

It is seen from the above analysis that in the A.S. USSR proton synchrotron resonance excitation of free oscillations is possible both in the injection process and in the acceleration process, as well as in extracting the particles from the chamber. These resonances can be avoided, however, by giving definite tolerances for the magnetic field, as was done in the technical project for the A.S. USSR proton synchrotron.

Resonance with Slow Phase Oscillations

The fundamental concept in deriving the phase equations is the use of a coordinate system composed of the instantaneous orbits and their normals. The accelerating field is expanded in a series of traveling waves along the equilibrium orbit. This gives an equation which makes it possible to develop a relation between the fast oscillations, phase oscillations, gap oscillations, etc. The phase equation is found by averaging over the fast oscillations.

In relatively small accelerators the frequency ω_1 of the phase oscillations is much higher than ordinary engineering frequencies. In the A.S. USSR proton synchrotron the frequency $\omega_1/2\pi$ of phase oscillations varies between 2000 and 700 cycles. Oscillations with such frequencies can occur both in the magnetic field and in the frequency and amplitude of the accelerating voltage.

The danger of these resonances is related to the "softness" of the system, which follows from low natural frequencies of the phase oscillations.

Exciting oscillations in the injection process is particularly dangerous, since this may cause the number of

particles captured into accelerating orbits to be decreased significantly, by as much as a factor of 10.

The excitation of oscillations in the accelerating process is not in itself dangerous, so long as the particles remain within a region of stability. The scattering of particles to the boundaries of the stability region, however, leads to losses. Due to oscillations in H, V_0, etc., the section of the stability region close to its boundaries is "cleaned" of particles. It may thus happen that the resonance particles begin to oscillate and then are lost due to sufficiently sharp oscillations of H with a frequency of the order of 600 cycles. The most dangerous is resonance with oscillations of the magnetic field and the frequency of the accelerating field.

As an example, let us consider resonance excitation by the harmonics of the magnetic field.

The phase equation is of the form

$$\frac{d}{dt}\left(\frac{E}{\omega_0^2 k F_0}\frac{d\alpha}{dt}\right) - \frac{eV_0\cos(\varphi_0+\alpha)}{2\pi} = -\frac{eV_0\cos\varphi_0}{2\pi} + Q, \tag{22}$$

where E is the energy; ω_0 is the frequency of the accelerating field; $\varphi = \varphi_0 + \alpha$ is the phase of the accelerating field; $k = 1 + \frac{n}{1-n}\frac{1}{\beta^2}$; F_0 is a coefficient equal to $1 - \frac{L}{\beta^2(1-n)(2\pi R + L)k}$ and accounting for the linear sections; V_0 is the sum of all the accelerating voltages, and Q is the resonance force.

$$Q = \frac{eR_0(2\pi R_0 + L)}{\pi c} h\Omega\cos\Omega t, \tag{23}$$

where $h\sin\Omega t$ is the oscillating part (or one of the terms of the Fourier series) of the magnetic field.

The phase equation is nonlinear. Therefore the treatment of resonance phenomena is extremely complicated. The equation may be solved in the linear approximation. It is then easy to find the amplitude of additional phase oscillations:

$$\alpha_{\max}^{\text{lin}} = \sqrt{\pi}\,\frac{h}{H(1-n)(2\pi R_0 + L)}\,\frac{\sqrt{2\pi}\,R_0\omega_0}{\sqrt{\dot{\omega}_1}},$$

where ω_1 is the rate at which the frequency of phase oscillations changes.

If no special measures are taken (such measures are, in general, provided), resonance with the second harmonic with a frequency of 1200 cycles of the magnetic field oscillations is extremely dangerous (the fundamental frequency of 600 cycles is obtained from the rectification of the 50-cycle 12-phase alternating current).

At the resonance point $\omega_1 = -10^3\pi$ and $\alpha_{\max}^{\text{lin}} \approx 3\cdot 10^2 h_2$ (here h_2 is given in oersteds). Thus h_2 must be much less than 0.01 oersteds. The magnitude of h_2 (the amplitude of oscillations in the magnetic field) which will cause these serious perturbations, is a million times less than the fundamental field; however, the rate at which the rapidly oscillating part of the field $h_2\Omega$ varies is 50 times less than dH/dt. For resonance, it is not the amplitude of the magnetic field oscillations which is of importance, but the rate of variation. We need therefore not be surprised at the small value of h_2.

From this example it is also seen that even if $h_2 \sim 0.01$ oersteds, it is necessary to take account of the nonlinearity of the phase equation.

The existing methods of nonlinear mechanics make it possible to solve this problem, considering the nonlinearity to be small. The calculations are based on the methods of N.M. Krylov, N.N. Bogoliubov, and Iu.A. Mitropol'skii.

In the case of small nonlinearities, we cannot consider the transition of particles through the boundary of the region of stability, but we can obtain a significantly more accurate value for the amplitude of oscillations. The rate of passing through resonance in the A.S. USSR proton synchrotron is small, and therefore even a small nonlinearity changes the result greatly. Indeed, in the linear approximation the amplitude of phase oscillations $\alpha_{\max} \to \infty$ as $\omega_1 \to 0$.

In accounting for a small nonlinearity, the amplitude of the oscillations remains finite even for $\omega_1 = 0$. The physical reason for this is clear. As the amplitude of phase oscillations increases, the frequency decreases and the particle leaves resonance. Such a system is called (according to N.M. Krylov and N.N. Bogoliubov) actively nonlinear, as opposed to passively nonlinear systems in which the amplitude is unbounded in the absence of damping.

Of great importance here is the direction of passing through resonance. If the time dependence and amplitude dependence of the oscillation frequency act in a given direction $\left(\text{that is, if } \frac{\partial \omega_1}{\partial t} \cdot \frac{\partial \omega_1}{\partial \alpha_{max}} > 0\right)$, then the nonlinearity itself plays the role of an "effective friction."

We shall look for a solution of Equation (22) in the form

$$c = a\cos(\tau+\psi) - \frac{a^2}{4}\left[1-\frac{1}{3}\cos(\tau+\psi)\right]\cot\varphi_0 - \frac{a^3}{192}\cos 3(\tau+\psi),$$

where $\tau = \int_0^t \omega_1 dt$ (here ω_1 is the frequency of phase oscillations). We may consider $\underline{a}$ and ψ the amplitude and phase of the oscillations. In general $\underline{a}$ and ψ depend on time, with the exception of the case in which $\psi = \pm \pi/2$, and $\underline{a}$ satisfies the algebraic equation

$$a^3 - \frac{16(1-\xi)a}{1+\frac{5}{3}\cot^2\varphi_0} \mp \frac{16D}{(1+\xi)\left(1+\frac{5}{3}\cot^2\varphi_0\right)} = 0, \tag{24}$$

where the minus sign corresponds to the stationary phase $\psi = \pi/2$, and the positive sign corresponds to the stationary phase $\psi = -\pi/2$. The constant $D = \sqrt{\frac{2}{\pi}}\,\alpha_{max}^{lin}\frac{\sqrt{\dot{\omega}_1}}{\omega} \approx h$, where $\underline{h}$ is given in oersteds.

Here ξ is the ratio of the perturbation frequency Ω to the frequency ω_1 of small phase oscillations.

Equation (24) has three different real roots if

$$-\frac{16(1-\xi)^3(1+\xi)^2}{D^2\left(1+\frac{5}{3}\cot^2\varphi_0\right)} < -6.5. \tag{25}$$

If Condition (25) is not satisfied, there exists only one real root. If the inequality sign is replaced by an equality sign, we obtain the condition for the existence of one multiple and one simple real root.

The multiple root is

$$|a_{mult}| = \frac{1{,}6D^{1/3}}{\left(1+\frac{5}{3}\cot^2\varphi_0\right)^{1/3}}. \tag{26}$$

The simple root is

$$|a_{simple}| = 2|a_{mult}|.$$

Figure 4 shows the dependence of the amplitude $\underline{a}$ on the ratio between the perturbation frequency and the frequency of phase oscillations.

An analysis of the stability of the stationary solution leads to the following results. The upper branches of the curves in Figure 4 correspond to the stationary phase $\psi = \pi/2$, and are stable. Of the two lower branches (for the stationary phase $\psi = -\pi/2$) one is stable, and the other is unstable. The boundary between these regions is the point a_{mult}.

If ξ is increased in the A.S. USSR proton synchrotron, the point describing the operation moves along the

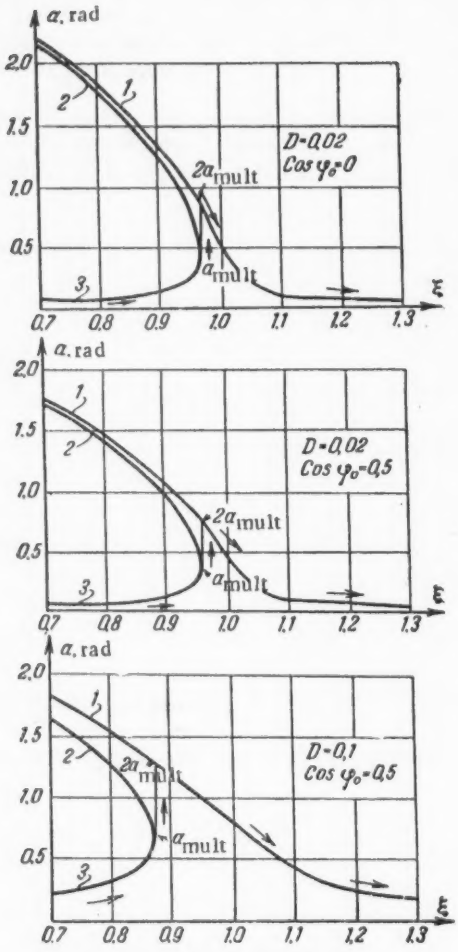

Fig. 4. Resonance curves for phase oscillations for various values of $\cos\varphi_0$ and the perturbation amplitude D, as a function of the ratio ξ of the perturbation frequency to the frequency of phase oscillations. 1) Upper stable branch; 2) lower unstable branch; 3) lower stable branch.

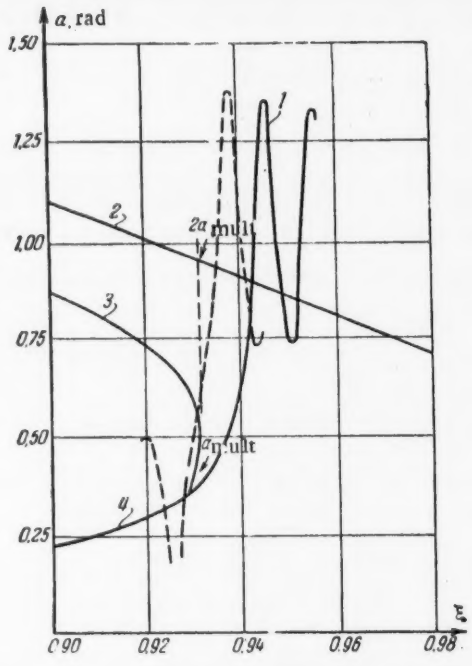

Fig. 5. The amplitude of phase oscillations for a slow change of the frequency of oscillation in the resonance region for two cases: the solid curve refers to an amplitude increasing from zero, and the dotted curve from $a_{init} \sim 0.2$; $D = 0.04$; $\cos\varphi_0 = 0.5$; $\delta = 0.0001$. 1) Resonance curve; 2) upper stable branch; 3) unstable branch; 4) lower stable branch.

lowest curve almost to the boundary of stability. The further behavior of this point can be considered only qualitatively, no matter how slowly the frequency of phase oscillations is changed.

Close to the boundary of stability, the amplitude of oscillations increases sharply and the point moves onto the upper stable branch. Since the transition is accomplished quite rapidly, the point no longer moves along the stationary curve, but oscillates about it. The final amplitude is greater than $2a_{mult}$ and less than $3a_{mult}$.

We note that the maximum amplitude is obtained when $\xi < 1$, which means that resonance "occurs" before the frequency of small phase oscillations becomes equal to that of the forced oscillations. The "displacement of resonance" increases with the perturbation.

These qualitative considerations can be verified by numerical integration of the equation with $D = 0.04$ and $d\xi/d\tau = 10^{-4} = \delta$. The initial conditions are chosen so that far from the resonance the amplitude of oscillation is equal to zero (that is, in agreement with the stationary curve). The result of integration is shown by the continuous curve in Figure 5. The case chosen by us corresponds to a large perturbation (the amplitude of oscillations according to the linear theory would be 5 rad). Therefore although the amplitude is found to be much smaller than in the linear case, it is almost equal to the limiting possible value.

If before resonance the particle was undergoing phase oscillations, then we cannot sum the oscillations in the linear case. This is illustrated in Figure 5 by the dotted curve obtained by numerical integration. Far from resonance the amplitude of oscillation is 0.2 rad. The increase of the amplitude in resonance comes about in an entirely different way and resonance "occurs" earlier, but the amplitude is hardly different from that obtained before. Thus a strong resonance levels all the amplitudes and "drives" the particle to the edge of the stability region.

We note that if the point describing the operation far from resonance were on the upper curve, instead of the resonance increasing the amplitude, it would decrease monotonically. In this case, however, in addition to the amplitude, the initial phase would also be of importance.

Comparison of the linear and nonlinear cases is most easily performed by comparing $2a_{mult}$ with α_{max}^{lin}.

$$2a_{mult} = \frac{3{,}2}{\left(1+\frac{5}{3}\cot^2\varphi_0\right)^{1/3}}\left(\frac{\dot{\omega}_1}{\omega_1^2}\right)^{1/6}\left(\alpha_{max}^{lin}\right)^{1/3}.$$

Thus, taking account of resonance allows us to reduce the tolerance on the magnitude of the field harmonics, etc. The A.S. USSR proton synchrotron was designed also to increase the rate at which the particles pass through resonance by rapidly changing V_0 (the accelerating voltage) in the region of resonant frequencies.

In addition to regular perturbations, an important role may also be played here by various noise-perturbations. This question has also been analyzed (only in the linear approximation), and definite tolerances have been established for the noise characteristics of the apparatus.

Injection

As is well known [2], a beam of 9 Mev particles travels a long distance through various magneto-electro-optical instruments and enters the chamber at the beginning of one of the quadrants. We shall consider here only the relation between the parameters of the beam entering the magnet and the injection efficiency, i.e., we shall calculate the number of particles captured into accelerating orbits.

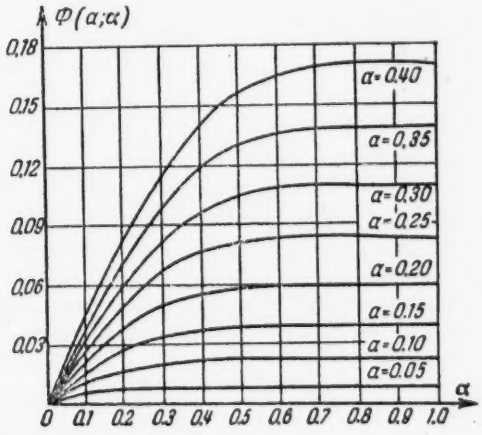

Fig. 6. A graph of $\Phi(a, \alpha)$ from Equation (31), according to M.S. Rabinovich [6].

If we knew the configuration of the magnetic field and the beam parameters, the problem would reduce essentially to calculating the orbit. We only know the tolerances in the magnetic field, and in the beam parameters. Therefore we must average over all allowable configurations and calculate the intensity of the beam of accelerated ions with an error less than a factor of 2.

A detailed analysis of the orbit made it possible to choose the following average motion. In a constant magnetic field, the particles injected into the chamber have on the average phases of free oscillation such that 50% of the particles are lost in the third revolution, and the rest in the sixth. Then in no case do we tolerate an error of more than 10-20%.

The beam enters the chamber with a homogeneous density and a thickness 2Δ and subtending an angle of $\pm \gamma_m$. The axis of the beam is displaced by an angle ϵ from the optimum direction.

The injection process is divided into two stages. First the accelerating voltage is turned off and the particles move in the alternating magnetic field in helical orbits. While the orbit has not moved from its initial position, there is a high probability that a particle will collide with the injector or the walls of the chamber. The fraction η_1 of the particles which do not collide with the injector or the chamber walls shall be called the particle capture

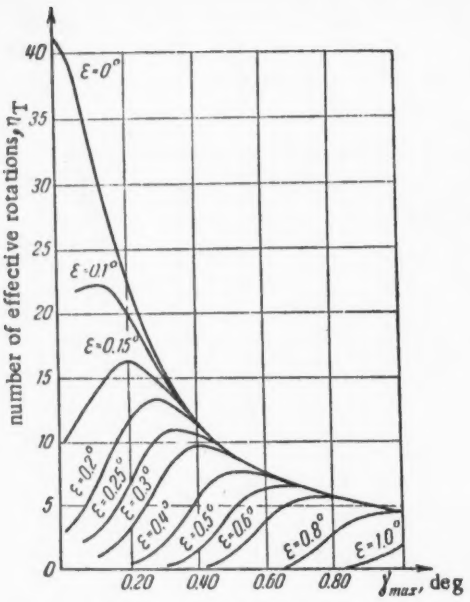

Fig. 7. The dependence of the number of effective rotations on the error in the admission angle ϵ and the horizontal divergence of the beam γ_{max}. $W_i = 10$ Mev; $\rho_i = 5$ cm; $dH/dt = 4000$ oersteds/sec; beam width 5 cm.

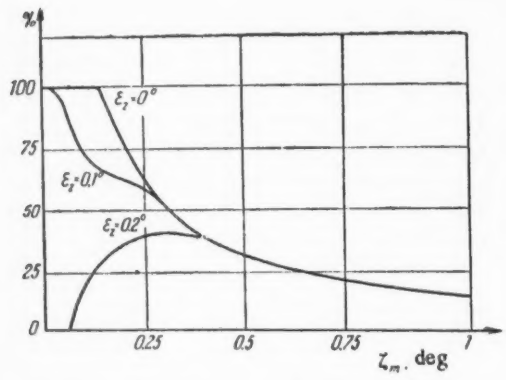

Fig. 8. The percent of the particles not colliding with the horizontal chamber walls for a given error in ϵ_z and a vertical divergence of ζ_m. D_z – vertical dimensions of the chamber. $2D_z = 25$ cm.

coefficient in the first stage of injection, and is given by

$$\eta_1 = \eta_\rho \cdot \eta_z, \tag{27}$$

where η_ρ is the probability that a particle will not collide with the injector, and η_z is the probability that a particle will not collide with a horizontal wall of the chamber.

In addition to the probability η_ρ, we shall calculate the number of effective rotations during the time of injection,

$$\eta_r = \eta_\rho \frac{\rho_1}{\Delta R}, \tag{28}$$

where ρ_i is the distance from the injector to the center of the chamber; ΔR is the pitch of the helical orbit of the particle ($\Delta R = 1.1$ cm for $W_i = 9$ Mev), and $\rho_i/\Delta R$ is the number of rotations of the helix during the first stage of injection.

When the orbit reaches the center of the chamber, the accelerating field is turned on. Of the particles captured in the first stage, only a fraction η_2 will be accelerated (this is the transient state coefficient). The remaining fraction of the particles ($1 - \eta_2$) either does not enter into the phase stability region and does not accelerate, or collides with the injector due to the excitation of radial phase oscillations.

The product of the coefficients $\eta_1 \cdot \eta_2$ shall be called the injection efficiency.

Let us introduce several dimensionless quantities:

$$\alpha = \frac{R_0 \Phi(\sigma_i)}{\rho_i}, \tag{29}$$

where α is the angle at which the particle is emitted, and $\Phi(\sigma_i)$ is given by Equation (9). The dimensionless angle varies between α_1 and α_2 ($\alpha_1 > \alpha_2$). The angle α between the beam axis and the optimal direction shall be denoted α_ϵ. Let us also write

$$a_1 = \frac{3\Delta R}{\rho_i}; \quad a_2 = 2a_1. \tag{30}$$

Then

$$\eta_r = \frac{\rho_i}{4\Delta R \cdot \bar{o} \cdot \alpha_{max}} \sum_{i=1}^{2} \sum_{k=1}^{2} [\Phi(a_i, \alpha_k) - \Phi(\bar{a}_i, \bar{\alpha}_k)], \tag{31}$$

where $\alpha_{max} = \frac{\alpha_1 - \alpha_2}{2}$, $\bar{o} \cdot \rho_i$ is the width of the particle beam, and $\Phi(\underline{a}, \alpha)$ is the function illustrated in Fig. 6.

Figure 7 shows a family of curves for η_T, which are typical for the A.S. USSR proton synchrotron. From these curves one sees the tolerance in the particle injection necessary to obtain almost 100% capture of the particles. These same curves show, however, that for stable and reliable capture, especially during tuning up, it is useful to have a beam with some angular aperture. In this case the number of particles captured is reduced, but the result will depend less critically on the parameters of the injection apparatus.

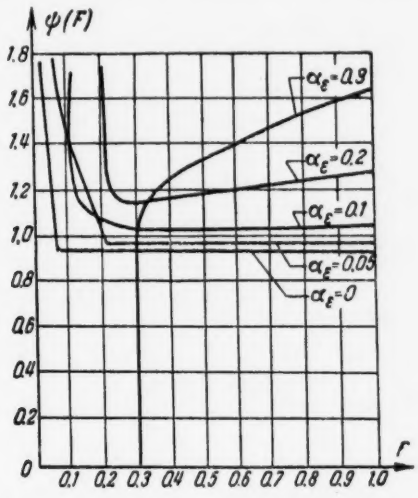

Fig. 9. The amplitude distribution function for a parallel beam after the first stage of injection.

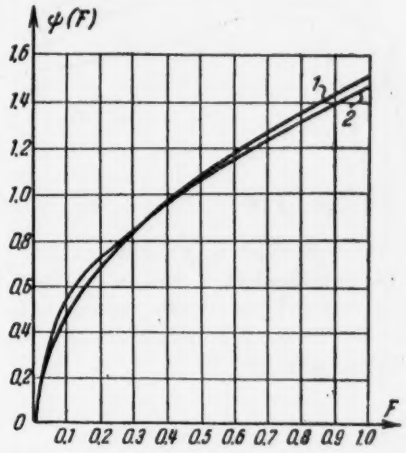

Fig. 10. The amplitude distribution function after the first stage of injection for a wide beam with a large angular aperture ($a_1 = 0.1$; $a_2 = 0.3$; $\bar{o} \geq 0.3$). 1) According to the approximate Equation (32); 2) according to the exact Equation (62) of Reference [6].

In order to calculate the capture coefficient in the first stage, we must also take account of collisions with the horizontal chamber walls, which means that we must calculate η_z (Figure 8).

Let us now consider the amplitude distribution of the particles after the first stage. Consider a parallel beam whose axis deviates from the optimum direction by an angle α_ϵ. The amplitude distribution of the particles is shown in Figure 9. We shall assume approximately that in this case the distribution is homogeneous if $F = \rho_{max}/\rho_i > \alpha_\epsilon$ (where ρ_{max} is the amplitude of oscillations, and ρ_i is the distance from the injector to the center of the chamber) and that the distribution function $\psi(F)$ vanishes for $F < \alpha_\epsilon$.

In this approximation we somewhat decrease the number of particles with small amplitudes of oscillation for very small α_ϵ, and increase this number for large α_ϵ.

If the beam has a large divergence angle, the amplitude distribution is given with sufficient accuracy by the equation

$$\psi(F)\,dF = \frac{3}{2}\sqrt{F}\,dF. \tag{32}$$

Figure 10 gives a comparison of the exact and approximate amplitude distribution functions.

During the second state of injection there arise radial phase oscillations. In order that particles which miss the injector in the first stage of injection fail to collide with it again, the condition

$$F + \frac{\rho_\varphi}{\rho_i} < 1, \tag{33}$$

must be satisfied, where ρ_φ is the amplitude of the radial phase oscillations, which is uniquely related to the phase oscillations. To the amplitude ρ_φ correspond two phases $\varphi_2 > \varphi_0$ and $\varphi_1 < \varphi_0$, between which the phase

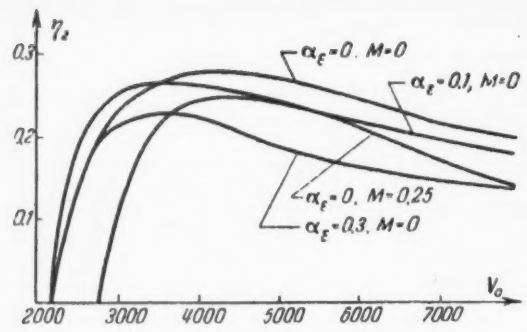

Fig. 11. The coefficient η_2 (the transient state coefficient) for a parallel beam with an angular uncertainty α_ε and an error M in the instant at which the field is turned on. V_0 is the amplitude of the accelerating field in volts.

Values of the Coefficient $\bar{\eta}_2$ (in percent)

Distance to injector		ρ_i=50 см						ρ_i=30 см			
Multiplicity	q	1		3		5		1		5	
The form of the function	$\psi(F)$	1	2F	1	2F	1	2F	1	2F	1	2F
Distribution in energy, %	0	23	—	30	—	34	--	—	—	—	—
	0.5	19	11	25	—	28	16	14	7	—	13
	1	13	7	17	—	18	10	10	5	—	8

oscillations take place. The magnitude of the phase oscillations $\varphi_2 - \varphi_1$ is a unique function of $\rho_\varphi/\bar{\rho}$, where $\bar{\rho}$ is the maximum possible amplitude of phase oscillations corresponding to motion at the boundary of the region of stability,

$$\bar{\rho} = R_0 \sqrt{\frac{eV_0 \sin\varphi_0 (1-\varphi_0 \operatorname{ctg}\varphi_0)}{\pi W_i n (1-n)\left[1-\frac{L}{n(2\pi R_0+L)}\right]}} \quad (34)$$

for $\beta^2 \ll 1$;

$$\varphi_2 - \varphi_1 = 2\pi\varepsilon\left(\frac{\rho_\varphi}{\bar{\rho}}\right). \quad (35)$$

The function $\varepsilon(\rho_\varphi/\bar{\rho})$ is given graphically, or by the approximate expression

$$\varepsilon\left(\frac{\rho_\varphi}{\bar{\rho}}\right) \approx \frac{2(1-\varphi_0\cot\varphi_0)^{1/2}\rho_\varphi}{\pi\bar{\rho}}\left[1+0{,}3\left(\frac{\rho_\varphi}{\bar{\rho}}\right)^2\right]. \quad (36)$$

At the beginning of the second stage of injection one of the following errors may arise; either the accelerating field is not turned on at the right time, or the energy of the beam (or the initial frequency of the accelerating field) has the incorrect value. In practice these two errors lead to the same result. If the beam of particles is not monoenergetic, then it is clearly impossible to turn on the high frequency voltage at the correct time for all the particles.

Let us assume that at the time when the accelerating field is turned on the instantaneous orbit is displaced from the mean orbit (by definition, the frequency of rotation on the mean orbit is equal to the frequency of the accelerating field) by a distance equal to $\rho_i M$. The value of M is related to the uncertainty in the energy ΔE_i by the expression

$$\rho_i M = R_0 \frac{\Delta E_i}{2(1-n)W_i} \quad (37)$$

or to the uncertainty Δt in the instant at which the field is turned on by the expression

$$\rho_i M = R_0 \frac{\dot{H}_i \Delta t}{H_i (1-n)}, \quad (38)$$

where H_i and $\dot{H}_i$ are the magnetic field and its time derivative at the instant of injection.

An uncertainty $\Delta\omega$ in the initial frequency will displace the mean orbit from which the calculations are performed by an amount

$$\rho_i M = R_0 \frac{\Delta\omega(2\pi R_0+L)}{\omega_0[n(2\pi R_0+L)-L]}. \quad (39)$$

According to the phase equation, the amplitude ρ_φ of radial phase oscillations is given by the initial phase φ_{init} and initial rate of change of the phase $\dot{\varphi}_{init}$ (or by the initial radial displacement $\rho_i M$):

$$\left[\left(\frac{\rho_\varphi}{\bar{\rho}}\right)^2 - \left(\frac{M\rho_i}{\bar{\rho}}\right)^2\right] = \frac{\sin\varphi_0 - \sin\varphi_{init} - (\varphi_0 - \varphi_{init})\cos\varphi_0}{2(\sin\varphi_0 - \varphi_0\cos\varphi_0)}. \tag{40}$$

As can be seen from Equation (40), φ_{init} is a many-valued function of $\left[\left(\frac{\rho_\varphi}{\bar{\rho}}\right)^2 - \left(\frac{M\rho_i}{\bar{\rho}}\right)^2\right]^{1/2}$. From Equation (40) we can find the two values $\varphi_{init\,1}$ and $\varphi_{init\,2}$ which have the smallest absolute value, form the combination $\varphi_{init\,2} - \varphi_{init\,1}$, and calculate the function

$$\varphi_{init\,2} - \varphi_{init\,1} = 2\pi\varepsilon_M\left(\sqrt{\frac{\rho_\varphi^2}{\bar{\rho}^2} - \left(\frac{M\rho_i}{\bar{\rho}}\right)^2}\right). \tag{41}$$

It is clear that the function ϵ_M differs from ϵ, as defined in (36), only in its argument.

According to Equations (40) and (41), $\varphi_{init\,2} - \varphi_{init\,1}$ is the dimension of the region of the initial phases in which for a given M the amplitude of radial phase oscillations is less than or equal to ρ_φ, and $\frac{\varphi_{init\,2} - \varphi_{init\,1}}{2\pi}$ is the fraction of particles with such phases. Therefore the fraction of particles with amplitudes between ρ_φ and $\rho_\varphi + d\rho_\varphi$ is given by

$$\frac{d\varepsilon_M}{d\rho_\varphi}\,d\rho_\varphi. \tag{42}$$

In the second stage, only those particles of this fraction will be captured whose amplitude of free oscillations fulfills the condition $\rho_{max} < \rho_i - \rho_\varphi$. If $\psi(F)$ is the amplitude distribution function of free oscillations, the fraction of particles satisfying this inequality is

$$\int_0^{1-\rho_\varphi/\rho_i} \psi(F)\,dF. \tag{43}$$

Multiplying (42) and (43) and integrating over all possible ρ_φ, we obtain the capture coefficient in the first stage of injection, namely

$$\eta_2 = \int_0^{\bar{\rho}} \frac{d\varepsilon_M}{d\rho_\varphi}\,d\rho_\varphi \int_0^{1-\rho_\varphi/\bar{\rho}} \psi(F)\,dF. \tag{44}$$

Let us interchange the order of integration in Equation (44), and integrate over ρ_φ, obtaining

$$\eta_2 = \int_0^{1-M} \varepsilon_M\left(\frac{\rho_i}{\bar{\rho}}\sqrt{(1-F)^2 - M^2}\right)\psi(F)\,dF. \tag{45}$$

Equation (45) is simpler, but it can be used to find the amplitude distribution function for radial phase oscillations after the second stage of injection; Equation (44) also gives the amplitude distribution function for free oscillations after the second stage of injection. If different particles have different values of M (different energies) with an energy distribution $\psi_M(M)$, the coefficient becomes

$$\bar{\eta}_2 = \int_0^{M_{max}} \eta_2 \psi_M dM, \tag{46}$$

Figure 11 shows graphs of η_2 for various values of α_ϵ and M. If the particles have a distribution in energies, the integration in Equation (46) for large injection angles [see Equation (32)] is quite complicated, and therefore in performing the calculations we use the distribution

$$\psi(F) = 2F, \tag{47}$$

instead of Equation (32), which reduces the value of $\bar{\eta}_2$ somewhat.

In using a multiple acceleration method with a frequency q times higher than the frequency of rotation, all the formulas remain valid if $\bar{\rho}$ in Equation (34) is replaced by a quantity $q^{1/2}$ times smaller.

The table gives the maximum value of $\bar{\eta}_2$ for an injection energy $W_i = 10$ Mev, a uniform energy distribution, and two values of ρ_i.

Thus, for $q = 1$, the maximum value of $\bar{\eta}_2$ is of the order of 25%.

We have briefly considered several theoretical problems of importance for the A.S. USSR proton synchrotron as well as for any other high-energy proton synchrotrons. The calculation performed makes it possible to choose parameters and tolerances which will assure its normal functioning. The theoretical methods developed were found to be convenient for calculations of accelerators.

Certain important theoretical questions are only mentioned here, and others are entirely neglected (for instance the problem of beam extraction, injection optics, etc.). We hope, however, that the present review will give some idea of the theoretical problems solved in developing the A.S. USSR proton synchrotron.

In conclusion, I consider it my pleasant duty to express my gratitude to V.I. Veksler, A.A. Kolomenskii and V.A. Petukhov for discussion of the problems considered.

LITERATURE CITED

[1] V.I. Veksler, A.A. Kolomenskii and M.S. Rabinovich, Physical Basis for the Design of the 10 Bev Proton Synchrotron (Report to the All-Soviet Conference on High-Energy Particles) Moscow, 1956.

[2] V.I. Veksler, D.V. Efremov, A.L. Mints, M.M. Veisbein, F.A. Vodonianov, M.A. Gashev, A.I. Zeidlits, P.P. Ivanov, A.A. Kolomenskii, E.G. Komar, I.F. Malyshev, N.A. Monoszon, I.Kh. Neviazhskii, V.A. Petukhov, M.S. Rabinovich, S.M. Sinel'nikov and A.M. Stolov, J. Atomic Energy 4, 22 (1956).

[3] M.S. Rabinovich and V.V. Mikhailov, An Investigation of Particle Motion in Proton Synchrotrons with Linear Segments, Report of the Phys. Inst. Acad. Sci. USSR, 1949.

[4] M.S. Rabinovich, A.M. Baldin and V.V. Mikhailov, On the Theory of Free Oscillations in an Accelerator with Linear Segments, Report of the Phys. Inst. Acad. Sci. USSR, 1950 (see also J. Exptl.-Theoret. Phys. 31, 993, 1956).

[5] M.S. Rabinovich, Theory of the Proton Synchrotron, RPIAS USSR, 1947.

[6] M.S. Rabinovich, Fundamental Theory of a Proton Synchrotron with a Segmented Magnet, Dissertation PIAS USSR, 1952.

[7] V.V. Mikhailov, The Influence of the Magnetic Field in the Gap on Particle Motion, RPIAS USSR, 1949.

[8] M.S. Rabinovich, A Theoretical Investigation of Resonance Phenomena in Accelerators, RPIAS USSR, 1952.

[9] A.M. Baldin and V.V. Mikhailov, Nearly Periodic Motion of Charged Particles in an Arbitrary Time-Independent Magnetic Field, RPIAS USSR, 1952.

[10] M. S. Rabinovich, A Theoretical Investigation of an Accelerator with a Variable Magnetic Field, RPIAS USSR, 1952.

Received August 6, 1956

THERMODYNAMICS OF THE EXTRACTION EQUILIBRIA FOR URANYL NITRATE

A.M. Rozen

The fundamental thermodynamic principles of the extraction equilibria for uranyl nitrate are examined. The equilibrium characteristics are associated with considerable nonideality of the aqueous phase – a strong electrolyte, and the organic phase -a practically undissociated nonelectrolyte.

It is shown that, at ionic strengths of up to 10, ion association in the aqueous phase does not significantly influence the distribution of uranyl nitrate. It is noted that in most instances the solutions of uranyl nitrate in the organic phase are close to regular solutions, and therefore there is no need to postulate solvation in the organic phase for interpretation of the equilibria. The effect of a salting out agent on the activity coefficient γ at constant concentration $\underline{x}$ of the latter is examined. It is shown that the relationship between $\gamma_{(x, m)}$ and the concentration of the salting out agent $\underline{m}$ is determined by the ratio of the Harned coefficient δ_V for the salting out agent to a quantity δ_e, characteristic for uranyl nitrate: $\log \gamma_{(x, m)}/\gamma_{(x,0)} = 2(\delta_U - \delta_S)J_S$, where $\gamma_{(x,0)}$ is the activity coefficient of uranyl nitrate in the absence of a salting out agent, and J_S is the ionic strength of the salting out agent. If $\delta_S < \delta_U$, then addition of salting out agent raises γ, and conversely; when $\delta_S = \delta_U$ (ammonium nitrate), γ is practically independent of the concentration of salting out agent. The value of δ_S decreases and the salting out agent becomes more effective with increasing number of molecules hydrating the cation. Equivalents of the salting out agents differ from chemical equivalents by activity coefficient corrections, and they can be only approximately constant.

The variation of the distribution coefficient with the degree of dilution or saturation of tributyl phosphate in extraction by mixed solvents, and the conditions of mutual displacement of the substances being extracted from the organic phase are examined. The role of nonideality of tributyl phosphate – dilutent solutions in the extraction of uranyl nitrate is demonstrated.

The parameters which determine the distribution of uranyl nitrate when different solvents and salting out agents are used are the distribution constant $\underline{k}$, the nonideality constant of the solvent λ, and δ_S. The most important parameter is the distribution constant $\underline{k}$, which varies several 1000-fold for different solvents. It is shown that the distribution curves have three characteristic regions, the extents of which depend on the value of $\underline{k}$ and the nonideality constant of the solvent λ.

1. Starting Principles

The basic characteristics of extraction equilibria of uranyl nitrate may be explained on the assumption that in the aqueous phase the salt is dissociated, while in the organic phase it is present as undissociated molecules, i.e.,

$$UO_2^{++} + 2NO_3^- \rightleftarrows UO_2(NO_3)_2, \qquad (1)$$

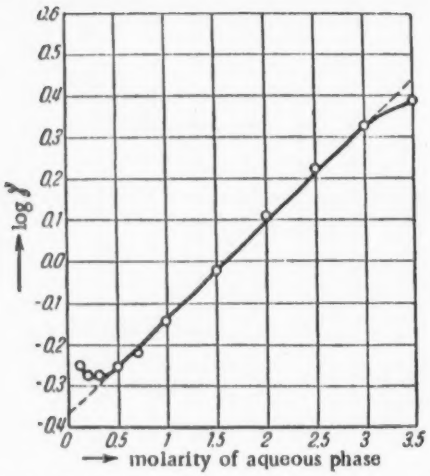

Fig. 1. Activity coefficient of uranyl nitrate in the aqueous phase from McKay's data [10].

and hence, by the law of mass action,

$$k = \frac{[UO_2(NO_3)_2]_{org}}{[UO^{++}][NO_3^-]^2}$$

and

$$[UO_2(NO_3)_2]_{org} = k[UO_2^{++}][NO_3^-]^2, \qquad (2)$$

where the square brackets indicate the activities of the molecules or ions.

Equations (1) and (2) should be regarded as the physicochemical interpretation of the thermodynamic distribution law for nonideal systems

$$a_{org}/a_{aq} = k, \qquad (3)$$

where a_{org} and a_{aq} are the activities of the salt in the organic and aqueous phases, and k is the distribution constant.

The activity of an electrolyte $K_\nu A_\mu$, giving (in this instance, in the aqueous phase) ν K^+ cations and μ A anions, is given by the expression

$$a_{aq} = [K]^\nu [A]^\mu = (K)^\nu \gamma_+^\nu (A)^\mu \gamma_-^\mu = (K)^\nu (A)^\mu \gamma^{\nu+\mu}, \qquad (4)$$

where (K) and (A) are the concentrations of the K and A ions, γ_+ and γ_- are their activity coefficients, $\gamma = \gamma_\pm$ is the average molar activity coefficient: $\gamma^{\mu+\nu} = \gamma_+^\nu \gamma_-^\mu$ (the average coefficient is introduced as it is impossible to determine the true activity coefficients of the ions).

In our case $\nu = 1$, $\mu = 2$, $K = UO_2^{++}$, $A = NO_3^-$, so that

$$a_{aq} = [UO_2^{++}][NO_3^-]^2 = (UO_2^{++})(NO_3^-)^2\gamma^3, \qquad (4a)$$

which is equivalent to Equation (2), since it follows from (3) that $a_{org} = ka_{aq}$. It is not necessary for the dissociation to be actually complete; Equations (4) and (4a) are, in fact, formal definitions of the activity coefficient γ: the activity a_{aq} is determined directly from experimental data, while γ is calculated from Equation (4a).

Thus the activity coefficients fully take into account all the effects which complicate the behavior of the aqueous phase – electrostatic interaction of the ions, association, etc.

The activity of uranyl nitrate in the organic phase can also be expressed as the product of the concentration (y, moles/liter) and the activity coefficient γ_e

$$a_{org} = [UO_2(NO_3)_2]_{org} = y\gamma_e. \qquad (5)$$

With (4a) and (5) taken into account, the Equation (2) for the distribution isotherm takes the form

$$y = kx(NO_3)^2\gamma^3/\gamma_e, \qquad (6)$$

where $x = (U) = [UO_2(NO_3)_2]$ is the concentration of uranyl nitrate in the aqueous phase.

The distribution coefficient will then be

$$\alpha = \frac{y}{x} = k(NO_3)^2\gamma^3/\gamma_3. \qquad (7)$$

If uranyl nitrate is the sole source of nitrate ions, then $(NO_3) = 2x$, and the distribution equation becomes

$$y = 4kx^3\gamma^3/\gamma_e. \tag{8}$$

In this case $\alpha \sim x^2$ and at low concentrations of uranyl nitrate the distribution coefficient tends to zero.

If a salting out agent is added to the aqueous phase, the concentration of NO_3 ions will increase: $(NO_3) = 2x + lm$, where l is the valency of the salting out agent and m_s is its concentration in moles/liter. The values of γ and of the distribution coefficient correspondingly increase; the latter no longer tends to zero with decreasing concentration of uranyl nitrate: when $x = 0$, $\alpha = kl^2m_s^2\gamma^3$.

Thus the action of salting out agent in the first instance is to increase the concentration of NO_3 ions in the solution (in addition, the activity coefficient of uranyl nitrate is changed; see below).

It must be pointed out that thermodynamic interpretation of extraction equilibria is often made difficult by lack of data on activity coefficient. However, the case of uranyl nitrate is relatively favorable: the activity coefficients of this salt in aqueous solution (Figure 1) have been determined [1] and subsequently revised several times [3]. If other nitrates (salting out agents, nitric acid) are present in the aqueous phase, their effect on the activity coefficient can be estimated by means of the modern theory of mixed electrolytes (Harned's rule [3, 4, 9]).

No information of any kind is available on activity coefficients in the organic phase; these coefficients can be found from the extraction equilibria with subsequent interpretation.

In particular, if it is known that a salt is extracted into an organic solvent with a definite number of water molecules n, and is solvated by q molecules of the solvent S, these effects can be taken into account directly. The extraction equation then assumes the form

$$UO_2^{++} + 2NO_3^- + nH_2O + qS \rightleftarrows UO_2^{++} + 2NO_3^- \tag{9}$$

and instead of Equation (6) we have•

$$y = kx\,(NO_3)^2\gamma^3 a_{H_2O}^n\,(S)^q/\gamma_e', \tag{10}$$

where a_{H_2O} is the activity of water, (S) is the volume concentration of the free solvent (not bound in the solvate), γ'_e is the activity coefficient which takes into account the residual nonideality of the organic phase. In other words, in this case

$$a_{org} = y\gamma_e = \frac{y\gamma_e'}{a_{H_2O}^n\,(S)^q}, \text{ i. e. } \gamma_e = \frac{\gamma_e'}{a_{H_2O}^n\,(S)^q}. \tag{11}$$

There is no sense in introducing corrections for hydration and solvation unless they represent a considerable part (90-100%) of the nonideality of the organic phase.

2. Some Literature Data

Several investigations [2, 5-14] have dealt with extraction equilibria of uranyl nitrate and their thermodynamic interpretation, the most important being those published by Glueckauf, McKay and others [2, 5-11]. In particular, it has been shown [5] that uranium enters most solvents (diethyl ether, methyl isobutyl ketone, cyclohexanone, etc.) with four molecules of water (n = 4); the paper [2] gives the distribution constants k and activity coefficients γ_e for a number of solvents.

To determine k it is necessary to compare Equation (8) with experimental data.

It must be remembered that activity coefficients of electrolytes greatly vary with the salt concentration (Figure 1). Therefore Equations (1-6) cannot be used even at high dilutions without taking γ into account. This is illustrated by Figure 2, in which the logarithms of the equilibrium concentrations of uranium in the aqueous and ether phases are plotted, for diethyl [2, 12] and dibutyl [2] ethers.

•It is possible to allow for solvation by the single term $(S)^q$ if all the extracted nitrate is in solvated form. The equation in Paper [2] differs from (10) in that only one of the terms γ_e or $(S)^q$ is introduced, as the authors assume that solvation is the sole cause of nonideality of the solution in the organic phase.

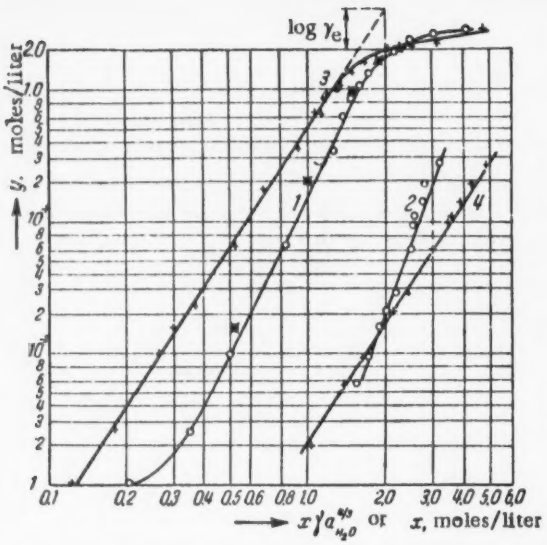

Fig. 2. Comparison of Equation (8) with experimental data. 1,3) Diethyl ether; 2,4) dibutyl ether; 1 and 2) with γ ignored; 3,4) with γ taken into account; O) data from [2]; ■) data from [12]; +) recalculated values.

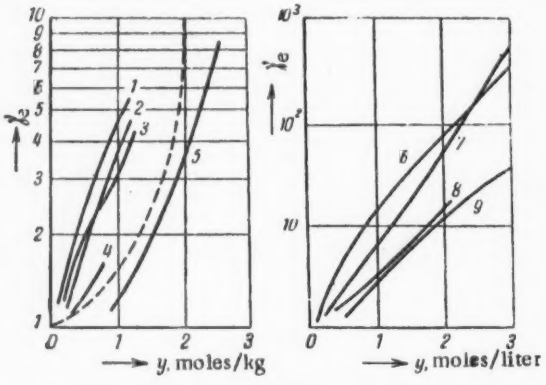

Fig. 3. Activity coefficients of uranyl nitrate in organic phases from the data in [2]. 1) Dibutyl cellosolve; 2) isoamyl acetate; 3) dibutyl carbitol; 4) diisopropyl ether; 5) diethyl ether; 6) cyclohexanone; 7) penta-ether; 8) methyl isobutyl ketone; 9) diethyl cellosolve; broken line represents γ_e in formation of solvate and for S/q = 2.

If γ = const, it follows from Equation (8) that $\log y = 3 \log x + C$, i.e., that the data, plotted in logarithmic coordinates, should fit on a straight line of slope factor 3. As Figure 2 shows, Curves 1 and 2, with the activity coefficients not taken into account, are not satisfactorily linear, and individual linear regions have slope factors different from 3. A different result is obtained if the activity coefficients for the uranium and water are used [2], $\log x\gamma a_{H_2O}^{4/3}$ being taken along the abscissa axis. Curves 3 and 4 then become linear, and have the theoretical slope factor of 3.

At high uranium concentrations in the organic phase the experimental curves in Figure 2 deviate from linearity. This is the result of nonideality of the solution in the organic phase – increase of the activity coefficient γ_e. The latter can be easily found from Figure 2, from the deviation from linearity, in the form of the difference $\Delta \log y = \log y - \log y_0 = \log \gamma_e$ (the values of $\log y_0 = \log x\gamma a_{H_2O}^{4/3}$ are found by linear extrapolation). Figure 3, taken from the paper [2], shows that the nonideality of the organic phase is very great; at high uranium concentrations the activity coefficients may reach 10^3.

The values of the activity coefficients may be determined more precisely [6-8], if it is taken into account that the organic solvent is dissolved in the aqueous phase, with a corresponding lowering of γ and a_{H_2O}

$$\gamma^3 a_{H_2O}^4 = \gamma_0^3 (a_{H_2O})_0^4 \cdot \psi,$$

where the subscript 0 refers to the pure aqueous solution. The correction factor ψ differs appreciably from 1.0 for diethyl ether. Thus, for x = 1.5 moles/liter, ψ = 0.92, and for x = 2.0 moles/liter, ψ = 0.75. For other solvents (less soluble in water) the correction is considerably less, and may be neglected in a number of cases.

The amount of water extracted together with the salt has also been determined more accurately [6, 7]. For many solvents the assumption that uranium in the organic phase is hydrated by n molecules of water, and the resultant simple relationship $m_{H_2O} = m_0 + nx$, $\gamma_e = \gamma'_e / a_{H_2O}^n$ (m_{H_2O} is the amount of water extracted into the organic solvent, in moles/liter) proved to be only a rough approximation. It was found [7] that $m_{H_2O} = m_0 + Ax + \frac{1}{2}Bx^2$ (where m_0 is a constant); this led to replacement of $a_{H_2O}^n$ in the equilibrium equation by $a_{H_2O}^{f - \beta y}$, where, for different solvents, f = 3.4-5.2 (f depends on $a_{H_2O}^4 \gamma^3$).

The influence of the concentration of the salting out agent on the activity coefficient of uranium has also been examined [9]. It was found that, for the same ionic strength of the solution, the activity coefficients differ in presence of different salting out agents (Figure 4), and their behavior may be represented with the aid of the Harned rule

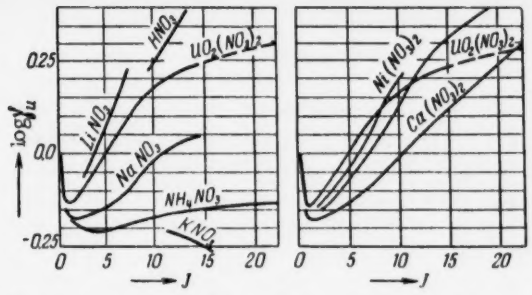

Fig. 4. Variation of the activity coefficients of uranyl nitrate (at tracer concentrations) with the ionic strength of the solutions (different salting out agents), from [9].

$$\frac{1}{2}\left[\log\gamma_{(x_1,\ s)} - \log\gamma_{(x_2,\ 0)}\right] = -\delta_s J_s, \qquad (12)$$

where $\gamma_{(x_1,\ m_s}$ is the activity coefficient in presence of moles of salting out agent; $\gamma_{(x_2,\ 0)}$ is the activity coefficient in absence of salting out agent, but for the same total ionic strength of the solution; and J are the concentration and the ionic strength of the salting out agent; δ_s is a coefficient which depends on the total ionic strength of the solution and on the nature of the salting out agent; we shall term it the Harned coefficient.

The values of δ_s, given in the paper [9] are shown in Figure 5; Figure 4 gives values of $\gamma_{(0,\ m_s)}$.

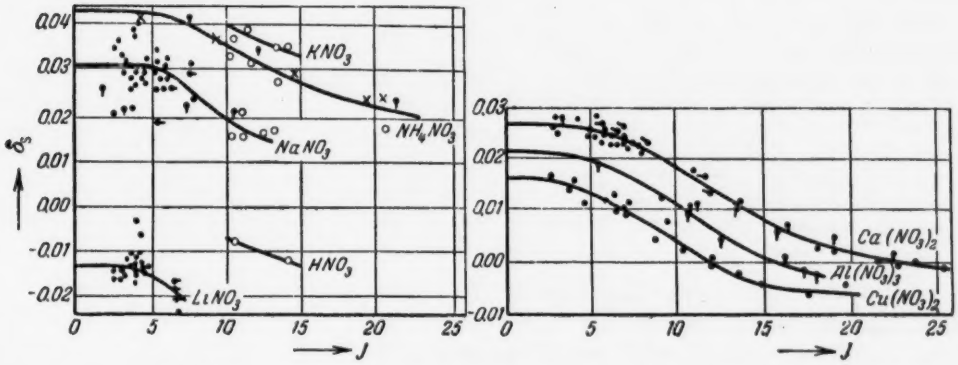

Fig. 5. Harned coefficients δ_s for various salting out agents in relation to the ionic strength, from the data in paper [9]. (x are values of δ_U calculated by the author).

3. Effect of Ionic Association on the Distribution of Uranyl Nitrate

It is still not clear to what extent association (or incompleteness of dissociation) influences the distribution of uranyl nitrate.

Several authors [15, 16] conclude from pH determinations and spectroscopic studies that association (formation of $UO_2NO_3^+$ ions) occurs, and that the stoichiometric association constant of the complex $k_s = 0.3$-0.5. As against this, spectroscopic determinations did not reveal association at UO_2 concentrations up to 0.1 mole/liter with 150-fold excess of nitrate ions [17].

It has also been stated [1] that the course of the activity coefficients indicates complete dissociation of uranyl nitrate in aqueous solution. It appears of interest to consider this question in rather more detail, especially as decisive importance is often attributed to association and formation of various complexes in extraction equilibria [18].

Since incompleteness of dissociation is automatically taken into account in the activity coefficients, it is necessary to determine whether the observed behavior of the activity coefficient of uranyl nitrate in the aqueous phase can be explained by incomplete dissociation.

Let us assume that deviations from ideality are caused by association only, and let us calculate the activity coefficients on this assumption. The calculation is simplest if the association proceeds according to the equation $UO_2^{++} + 2NO_3^- \rightleftharpoons UO_2(NO_3)_2$, so that

$$[UO_2][NO_3]^2/[UO_2(NO_3)]^+ = k_g.$$

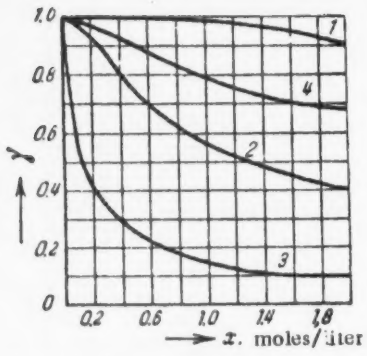

Fig. 6. Activity coefficient of uranyl nitrate in the aqueous phase, calculated on the assumption that nonideality of the solution is caused by ionic association. 1,2,3) formation of undissociated molecules; k_g = 100; 1.6; 0.016; 4) formation of the complex UO_2NO_3, k_s = 0.3; x) uranium concentration.

Let the degree of association be

$$\beta\ (\beta = [UO_2(NO_3)_2]/(UO_2)),$$

and it is then easy to show that the distribution equation takes the form $y = kx^3(1-\beta)^3/\gamma_e$. Comparing this with (6a), we have $\gamma = 1 - \beta$, where $\beta/(1-\beta)^3 = x^2/k_g$. For formation of $UO_2NO_3^+$ analogously we find

$$\gamma = \sqrt[3]{(1-\beta)\left(1-\frac{\beta}{2}\right)^2},$$

where $\beta/(1-\beta)(2-\beta) = k_s x$.

Values of γ calculated by these formulas are given in Figure 6; here the stability constant $k_s = 0.3$ (Curve 4) was assumed; since the dissociation constant is not known, the calculation was performed for $k_g = 100$ (Curve 1), 1.6 (Curve 2), and 0.016 (Curve 3).

Comparison of Figures 1 and 6 shows that the actual behavior of the activity coefficients has nothing in common with the above calculations. If it is assumed that association is the main cause of the observed nonideality, the activity coefficients should only decrease with increasing uranyl nitrate content in the aqueous phase. In fact, they greatly increase (with the exception of the region of very low concentrations).

Thus, the behavior of γ at ionic strengths up to 10 (uranyl nitrate molalities up to 3 moles/liter of water) contradicts the assumption of the significant role of ion association in the aqueous phase. This conclusion is also valid for more complex association than that considered; in such cases we would have $\gamma = 1/(1 + \Sigma A_k NO_3^k)^{1/3}$, i.e., γ could only decrease with increasing uranyl nitrate concentration.

It is possible that the retardation in the increase of γ observed in concentrated solutions (at $J > 10$, Figure 4) is caused by association (such retardation is not found for other strong electrolytes). However, such conclusions are qualitative in character, as there is no exact theory of concentrated electrolyte solutions.

There are better grounds for the explanation that the less effective extraction of uranyl nitrate (i.e., decrease of γ) in presence of phosphate and sulfate ions is the result of complex formation with these ions.

Evidently, extraction equilibria of uranyl nitrate essentially belong to the class of equilibria which do not involve changes of the chemical composition of the substance in the aqueous phase. Control of extraction in such cases reduces to addition of salting out agents, which increase the activity a_{aq} of the substance. In extraction with changes in the chemical composition of the substance in the aqueous phase, inorganic or organic additions act as complex formers which convert the substance into an extractable form, i.e., the distribution constant is changed (this class includes the extraction of chlorides of Fe^{2+}, Co^{2+}, Ni^{2+} by alcohols, which only occurs in presence of HCl or $CaCl_2$, which convert the cations into complex anions of the type of $FeCl_4^{2-}$, $CoCl_4^{2-}$). It is true that individual instances are known of extraction of uranyl nitrate in the form of an anion, trinitrouranyl (with tetrabutyl ammonium and other complex formers [26]). However, only the use of complex formers (for example, tributyl phosphate) in the organic phase is of practical significance.

4. Nonideality of Uranyl Nitrate Solution in the Organic Phase

The nonideality of organic solutions of uranyl nitrate is very great. Figure 3 shows that in the majority of cases (in practice, with the exception of diethyl ether and cyclohexanone) the behavior of the activity coefficients γ_e at low concentrations of uranyl nitrate is described in fair approximation by the linear relationship

$$\log \gamma_e = \lambda y, \qquad (13)$$

where y is the concentration of uranyl nitrate in the organic phase. The authors of the paper [2] consider that Equation (13) is purely empirical and has no physical meaning; they prefer not to use it and attempt to attribute the nonideality of the solutions in the organic phase solely to solvate formation.

However, this viewpoint is not well founded. In fact, as has been shown by Krichevsky [23], Equation (13) is a general thermodynamic law for dilute solutions of nonelectrolytes. The extensive class of the so-called regular solutions [19] obey the relationship $\log \gamma_e \approx a(1 - by)^2$ (where a is the nonideality constant) over the whole concentration range, which is in good agreement with the course of Curves 1, 2, 3, 6, 9 (Figure 3), and which gives (13) for low values of y. Since uranyl nitrate is dissociated very slightly in the organic phase, it is quite natural that the relationship characteristic for nonelectrolytes should be obeyed. There is no doubt that in a number of cases (for example, in extraction by tributyl phosphate [14]) solvation does occur, but there are not adequate grounds for ascribing the observed effects in all solvents to solvate formation.* Sometimes, in order to obtain agreement with experimental data, a variable degree of solvation q is assumed (for example, for cyclohexanone) in the range of 11 to 3 [2]. Similar bias has been shown earlier in well known controversies concerning the chemical and physical theory of solutions, and it does not require more detailed discussion.

It is merely necessary to point out that even in presence of solvates the causes of the nonideality of uranyl nitrate solutions in the organic phase are not confined to solvation.

5. Effect of Salting Out Agent on the Activity Coefficient of Uranyl Nitrate

The Harned rule [Equation (12)] relates the activity coefficient of two solutions to different uranyl nitrate contents (x_1 and x_2), but at the same ionic strength J. It would be interesting to find how addition of salting out agent affects the activity coefficient at constant uranyl nitrate concentration (i.e., when $x_1 = x_2$). For this, we first establish the relationship between x_1 and x_2. From the condition that the ionic strengths are equal we have

$$J_1 = J'_U + J'_S = 3x_1 + J_S = J_2 = 3x_2,$$

and hence $x_2 = x_1 + J_S/3$. On the other hand, as Figure 1 shows, for a solution of uranyl nitrate at x > 0.3 mole/liter, we can also write the linear equation

$$\log \gamma_{(x,\,0)} = \log \gamma_* + bx = \log \gamma_* + 2\delta_U J_U, \quad (14)$$

where at 0.3 mole/liter < x < 2.0 moles/liter, b = 0.292, $\delta_U = b/6 = 0.039$, γ_* is a constant. Using Equation (14), we have:

$$\log \gamma_{(x_2,\,0)} = \log \gamma_{\left(x_1 + \frac{J_S}{3},\,0\right)} = \log \gamma_{(x_1,\,0)} + \frac{b}{3} J_S = \log \gamma_{(x_1,\,0)} + 2\delta_U J_S . \quad (14a)$$

Substituting (14a) into Equation (7) we find that at J < 6, when δ = const,

$$\log \frac{\gamma_{(x,\,m_S)}}{\gamma_{(x,\,0)}} = 2(\delta_U - \delta_S) J_S \cong 2(0.04 - \delta_S) J_S . \quad (15)$$

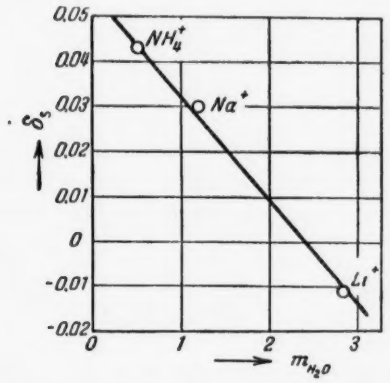

Fig. 7. Variation of the Harned coefficient for univalent ions with the degree of hydration of the cation.

Thus, the salting out agent not only increases the concentration of NO_3 ions, but changes the activity coefficient of uranyl nitrate according to Equation (15). The nature of the influence of the salting out agent on the activity coefficient depends on the ratio of δ_U to δ_S. If $\delta_S < \delta_U = 0.04$, the activity coefficient will increase on addition of salting out agent. As Figure 5 shows, this is the case for most salting out agents ($\delta_S \leq 0.03$). It is clear that a salting out agent is increasingly effective for lower values of δ_S (for example, $LiNO_3$, for which δ_S =

*We may point out that if solvates are formed the variation of γ_e with y should be represented by a curve of the form shown by a broken line in Figure 3, as when y — S/q, γ_e — ∞.

TABLE 1

Salting out agent		Trivalent	Bivalent		Univalent	
		Al^{3+}	Ca^{++}	UO_2^{++}	Na^+	NH_4^+
Salting out equivalents with the use of	diethyl ether	1	1.78	1.2	4.55	7.2
	butyl acetate	1	1.72	1.4	4.0	6.2
Chemical equivalents		1	1.5		3	
Equivalents from ionic strength		1	2		6	

$= -0.015$, is better than $NaNO_3$, for which $\delta_s = 0.03$).

If $\delta_s \approx \delta_U$, the activity coefficient of uranyl nitrate will be practically independent of the added salting out agent. This is so for NH_4NO_3, for which $\delta_s = 0.04$ (Figure 6). If $\delta_s > \delta_U$, then γ will decrease with addition of the salting out agent (KNO_3). Thus, the effectiveness of the salting out agent is characterized by the Harned coefficient, δ_s, which depends on the properties of the cation. The determining factor is probably the tendency of the cation to hydration; the more water is bound with the cation, the lower will be δ_s and the more effective the salting out agent. This is illustrated by the graph in Figure 7, based on the values of δ_s for univalent nitrates, given in Figure 5, and the effective number of water molecules m_{H_2O} hydrating the cations (according to [3], for NH_4^+, Na^+ and Li^+ $m_{H_2O} = 0.5$; 1.2; 2.8). Approximately, $\delta = 0.055\text{-}0.024\ m_{H_2O}$, so that for univalent salting out agents

$$\log \frac{\gamma(x, m)}{\gamma(x, 0)} \approx (-0{,}032 + 0{,}048\, m_{H_2O})\, m_s.$$

The qualitative aspect of the relationship between the effectiveness of the salting out agent and its power to bind water (this relationship was pointed out by V.I. Kuznetsov [20]) is relatively simple: hydration of the ions of the salting out agent decreases the amount of free water and increases the activity of uranyl nitrate owing to increase of its effective concentration.*

A few comments must be made on the salting out equivalents introduced in the paper [12]. If the distribution coefficient α was determined only by the concentration of the nitrate ions, equal changes of α would be produced by additions of chemically equivalent amounts of salting out agents. Thus, 1 mole of $Al(NO_3)_3$ would correspond to 3/2 mole of a bivalent and 3 moles of a univalent salting out agent, i.e., nitrates of valency 3, 2 and 1 would have equivalents in the proportion 1 : 1,5 : 3. If only the activity coefficients, determined by the ionic strength, were significant, then equivalent changes of the distribution coefficient would be produced by additions of amounts of salting out agent having the same ionic strength. Since the ionic strengths of one mole of a uni-, bi-, and trivalent nitrate are 1, 2 and 6 respectively, additions of the salting out agent in the proportion $1/J_3$: $: 1/J_2 : 1/J_1 = 1/6 : 1/3 : 1 = 1 : 2 : 6$.

Since both factors operate simultaneously, the equivalents can be only approximately constant at different concentrations of uranyl nitrate and salting out agents. Because of the different values of δ_s, the equivalents of different salting out agents of the same valency must be different; the greater the value of δ_s (i.e., the less effective the salting out agent), the higher the equivalent must be.

*If we attempt to interpret the increase of activity coefficients with increasing strong electrolyte concentrations as the consequence of hydration of the ions, then, for uranyl nitrate, $a \sim a_{H_2O}^{-m_0}$ and when $x = 0$

$$\gamma \sim a_{H_2O}^{-m_0/3} \sim (1 - m_{H_2O} m_s / c_0)^{-m_0/3},$$

where m_0 is the number of water molecules hydrating the cation UO_2^{2+}, $c_0 = 55$ moles/liter is the original concentration of water.

From the condition that the distribution coefficients are equal, it is possible to use Equation (7) to determine the ratio of the equivalents E_2 and E_1. In the case of tracer concentrations of uranyl nitrate, $E_2/E_1 = (\gamma_1/\gamma_2)^{3/2}$; hence, using Equation (10), we find for univalent nitrates as salting out agents, $\log E_2/E_1 = 3(\delta_2 E_2 - \delta_1 E_1)$. Assuming $E_1 = 1$ for $NaNO_3$, and using the values of δ given in Figure 7, we find for NH_4NO_3, $E_2 \approx 1.3$, and for $LiNO_3$, $E_3 \approx 0.75$. Calculations based on experimental data [21] gave $E_2 = 1.43$-1.5, $E_3 = 0.6$-0.76.

Table 1 gives the values of the equivalents of the salting out agents given in the paper [12], the chemical equivalents, and the equivalents based on the ionic strength.

The table shows that the values given lie within the indicated limits, closer to those based on the ionic strength. The equivalents for NH_4NO_3 are higher than for $NaNO_3$, as $\delta_{NH_4NO_3} > \delta_{NaNO_3}$. The differences between the equivalents for the two solvents depend on differences of the constants K and χ.

It must be pointed out that at high concentrations of uranyl nitrate or salting out agents, beyond the maximum of the distribution coefficient, the equivalents do not remain even approximately constant.

6. Extraction by Mixed Solvents

In recent times extraction by mixed solvents, for example by tributyl phosphate with diluents (these are usually hydrocarbons, inert with respect to extraction, introduced to decrease the viscosity and density of the solvent) has acquired some importance.

Of interest from the thermodynamical standpoint is the property of tributyl phosphate (TBP) of forming relatively stable solvates with actinides and many other elements [11, 22], so that it is possible to take quantitatively into account a considerable proportion of the nonideality of the solutions in the organic phase (see [14]).

For uranyl nitrate, which forms a disolvate with TBP [11, 14, 22], the distribution Equation (10) takes the form [14]*

$$y = k_U x (NO_3)^2 \gamma^3 T^2 \gamma_T^2 / \gamma_e = \tilde{k}_U x (NO_3)^2 T^2, \tag{16}$$

where T is the concentration of free TBP, $T = T_0 - 2y = cT_{100} - 2y$, T_0 is the initial concentration of TBP in moles/liter, $T_{100} = 3.68$ moles/liter is the concentration of undiluted TBP, c is the volume fraction of TBP in the diluent, γ_T and γ_e are the activity coefficients of TBP and uranyl nitrate solvate, $\tilde{k}_U$ is the apparent distribution constant.

Figure 8 shows the distribution of uranyl nitrate in extraction by TBP diluted with saturated hydrocarbons (70-250 °C). For 100, 50, 40, 30, 20 and 10% TBP the values of the constant $\tilde{k}_U$ were [14] respectively 30, 51, 53, 63, 66 and 79. As Figure 8 shows, at a constant dilution of TBP the solvation concept expresses the nonideality of the organic phase almost quantitatively (with the exception of 100% TBP, when the relative concentrations of uranyl nitrate in the organic phase are high and changes of γ_e must be taken into account). As has been shown [14], the nonideality of the solvated uranyl nitrate solution in TBP is relatively high; (the nonideality constant $A \sim -RT$). On passing from one dilution to another it is necessary to take into account the nonideality of the TBP-diluent solution, which in this case assists extraction (the effective constants increase with dilution, $\gamma_T > 1$).

Approximate evaluation of γ_T and γ_e by means of the thermodynamic relationships for multicomponent systems showed [14] that TBP-diluent solutions are nearly regular [19, 23], i.e., $\log \gamma_T \approx a(1-c)^2$.

The distribution of nitric acid at concentrations up to 5 moles/liter can be to a good degree of approximation represented by an equation based on the assumption that a monosolvate [14, 24, 25] is formed with TBP**

$$N_y = \tilde{k}_H N_x (NO_3) T, \tag{17}$$

*When TBP is used, water is not extracted with the uranyl nitrate, and $n = 0$. As the distribution of a number of substances is considered in this section, the constant for uranyl nitrate is designated with the subscript "U," for nitric acid by "H," etc.

**At high HNO_3 concentrations more acid passes into the TBP than would correspond to the monosolvate: at $N_x = 11$ moles/liter, $HNO_3/TBP = 1.2$.

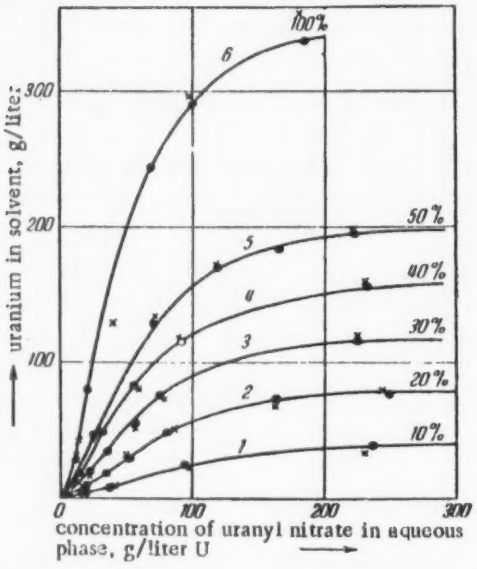

Fig. 8. Distribution of uranyl nitrate in extraction by TBP diluted with kerosene, according to data in the paper [14]. 1-6) volume fractions of 10, 20, 30, 40, 50 and 100% of TBP in kerosene; O) experimental data from [22]; x) calculated from Equation (16) with the use of average values, for each dilution, of the effective constants $\tilde{k}_U = k_U \gamma_T^2/\gamma_e$.

where N_y and N_x are the acid concentrations in the organic and aqueous phases, $\tilde{k}_H = k_H \gamma_H^2 \gamma_T/\gamma_e$ at $0.5 < N_x < 5$ moles/liter, $\tilde{k}_H \approx \text{const} = 0.2$ [24].

It is of interest to predict the simultaneous distribution of uranyl nitrate and nitric acid from data on their individual distributions, on the assumption that the activity coefficient of uranyl nitrate γ is determined by the total ionic strength of the solution ($\delta_{HNO_3} = 0$), while TBP is bound by both components, i.e., $T = T_0 - 2y - N_y$. This can be done [14], by writing Equations (16) and (17) in the form

$$y = f_U (T_0 - 2y - N_y)^2, \quad N_y = f_H (T_0 - 2y - N_y)$$

and solving them simultaneously, which gives

$$y = \frac{1}{2}\left[T_0 - (\sqrt{1 + 8FT_0} - 1)/4F\right]; \qquad N_y = (T_0 - 2y) f_H/(1 + f_H), \tag{18}$$

where

$$F = f_U/(1 + f_H)^2;$$
$$f_U = \tilde{k}_U x (NO_3)^2 = \bar{k}_U \gamma^3 x (2x + N_x)^2;$$
$$f_H = 0{,}2 N_x (2x + N_x).$$

As can be seen in Figure 9, taken from the paper [14], very good agreement was found between the predicted and calculated values of $\underline{y}$. The agreement for the acid was somewhat worse (see Figure 11 in the paper [14]), and when $x > 200$ g/liter the distribution coefficient of HNO_3 increased with increase of $\underline{x}$ instead of decreasing as predicted by Equation (15). The possibility is not excluded that this is caused by formation of a mixed solvate $UO_2(NO_3)_2 \cdot HNO_3 \cdot TBP$* (with apparent distribution constant $\tilde{k} \sim 10^{-3}$), which causes additional extraction of acid to occur

$$N_y'' = \tilde{k} (NO_3)^3 x N_x.$$

Several characteristic features of equilibria involving TBP depend on the fact that the distribution coefficients depend on the concentration of free TBP, i.e., on the degree of dilution of TBP or on the degree of its saturation with the extracted compounds $\epsilon = T/qy$. Since $\epsilon \leq 1$, at saturation $y = T/q$. Therefore the initial increase of the distribution coefficients ($\alpha \sim x^3$) is replaced at high concentrations of the extracted substance by a decrease obeying the T/qx law, i.e., by "self-displacement." If several compounds are extracted simultaneously, they mutually displace each other from the organic phase. For example, nitric acid at first salts out uranyl nitrate and then, at high enough concentrations, binds TBP and displaces uranium from the organic phase (Figure 10). Uranyl nitrate acts similarly at tracer concentrations of nitric acid. This follows from Equations (16) and (17), according to which $\alpha_U = (\tilde{k}_U/\tilde{k}_H^2)\alpha_H^2$;** at tracer concentrations of uranyl nitrate α_U reproduces the variation of α_H^2 with the acid concentration, while at $HNO_3 \to 0$, $\alpha_H \sim \sqrt{\alpha_U}$. The increase in the distribution coefficients of americium at high HNO_3 concentrations may be explained by a change in the chemical mechanism – by extraction of americium in the form of the acid $H_pAm(NO_3)_{3+p}$, i.e., formally, by formation of mixed solvates in which one or several molecules of TBP are replaced by HNO_3.*** For a trivalent nitrate, solvated with

*That is, transition to a second extraction mechanism.

**α_U and α_H are the distribution coefficients of uranium and HNO_3.

***If the distribution constant of the mixed solvate is low enough, the minimum of α may not be reached.

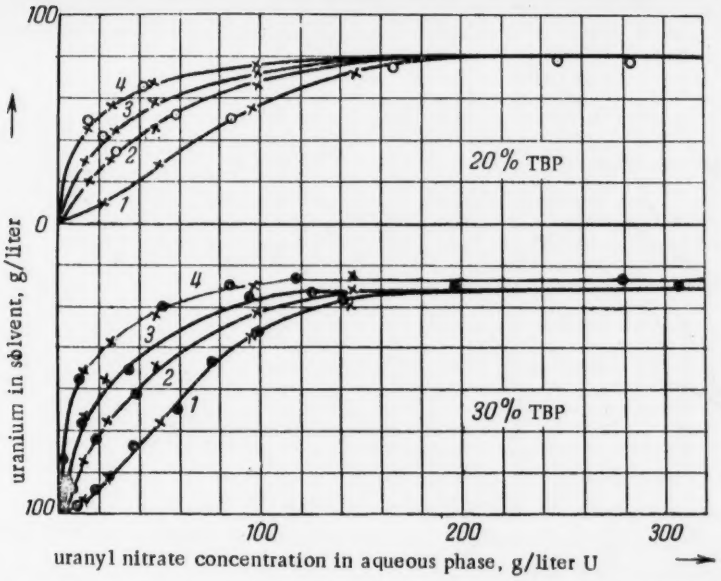

Fig. 9. The distribution of uranyl nitrate in the presence of nitric acid according to data in the paper [14] (extract TBP, diluted with kerosene): 1, 2, 3 and 4) correspond to nitric acid concentration 0.05, 0.5, 1 and 2 moles/liter; O and ●) experimental data; x) calculated according to Equations (16) and (18).

three molecules of TBP, a mixed solvate with one, two and three molecules of acid will cause [14] at high acidity an increase of the distribution coefficient conforming to the law $\sim(NO_3)$, $(NO_3)^5$ and $(NO_3)^9$, while according to the data in [11] $\alpha_{Am} \sim (NO_3)^{6-7}$, i.e., p = 2-3 (if the degree of solvation q remains unchanged, then when p = 3, $\alpha \sim (NO_3)^3$). In general, if the microelement is extracted in conformity with the equation

$$\alpha = \tilde{k}(NO_3)^m T^q,$$

then in absence of mixed solvates uranyl nitrate displaces it from the organic phase under the condition that q > > $^2/_3$m (nitric acid, when q > m/2). Thus, by saturating TBP, it is possible to decrease the extraction of a number of microelements.

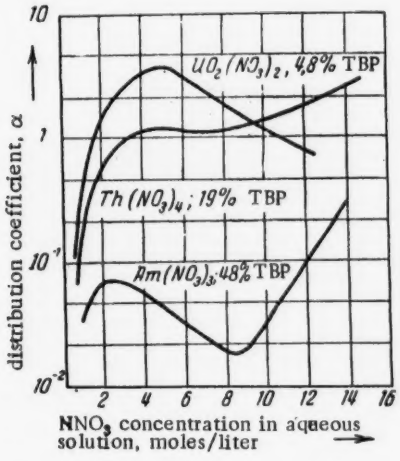

Fig. 10. Variation of distribution coefficients of certain actinides with nitric acid concentration, in extraction by TBP with diluents; based on data from [11].

The dependence of the distribution coefficient (at tracer concentrations of the element) on the dilution of TBP is generally used for determination of the number q of TBP molecules entering the solvate; since $\alpha \sim T^q$, q is found from the slope of the $\log\alpha = f(\log T)$ curve. It must be remembered that owing to the nonideality of the TBP-diluent solution the logarithmic slope $\tilde{q} = d\log\alpha/d\log T$ coincides with q only at high dilutions, when γ_T = const, or at $c_T = 100\%$, when $\gamma_T = 1$. In the general case $\tilde{q} \neq q$; for regular solutions $\ln\gamma \cong a(1-c)^2$; since $\alpha \approx T^q\gamma^q$, then $\tilde{q} = q - 2aqc(1-c)$. If a > 0, then at intermediate concentrations $\tilde{q} < q$, and at a < 0, $\tilde{q} > q$. This accounts for the deviation from the linear relationship $\log\alpha = f(\log T)$ found in [11]. The general picture for tracer concentrations of uranyl nitrate is shown in Figure 11. If a > 0, then nonideality of the TBP-diluent solution improves extraction, if a < 0, it worsens it. Thus, the distribution data in Figure 11 give an indication of the nonideality of the

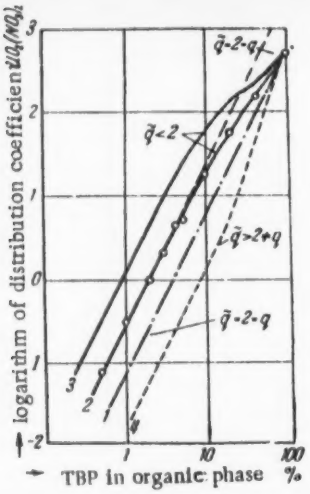

Fig. 11. Logarithm of the distribution coefficient of uranyl nitrate (at tracer concentrations of uranium) vs. the logarithm of the TBP concentration in the solvent. 1) Ideal solution; TBP-diluent; $a_1 = 0$; 2,3,4) nonideal solutions, with $a_2 > 0$; $a_3 > a_2$; and $a_4 < 0$ respectively; O) data from [11]; ●) data from [14].

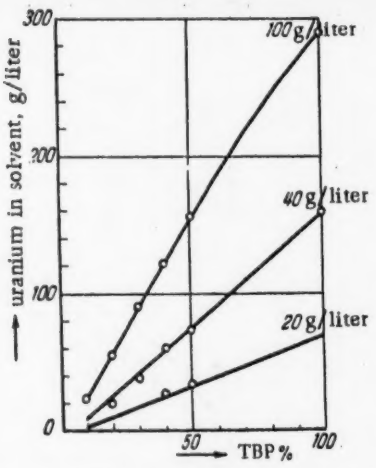

Fig. 12. Variation of uranyl nitrate distribution with concentration of TBP in the solvent, from the data in [14] for various concentrations in the aqueous phase.

TBP-diluent solution.

In conclusion we note that the quadratic relationship $y \sim c^2$ applies only at concentrations of uranyl nitrate in water up to ~1 g/liter. As x increases, the $\alpha = f(T)$ relationship approaches linearity (Figure 12) [14].

7. The Basic Distribution Parameters

With (11) and (15) taken into account, the distribution equation takes the form

$$y = kx\,(NO_3)^2 \frac{\gamma_*^2}{\gamma_e} \cdot 10^{6(\delta_U - \delta_S)J_S}, \qquad (19)$$

where $NO_3 = 2x + \ell m_s$, $\gamma_e \approx e^{\lambda y}/a_{H_2O}^n$.

It follows from Equation (19) that:

a) the solvent can be basically characterized by two constants: the distribution constant k and the nonideality constant λ (or the degree of solvation q; in that case

$$\gamma_e \sim (S)^q \sim \frac{1}{(1-\epsilon)^q} = \frac{1}{\left(1-\frac{q}{S_0}y\right)^q},$$

where ε is the degree of saturation of the solvent by the solvate). The degree of hydration n is not so important for the distribution;

b) the aqueous phase is characterized by quantities pertaining to uranium

$$(\gamma_U = \gamma_* \cdot 10^{2\delta_U J_U}),$$

and also by the individual nature of the salting out agent (δ_S).

Thus, three basic quantities vary in systems with different solvents and salting out agents; K, λ (or q), and δ_S. The decisive factor is the distribution constant K, which shows thousandfold variations for different solvents.

TABLE 2

No.	Solvent	Distribution constant			Free energy change
		absolute value of 4k	k/k_{dee}	k/k_{dbe}	$F = \Delta RT \ln k/k_{dbe}$ cal/mole
1	Dibutyl ether (dbe)	0.0025	0.0055	1.0	0
2	Diisopropyl ether	0.012	0.026	4.7	900
3	Isoamyl acetate	0.06	0.13	29	2000
4	Diethyl ether (dee)	0.46	1.0	180	3050
5	Methyl isobutyl ketone	0.75	1.63	300	3400
6	Cyclohexanone	29.5	64	11,600	5500
7	Tributyl phosphate (mixed with 80% kerosene)	252	550	10^5	6600

This is illustrated in Table 2, where, for comparison, the constant for diethyl or dibutyl ether is taken as unity. The nonideality constant varies from 0.7 for diisopropyl ether to ~2 for penta-ether and $\sim 4/T_0$ for TBP.

The values of the constants for solvents Nos. 1-3, 5-6 have been recalculated from data in [2], for diethyl ether, from [2] and [12], and for tributyl phosphate from [14].

The value of the distribution constant* to some extent characterizes the energy (strength) of the bond between uranyl nitrate and the solvent. However, it is not correct to regard the constant (or extraction efficiency) as a measure of bond strength. $\Delta F = \Delta E - T\Delta S$ (S is the entropy) and $\Delta F \neq \Delta E_{bond}$ (as there are no grounds for neglecting the entropy term).

8. Form of the Distribution Curves

The characteristic form of the distribution curves is shown in Figure 13. In absence of a salting out agent the equilibrium curve may have three characteristic regions: initial – concave (1); middle – convex (2); and final – flat, approaching to horizontal (3). The concavity of the first region is the consequence of the dissociation of the uranyl nitrate molecule into three ions, with the consequent $y \sim x^3$ distribution law. The transition from a concave to a convex isotherm and the formation of the second region is the result of the sharp increase of nonideality (i.e., of the activity coefficient γ_e) or uranyl nitrate solution in the organic phase as the latter becomes saturated with uranium: $y \sim x^3/\gamma_e \approx x^3 e^{-bx^3}$. Finally, the last region corresponds to complete saturation of the organic phase with uranium.

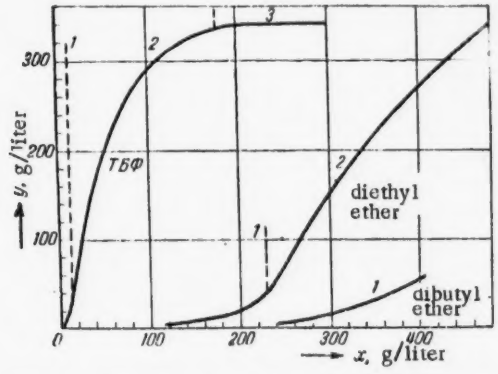

Fig. 13. Characteristic regions of the distribution curves (y and x are the concentrations of uranyl nitrate in the organic and aqueous phases in g/liter).

The extents of these regions vary for different solvents according to the distribution constant K and nonideality constant λ. For example, in the case of dibutyl ether (4k = 0.0025) only the first region appears – so little uranium passes into the ether that nonideality of the ether phase has no effect (compare Figure 2). For diethyl ether (4k = 0.46), the initial region extends only up to 1.0 mole/liter of uranium in the aqueous phase, after which the nonideality of the solution in the organic phase becomes considerable and the second region of the curve appears. For tributyl phosphate (4k = 250) all three regions are found, the first being very small (because of the strong nonideality of the organic phase).

Thus, a peculiarity of extraction solvents with high distribution constants (such as cyclohexanone, tributyl

*The constant increases with increasing oxygen/carbon ratio in the solvent.

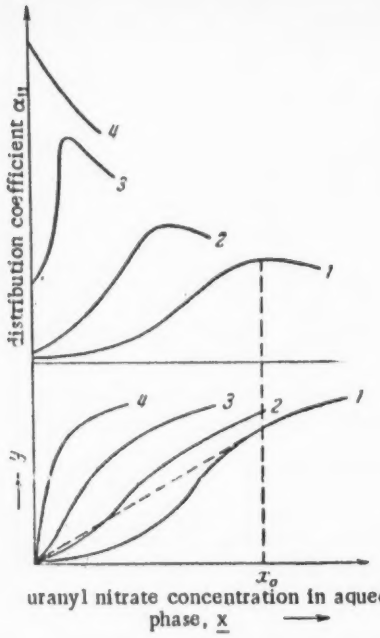

Fig. 14. Form of the distribution curves and the $\alpha = f(x)$ relationship in presence of salting out agents. 1) No salting out agent; 2,3,4) with increasing amounts of salting out agent. The broken lines represent construction of the tangent for finding the maximum α when $dy/dx_0 = y/x_0$.

phosphate, penta-ether) is the extremely restricted region of dilute solutions (short initial region), which makes it possible to attain relatively high distribution coefficients without using salting out agents.

The dependence of the distribution coefficient of uranyl nitrate α_U on the concentration in the aqueous phase (Figure 14) is also related to the form of the distribution curves. The initial (concave) region of the curves corresponds to increase of the distribution coefficient with increase of x. In the second region the increase of α slows down; if the region is long enough, α passes through a maximum (the concentration x_0 corresponding to maximum α can be found by constructing a tangent to the distribution curve, see Figure 14). Finally, the third region corresponds to a decrease of α by the 1/x law. Thus, the distribution coefficient maxima are the consequence of nonideality of the organic phase.

If a salting out agent is present in the aqueous phase, as its concentration increases the maxima of α should be displaced toward the coordinate origin, since $\alpha \sim (NO_3)^2 e^{-\lambda y}$ and the higher the concentration of salting out agent, the more uranyl nitrate will pass into the organic phase and the earlier will the nonideality of the organic phase take effect. At high enough concentrations of salting out agent, when $(d^2y/dx^2)_{x=0} = 0$, the concave region on the distribution curve disappears (at $l m_s \sim 1/\lambda^{1/3}$). The maximum of the distribution coefficient disappears at the same time.

LITERATURE CITED

[1] R.Robinson, J. Am. Chem. Soc. 64, 1469 (1942); 73, 1840 (1951).

[2] E. Glueckauf, H. McKay and A. Mathieson, Trans. Farad. Soc. 47, 437 (1951).

[3] R.Robinson and R. Stokes, Electrolyte Solutions (London, 1955), p. 320.

[4] H. Harned and B. Owen, The Physical Chemistry of Electrolyte Solutions (Foreign Lit. Press, Moscow, 1952). [Russian translation].

[5] H. McKay and A. Mathieson, Trans. Farad. Soc. 47, 428 (1951).

[6] A. Gardner, H. McKay and D. Worren, Trans. Farad. Soc. 48, 997 (1952).

[7] A. Gardner and H. McKay, Trans. Farad. Soc. 48, 1099 (1952).

[8] H. McKay, Trans. Farad. Soc. 48, 1103 (1952).

[9] J. Jenkins and H. McKay, Trans. Farad. Soc. 50, 107 (1954).

[10] H. McKay, Chem. and Ind. 51, 1549 (1954).

[11] H. McKay, Tributyl Phosphate for Extraction of Nitrates of the Actinide Elements, Symposium, Chemistry of Nuclear Fuel (United Sci.-Tech. Press, Moscow, 1956).

[12] S. Karpacheva and L. Kharkhorina, J. Inorg. Chem. 4 (1957).

[13] L. Katzin and J. Sullivan, J. Phys. Colloid. Chem. 55, 346 (1951).

[14] A. Rozen and L. Kharkhorina, J. Inorg. Chem. 8 (1957).

[15] R. Betts and R. Michels, J. Chem. Soc. Suppl. No. 2, 286 (1949).

[16] S. Ahrland, Acta Chem. Scand. 5, 1151, 1271 (1951).

[17] N. Komar and Z. Tretyak, J. Anal. Chem. 10, 236 (1955).

[18] S. Irving, J. Chem. Soc. (London) 1841 (1949).

[19] J. Hildebrand, Solubility of Nonelectrolytes (New York, 1936).

[20] V. Kuznetsov, Progr. Chem. 23, 654 (1954).

[21] V. Vdovenko and T. Kovaleva, Radiochemical Symposium of the Leningrad State University (Leningrad, 1956), p. 43.

[22] S. Karpacheva, L. Kharkhorina and A. Rozen, J. Inorg. Chem. 6 (1957).

[23] I. Krichevsky, Phase Equilibria in Solutions (State Sci.-Tech. Press, Moscow, 1952); see also I. Krichevsky and A. Ilyinskaya, J. Phys. Chem. 19, 621 (1945).

[24] V. Fomin and E. Maiorova, J. Inorg. Chem. 1, 1703 (1956).

[25] H. McKay, K. Alcock, S. Grimley, T. Heavy and J. Kennedy, Trans. Farad. Soc. 52, 39 (1956).

[26] L. Kaplan and R. Hildebrand, J. Inorg. Nucl. Chem. 2, 153 (1956).

Received October 10, 1956

MECHANISM OF FORMATION OF ZIRCONIUM SPONGE IN ZIRCONIUM PRODUCTION BY THE MAGNESOTHERMIC PROCESS

F.G. Reshetnikov and E.N. Oblomeev

The mechanism of formation of zirconium sponge in the production of zirconium by the magnesothermic process has been investigated by introducing into the reducing agent a very soluble but not very volatile additive (aluminum, tin) acting as marked atoms. It was found that the growth of the zirconium sponge on the wall of the reaction crucible above the level of the molten bath is the result of the reaction of zirconium chloride vapor with molten magnesium as the latter ascends by capillary action through the previously formed sponge. The amount of zirconium chloride reacting with magnesium in unit time depends more upon the perimeter of the crucible than upon the surface area of the bath. To intensify the reduction of zirconium chloride by magnesium, it is recommended that partitions be placed in the crucible to act practically in the same way as the crucible wall.

The production of magnesothermic zirconium, competing in purity with zirconium iodide, depends upon the degree of perfection of the magnesothermic method.

In atomic energy engineering, zirconium is used in the form of corrosion-resistant alloys [1] (with small additions of tin, iron, nickel). In magnesothermic zirconium, the addition of tin neutralizes the harmful effect of nitrogen; it is thus possible to produce alloys whose properties are equal to those of alloys prepared on the basis of zirconium iodide.

One of the most important operations in the magnesothermic method is actually the reduction of zirconium chloride by magnesium, upon which depend to a considerable degree the purity and properties of the metal obtained.

In contrast to the majority of metallurgical thermal processes, in the present process, the magnesium reduces gaseous zirconium chloride, the vapor pressure of the latter attaining 1 atmos even at 331°C.

The reaction of zirconium chloride with magnesium results in the formation of metallic zirconium in the form of a porous mass – sponge – and magnesium chloride. A temperature of the order of 800-850°C is maintained in the reaction crucible. In these conditions, the zirconium which melts at about 1860°C, remains in the solid state in sponge form, and the magnesium chloride and excess of metallic magnesium are in the molten state.

Figure 1 shows the typical distribution of the fusion products (cross-section of crucible contents after the reaction). The purest part of the zirconium is the upper, ramified and entirely porous sponge A. Its yield depends upon the temperature conditions of the process and in our experiments is about 75% of the total amount of metal.

The location of the upper part of the sponge is noteworthy. It is mainly situated above the level of the liquid bath in the reaction crucible.

In Reference [2], it is pointed out that the yield of this sort of high-grade zirconium sponge is altogether only 35%. A diagrammatic distribution of the different sorts of zirconium sponge is given and it is pointed out that the bottom part of the sponge C is formed in the initial reaction period. In our opinion, this also refers to the lateral part of the sponge B, the amount of which is usually not very large.

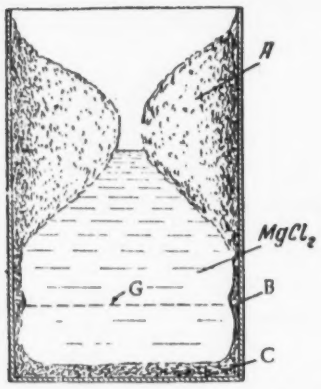

Fig. 1. Distribution of fusion products (G – original level of magnesium; for other references, see text).

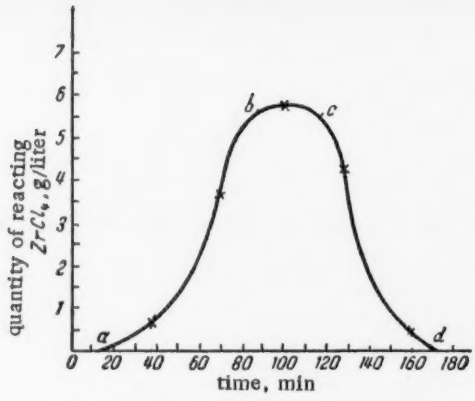

Fig. 2. Variation, with time, of quantity of zirconium chloride reacting with magnesium.

The investigation we have made has enabled us to make the following suppositions regarding the sequence and mechanism of formation of the different parts of the zirconium sponge.

In the initial stage of the reduction process, the zirconium chloride reacts with magnesium on the surface of the molten magnesium bath. The reaction proceeds mainly on the crucible walls, which may be due to the higher temperature and the catalytic action of the crucible wall. The zirconium formed at this moment absorbs a mixture of oxygen and nitrogen (zirconium is a good getter) from the gaseous medium and falls to the bottom of the crucible; a small portion of the zirconium remains on the crucible walls forming the side sponge. In the initial stage, the reaction of the magnesium vapor with zirconium chloride may be reduced to zero if the heating of the reaction crucible with the magnesium lags behind the supply of zirconium chloride. In the opposite case, the formation of a black powder ($Zr + MgCl_2$) is observed.

The upper part of the sponge is formed in the next stage. It has been found experimentally that the upward growth of this part of the zirconium sponge considerably outstrips the rise in level of the molten bath of metallic magnesium and magnesium chloride. This phenomenon is observed when the temperature conditions have become established and the temperature of the reaction crucible has reached 800-850°C. It could be assumed that the upper part of the sponge, situated above the level of the molten bath, is formed by the reaction of zirconium chloride vapor with magnesium vapor. At this temperature, the pressure of the latter is about 40 mm Hg [3]. The probability of such a process increases with decrease in the supply of zirconium chloride vapor, when considerable rarefaction may occur in the apparatus.

The character of the location of the upper part of the sponge, the presence in the latter of a considerable amount of excess metallic magnesium and also the absence of metallic magnesium in the apparatus outside the reaction crucible, however, suggest that the magnesium, which wets zirconium well, ascends through the zirconium sponge by capillary action and reacts with the zirconium chloride vapor on the large surface offered by the sponge. A gradual and continuous upward growth of the zirconium sponge takes place in this way. The crucible walls also play some part in this process but only after they have been covered with a thin layer of zirconium. Subsequently, the magnesium ascends through the zirconium sponge.

To verify these assumptions, 3% of aluminum, forming a very soluble but not very volatile additive, was introduced into the magnesium. The vapor pressure of aluminum at 850°C does not exceed 0.001 mm Hg. The zirconium sponge obtained by reduction with such an alloy was analyzed in different parts for its aluminum content. The results of the analyses are given below.

Similar results were obtained when a small quantity of tin was added to the magnesium.

The figures given in the table show a completely regular distribution of aluminum in the different parts of the zirconium sponge. The maximum amount of aluminum is contained in the bottom part of the sponge, a some-

Aluminum content of upper sponge, %		Aluminum content of bottom sponge, %
close to crucible center	close to crucible wall	
2.17	2.31	2.45
1.44	3.26	4.92
0.26	2.05	2.87

what smaller amount is contained in the upper part of the sponge, situated relatively close to the crucible wall and still less in the upper part of the sponge, situated close to the center of the crucible. Such a distribution of aluminum throughout the entire zirconium sponge undoubtedly indicates that the magnesium, with the aluminum dissolved in it, ascends by capillary action through the zirconium sponge and reacts on the surface of the latter with the vapor of $ZrCl_4$. A similar mechanism has been observed in the formation of titanium sponge, but was detected by a less strict method [4].

The lower aluminum content in the center of the upper part of the sponge in comparison with the content closer to the crucible wall indicates that magnesium in vapor form also takes part in the formation of the upper part of the sponge. The magnesium left in the crucible becomes richer in aluminum, due to partial vaporization, which results in an appreciable increase in aluminum in the bottom part of the sponge. The reaction of magnesium vapor with zirconium chloride leads to an increase in the bottom part of the sponge and towards the end of the process, to the formation in different parts of the apparatus of a friable black powder, consisting basically of a mixture of finely dispersed metallic zirconium with magnesium chloride.

Figure 2 shows a curve of the rate of reduction of zirconium chloride by magnesium. It was constructed from the descent of an indicator (Co^{60}) situated on the chloride in the vaporizer and enabling the rate of volatilization of $ZrCl_4$ and its reaction with the molten magnesium to be recorded.

It will be seen from the plot that as the zirconium sponge grows, the quantity of $ZrCl_4$, reacting with magnesium in unit time, increases (section ab). The section bc corresponds to the maximum rate of reduction of zirconium chloride, as determined by the rate of its admission. The section cd corresponds to the completion of the reduction process, connected with the cessation in the supply of $ZrCl_4$. These data likewise confirm that in the formation process of the higher grade upper part of the zirconium sponge, the predominant part is played by the reaction of $ZrCl_4$ with magnesium ascending by the action of capillary forces through the previously formed sponge. If the essential factor in this process was the reaction of $ZrCl_4$ with magnesium vapor or with the surface of the molten magnesium bath, its velocity would diminish with time, since the surface of the molten magnesium diminishes with the growth of the zirconium sponge.

Some authors [5] support the view that the heavier magnesium chloride formed in the reduction process descends to the bottom, and the lighter metallic magnesium floats, i.e., it is always on the top.

In numerous experiments we have carried out with the usual excess of reducing agent (25%) and also with a much greater excess (up to 1000%), the opposite was always observed: the magnesium chloride was on the top and the metallic magnesium below, rising fairly high at the crucible walls and forming a pronounced concave surface. This may evidently be explained as follows. With increase in temperature, the specific gravities of magnesium and magnesium chloride become very close. While at room temperature they are respectively equal to 1.74 and 2.33, at 780°C they become 1.545 and 1.667 [6]. The zirconium formed in the reduction process dissolves partly in the magnesium, increasing the specific gravity of the latter. The solubility of zirconium in magnesium at 600°C is 0.43% and at 900°C, it is 0.7% [7]. Finally, magnesium wets the crucible walls very well, especially when they are covered with a layer of zirconium, while magnesium chloride is lyophobic with respect to the walls of the steel crucible and to zirconium. All this explains the observed positions of metallic magnesium and magnesium chloride. Thus, after a certain quantity of magnesium chloride has been formed, the zirconium tetrachloride vapor no longer has any direct contact with the surface of the molten magnesium, and reacts above the surface of the molten magnesium chloride only with that part of the magnesium which, by capillary forces, ascends through the zirconium sponge formed along the crucible wall. The magnesium chloride formed at the same time flows downward. These processes lead to the growth of the zirconium sponge upwardly and towards the crucible center, with the formation of the upper part of the sponge as shown in Figure 1.

Such location of the metallic magnesium does not, of course, exclude its partial vaporization and the reaction of magnesium vapor with zirconium chloride vapor.

The mechanism described for the formation of zirconium sponge permits one to conclude that the quantity

of zirconium chloride reacting with magnesium in unit time, other conditions being the same, will depend not so much on the cross-sectional area of the reaction crucible as upon its perimeter, since the formation of sponge proceeds mainly at the crucible walls. If crucibles of large dimensions are used, therefore, it would obviously be expedient to provide them with additional surfaces in the form of partitions or crosspieces, which would practically play the same part in the formation of the zirconium sponge as the walls of the crucible itself. Such partitions ought to extend almost to the bottom of the crucible, i.e., they should dip into the molten magnesium. They should preferably be made of material which does not contaminate zirconium, for example sheet zirconium.

The observations made permit a more correct approach to the choice of the optimum temperature conditions for heating the reaction crucible and vaporizer, the increase in the yield of high-grade zirconium sponge and the construction of the reaction crucible for the intensification of the magnesothermic process of zirconium production.

LITERATURE CITED

[1] D.E. Thomas, Metallurgy of Nuclear Energy Production and Effect of Radiation on Materials (Papers read by foreign scientists at the International Conference on the Peaceful Uses of Atomic Energy), Metallurg. Press, 1956, p. 376.

[2] S.M. Shelton and E. Dilling, The Manufacture of Zirconium Sponge, Zirconium and Zirconium Alloys, E.F.M., 1953.

[3] D.R. Stell, Vapor Pressure Tables of Individual Substances, IL, 1949. [Russian translation].

[4] W.J. Kroll, Metall. 9 (9/10), 366-376 (1955).

[5] H.L. Gilbert and C.Q. Morrison, Chem. Eng. Progress, No. 7 (1955).

[6] Kh.L. Strelets, A.Yu. Taits and B.S. Gulyanitsky, Metallurgy of Magnesium, Metallurg. Press, 1950.

[7] O.A. Carson and D.T. Austin, Can. Min. J. 73, 70-75 (1952).

Received November 14, 1956

LETTERS TO THE EDITOR

PARITY NONCONSERVATION IN WEAK INTERACTIONS

(Review)

A.P. Rudick

I. Theoretical Investigations

The recently performed experimental studies of the properties of "strange" particles, that is, of hyperons and K-mesons, has led, among other things, to the establishment of the following fundamental facts: the charged K^+-meson can decay in two ways, namely

$$K_1^+ \to \pi^+ + \pi^0, \tag{1}$$
$$K_2^+ \to \pi^+ + \pi^+ + \pi^-. \tag{2}$$

In addition, it has been experimentally established that such physical characteristics of the K^+-meson as its mass ($m = 966$), its spin ($s = 0$), and its lifetime ($\tau = 1.3 \cdot 10^{-8}$ sec) are identical with those of the K_1-meson and the K_2-meson.

On the other hand, it has been known for a long time that π-mesons are pseudoscalar particles, which means that the wave function which describes the π-meson changes sign under space inversion, that is, under change of sign of all the space coordinates. Since it is also established that the π-mesons emitted in Reactions (1) and (2) are emitted in the S-state, it follows that the final state in Reaction (1) is described by a scalar (with respect to space inversion), and that in Reaction (2) by a pseudoscalar.

Thus, the fact that the K^+-meson can decay according to both (1) and (2) leads to one of the following two possibilities:

I. Either the K_1^+-meson and K_2^+-meson are different particles having the same mass, spin and lifetime, and differ only in their intrinsic parities (the K_1^+-meson is a scalar, and the K_2^+-meson is a pseudoscalar).

II. Or the K_1^+-meson and the K_2^+-meson are the same particle with a definite intrinsic parity, but in one of the Reactions (1) or (2) parity is not conserved.

The conclusions following from the first and second possibilities were analyzed in detail in the works of Lee and Yang. They established the fact that special experiments can be performed to determine which of the possibilities actually is fulfilled in nature.

Let us consider the possibility of parity nonconservation. Lee and Yang [1] suggested that the nonconservation of parity is not a particular property only of those weak interactions involving K-mesons, but that parity is not conserved in any weak interactions (for instance in β-decay). The nonconservation of parity is a characteristic property differentiating weak interactions from strong (electromagnetic and π-meson-nucleon) interactions, in which, as has been experimentally established for a long time, parity is conserved. It should be noted that Lee's and Yang's hypothesis that parity is not conserved in weak interactions was an extremely daring physical assertion, since it was previously considered completely obvious and necessary that the parity conservation law be absolutely strict. The analysis performed by Lee and Yang, however, showed that in previous investigations of weak interactions, it was always scalar quantities that were measured, and these are not sensitive to whether or not the parity is conserved. The nonconservation of parity can be established by an experiment (involving only one interaction) only if the quantity measured is a pseudoscalar.

Lee and Yang suggested several experiments whose results would make it possible to establish whether parity is conserved in weak interactions. In the case of nonconservation the following phenomena should be observed:

1. The angular distribution of electrons in the β-decay of polarized nuclei should be of the form

$$W(\vartheta) \approx 1 + a\cos\vartheta, \tag{3}$$

where ϑ is the angle between the spin axis of the decaying nucleus and the direction of motion of the electron. The quantity a, for allowed β-decay with $\Delta I = -1$, is given by

$$a = \frac{v}{c}\frac{\langle I_z\rangle}{I} f, \tag{4}$$

where v is the electron velocity; I is the spin of the decaying nucleus; $\langle I_z\rangle$ is the expectation value of the projection of the spin along the z axis, and $f \leq 1$ is a function of certain constants which define the degree of parity nonconservation. If parity is conserved in β-decay, then $f = 0$.

2. In successive β-γ-decays, the γ-ray emitted should be circularly polarized if parity is not conserved.

3. In successive π-μ-e decays

$$\begin{array}{l} \pi \to \mu + \nu \\ \quad\downarrow \\ \quad e + \nu + \tilde{\nu} \end{array} \tag{5}$$

there should be a correlation between the directions of motion of the μ-meson and the electron. The angular distribution of the electrons in the π-meson rest-system should be of the form

$$W(\varphi) = 1 + b\cos\varphi, \tag{6}$$

where φ is the angle between the directions of the μ-meson and the electron, and b is a function which depends on the type of decay theory and constants which determine the degree of parity nonconservation. We note that in π-μ-e decays, the measured quantity $b\cos\varphi$ is a scalar, but that nevertheless, because the angular distribution of the electrons appears in this function, it can be used to observe parity nonconservation. This is related to the fact that in the successive decays of the π-meson and the μ-meson parity nonconservation may occur twice; in each of these decays nonconservation leads to the appearance of a pseudoscalar quantity, but in the final result only the product of these quantities appears, and this is a scalar.

4. If parity is not conserved one should observe various correlation phenomena in the decay of polarized Λ- and Σ-particles. Further theoretical investigations [2, 3], refer to the question whether parity nonconservation in weak interactions would lead to the failure of any other conservation laws. It had already been shown by Pauli and Lüders [4] that the relation between the spin and statistics of a particle requires the invariance of the interaction Hamiltonian under the product of the three transformations space inversion I, time inversion T (that is, replacement of t by $-t$), and charge conjugation C (that is, transformation from the particle to the antiparticle). The Pauli-Lüders condition can be symbolically written

$$ITC = 1. \tag{7}$$

If it is assumed that parity nonconservation in weak interactions does not cause failure of the relation between spin and statistics (this seems an entirely valid assumption, since experiment verifies the connection between spin and statistics), then it follows that parity nonconservation

A) either leads to noninvariance in weak interactions also under time inversion and charge conjugation, but so that Relation (7) holds as previously,

B) or, again in weak interactions, leads to noninvariance with respect to

B') only time inversion, maintaining the invariance under charge conjugation and Relation (7),

B") only charge conjugation, maintaining the invariance under time inversion and Relation (7).

The more probable of these is one of possibilities B, since the existence of the long-lived K^0-meson which was recently predicted [5] and experimentally observed [6] is easily explained in this case on the basis of invariance under either charge conjugation (case B') or time inversion (case B"); the short-lived K_1^0-meson has even charge parity in case B', and has even "time parity" in case B", and the long-lived K_2^0-meson has odd charge parity (case B') or odd "time parity" (case B"). Then case B' and B" should give different states for the three π-mesons emitted in K_2^0-decays: in case B" the three π-mesons can be in the S-state, and in case B' the three π-mesons cannot be in the S-state.

In case B', the experiments suggested by Lee and Yang could not be used to discover whether or not parity is conserved, although these experiments would be decisive in case B". Ioffe [7] has indicated what experiments can be performed to observe parity nonconservation in both cases B' and B".

A profound physical approach to the solution of the question of which conservation laws remain valid in weak interactions is to be found in the work of Landau [8]. Landau noted the fact that the nonconservation only of parity would be extremely strange, since this would lead to the asymmetry of space with respect to inversion, whereas it is well known that space is actually entirely isotropic (this isotropy leads to the conservation of angular momentum). Landau finds the solution to these difficulties in the assumption that weak interactions fail to conserve in addition to spatial parity, also charge parity; but their product, which Landau calls the "combined parity,"* is conserved. The assertion that in spite of their nonconservation of spatial parity, weak interactions conserve the combined parity, enabled Landau to make an extremely interesting hypothesis [9] on the possibility of the existence of a two-component neutrino (a similar hypothesis was also made by Lee and Yang [10] and by Salam [11]). As is well known, the neutrino, which has spin 1/2 and thus satisfies the Dirac equation, is in general described by a four-component wave function. If it is assumed, however, that the combined parity is conserved in weak interactions and that spatial parity fails to be conserved in a well-defined way (with those constants being equal, in the interaction Hamiltonian, which multiply the terms that alter and leave unaltered the spatial parity), the neutrino can be described by a two-component wave function, but if and only if the neutrino mass vanishes. Thus the fact that the neutrino mass is exactly equal to zero is no longer a coincidence, but follows necessarily from the theory.

The two-component neutrino introduced by Landau has a remarkable property: its spin can be directed either only parallel or only antiparallel to the momentum (and correspondingly, the spin of the antineutrino is directed only antiparallel or only parallel to the momentum). On the basis of this property, the two-component neutrino was called the "longitudinal neutrino." It follows from this property that all the correlation effects in the experiments involving the neutrinos which were suggested by Lee and Yang are maximal, since parity nonconservation in weak interactions is maximal in the case of the longitudinal neutrino.

In particular, in π-μ-e decays the quantity $\underline{b}$ is

$$b=\frac{1}{3}\frac{2\lambda_1\lambda_2}{\lambda_1^2+\lambda_2^2}, \tag{8}$$

if the neutrino is longitudinal, where the constants λ_1 and λ_2 characterize the amount of vector and pseudovector interaction between the muon and electron. We note here the following very important situation: for a longitudinal neutrino, it follows necessarily that both a neutrino and an antineutrino are emitted in the muon decay $\mu \rightarrow e + \nu + \tilde{\nu}$. In this case the Michel parameter** is $\rho = 0.75$, which is in good agreement with the most recent experimental data. If two neutrinos were emitted in μ-e decay then we would have $\rho = 0$ for the longitudinal neutrino, and this is in obvious disagreement with experiment. Landau [9] also proposed an experiment to verify the longitudinal neutrino hypothesis in β-decay. He established the fact that if parity is not conserved, the electrons emitted in β-decay will be longitudinally polarized. For the longitudinal neutrino, this polarization will have the same magnitude as the ratio of the electron velocity to the velocity of light.

---

*In view of Relation (7) the combined parity is the same as "time parity."

**The electron energy spectrum in μ-e decay is related to the Michel parameter ρ by the equation

$$\frac{dN}{N}\sim\varepsilon^2[(1-\varepsilon)+\frac{2}{9}\rho(4\varepsilon-3)]d\varepsilon,$$

where ϵ is the ratio of the electron energy to its maximum possible value.

II. Experimental Results

Very recently there have appeared short preliminary communications on several experimental observations of parity nonconservation in weak interactions involving the neutrino.

1) Angular Distribution of the Electrons in β-decay of Polarized Nuclei

Wu and co-workers [12] have investigated the angular distribution of electrons emitted in the β-decay of polarized Co^{60} nuclei. Polarization of the Co^{60} nuclei, a 50μ layer of which was grown on a CeMg nitrate crystal, was achieved by the Rose-Gorter method. The fundamental experimental difficulty was that of locating the anthracene crystal scintillation counter (3 cm in diameter and 1.6 mm thick), which was to record the decay electrons, sufficiently close to the Co^{60}, that is, where the absolute temperature must be only fractions of a degree. It was possible to place the scintillation counter at a distance of 2 cm from the Co^{60}.

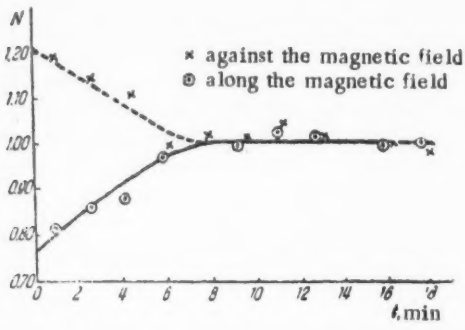

Fig. 1. The asymmetry of the emitted electrons in the experiment of Wu and co-workers [12]. The ordinate indicates the counting rate N of the scintillation counter normalized to unity for the warm sample.

The degree of polarization of the Co^{60} nuclei was found by recording the γ-rays which follow β-decay. This was done with the aid of two NaI crystal counters above and at the sides of the source. The experiment was performed in the following way: after cooling the CeMg nitrate crystal, which took 20 sec, both the electrons and their accompanying γ-rays were counted for 18 min. The difference between the counting rates of the equitorial and polar NaI crystals was used to determine the change of the Co^{60} polarization in time. After 6 min the γ-counter counting rates became equal, so that the Co^{60} nuclei were entirely unpolarized. By changing the direction of the magnetic field, the Co^{60} nuclei could be polarized either in the direction of the scintillation counter or in the opposite direction. The time change of the counting rate of the scintillation counter for the two directions of the magnetic field, which is shown in Figure 1, made it possible to determine the magnitude of a [Equation (3)], which was found to be −0.4. This indicates that more electrons are emitted in the direction opposite to the spin of the Co^{60} nucleus, than along it. The absolute value of a obtained is not in contradiction to the longitudinal neutrino hypothesis.

2) Asymmetry of the Angular Distribution in π-μ-e Decay

Lederman and co-workers [13] investigated the angular distribution of electrons in π-μ-e decay. The experimental arrangement is shown in Figure 2. A beam of 85 Mev π^+- or π^--mesons is passed through a 20 cm layer of carbon. Since the mean free path of a π-meson of this energy in carbon is 12.5 cm, almost all the π-mesons are stopped in the carbon. The μ-mesons, produced by in-flight decay of the π-mesons, are stopped by a target along the path of the original meson. This target was made of one of three substances: carbon, polyethylene, or calcium. The target was placed in a solenoid. The magnetic field due to the solenoid caused the spin of the μ-meson to precess. At the side of the target were located electron counters gated with some delay by two counters which record μ-mesons passing through the carbon filter. A layer of matter is placed in front of the second electron counter, and by changing its thickness it was possible to determine the lower energy bound of the electrons (positrons) recorded.

Measurements were taken with various currents in the solenoid (the magnetic field was as large as 50 gauss). From the dependence of the number of electrons (positrons) recorded by the counters on the magnetic field strength (Figure 3), the following conclusions were made:

1. The μ^+-mesons beam is strongly polarized.

2. The angular distribution of the decay positrons is that given by Equation (6). The magnitude of b is $-1/3$ (with an estimated error of 10%). This means that the positrons leave overwhelmingly in the direction opposite to that of the μ-meson motion.

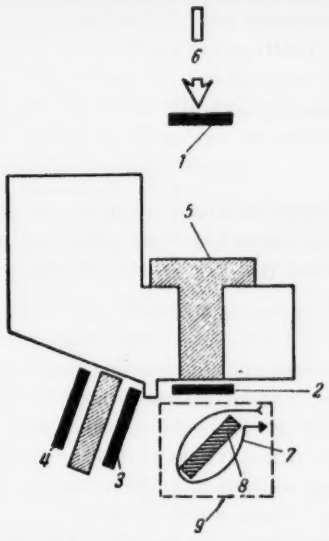

Fig. 2. The experimental arrangement of Lederman and co-workers [13]. 1, 2) Initiating counters (10 x 10 cm); 3, 4) electron counters (15 x 13 cm); 5) carbon absorber to stop π-mesons; 6) 85 Mev π-meson beam; 7) magnetizing current; 8) target; 9) magnetic shield.

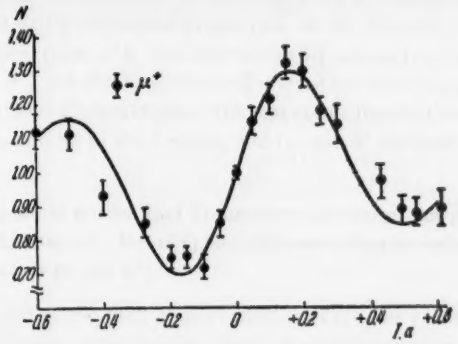

Fig. 3. The dependence of the counting rate for decay positrons from the reaction $\mu^+ \rightarrow e + \nu + \tilde{\nu}$ on the current I in the solenoid. The ordinate gives the counting rate N relative to zero applied field.

3. The gyromagnetic ratio for the free μ-meson is found to be $g = 2.00 \pm 0.10$, which means that the μ-meson has no anomalous magnetic moment.

4. The energy dependence of the μ-e asymmetry is weak.

5. The asymmetry for μ^--mesons is much smaller than that for μ^+-mesons; the value of $\underline{b}$ for μ^--mesons was found to be $-1/20$.

3) The Energy Dependence of the Angular Asymmetry in π-μ-e Decay.

As was shown by Landau [9], for the longitudinal-neutrino theory the angular and energy distribution of the electrons from π-μ-e decay is of the form

$$\frac{dN}{N} = 2\varepsilon^2 d\varepsilon \left[(3-2\varepsilon) + 3b(2\varepsilon-1)\cos\vartheta\right], \tag{9}$$

where ϵ is the ratio between the electron energy and its maximum possible value, and $\underline{b}$ is given by Equation (8). It follows from Equation (9) that the angular asymmetry is strongly energy dependent.

In the original experiments of Lederman and co-workers [13], a weak energy-dependence was observed for the angular asymmetry in π-μ-e decay. Later, however, Lederman and co-workers performed more careful experiments to measure the dependence of the angular asymmetry on the electron energy, and these showed that this dependence is that which may be expected on the basis of the longitudinal-neutrino theory.

Recently Vaisenberg and Smirtinskii [14] have made available results of examinations of correlation in π^+-μ^+-e^+-decay, as observed in Ilford 9-5 emulsions exposed in the stratosphere. Of great interest is the measurement they have performed of the dependence of the angular asymmetry on the positron energy. Of a total number of 2334 π^+-μ^+-e^+-decays investigated, they found 120 cases in which the positron track in the emulsion was longer than 1 mm, which is necessary in order to be able to measure the positron energy on the basis of multiple scattering. The error with which the positron energy was determined varied within the limits of 10-25%, depending on the length of the track. The magnitude of the effect observed and the statistical error of the results can be seen from the following example: by considering positrons of various energies emitted in the forward direction between 0 and 45° and in the backward direction between 135 and 180°, it was established that for energies greater than 25 Mev, 27 positrons were emitted in the forward direction, and 37 positrons in the backward direction; for energies greater than 40 Mev, 6 positrons were emitted in the forward direction, and 21 in the backward direction.

Thus, the energy dependence of the angular asymmetry obtained in experiment is in satisfactory qualitative agreement with the longitudinal-neutrino theory.

4. Electron Polarization in β-decay

Landau's prediction [9] of longitudinal electron polarization in β-decay has been the subject of several experiments [15-17].

The electron polarization was found on the basis of angular asymmetry resulting from single scattering. Since this symmetry is observed only for electrons polarized in the transverse direction, it is necessary to transform the longitudinal electron polarization into a transverse polarization. This was done by passing the longitudinally polarized electrons through an electric field which does not change the spin direction but changes the direction of motion of the electron (when a longitudinally polarized electron moves in a magnetic field, the spin always remains directed along the electron motion).

The experiment of Alikhanov and co-workers [16] was performed on an apparatus operating according to a velocity selection method. The electrons from the β-source are passed through magnetic and electric fields. When the electron velocity is $v = cE/H$ it travels in a straight line. The angle by which the spin direction is changed is $\varphi = 300\ Hl/pc$ (where H is the magnetic field strength in oersteds, l is the electron path in the magnetic field in centimeters, p is the electron momentum in ev/c, and c is the velocity of light). The design of the apparatus had the following advantages:

1) the electron spin could be turned through any angle (which makes it possible to work with a wide range of electron velocities);

2) the resolving power of the apparatus could be decreased by varying E and H (and maintaining E/H constant), which greatly increases the intensity, and hardly alters the measured effect;

3) due to the simple geometry, it is easily possible to obtain the necessary accuracy in constructing the apparatus. Changing the electric and magnetic fields to their opposite values excluded asymmetries due to the apparatus.

On leaving the apparatus the electrons were scattered by a gold foil. The scatterer was placed at an angle of 45° to the electron beam. Two Geiger counters in coincidence were used to record electrons passing through the foil and those scattered through an angle of 90 ± 4°. The counters were separated by an absorber to eliminate low-energy electrons. The counters, together with the scatterer, could be rotated to any angle about the axis passing through the beam center.

A strontium-yttrium source was used. The maximum β-energy from Sr^{90} is 540 kev (β-decay with a parity change $\Delta I = -2$), and the maximum β-energy from Y^{90} is 2260 kev (β-decay with a parity change $\Delta I = +2$).

The measurements were performed at two electron energies: 300 kev (electrons from Sr β-decay) and 1000 kev (electrons from Y β-decay).

At an electron energy of 300 kev (E = 18.3 kv/cm, H = 79 oersteds, v/c = 0.775, and the angle of spin orientation is about 50°), the following series of measurements were performed: I) with a source thickness of about 4 mg/cm² and a scatterer thickness of 0.537 mg/cm²; II) with a source thickness of 1.5 mg/cm² and a scatterer thickness of 0.537 mg/cm²; III) with a source thickness of about 4 mg/cm² and a scatterer thickness of 0.17 mg/cm².

In all cases no asymmetry was observed in the plane of rotation of the spin, but an asymmetry was observed in a plane perpendicular to it. When the fields were replaced by their negatives, the asymmetry changed sign. The sign of the asymmetry corresponded to electrons emitted in β-decay being polarized antiparallel to their direction of motion.

The degree of polarization of the electrons was the following: in experiments I, (0.63 ± 0.09) v/c, and in experiment II, (0.77 ± 0.16) v/c.

The difference between I and II makes it possible to account for depolarization in the source.

On the other hand, comparison of the scattering intensities in I and III made it possible to determine the amount of multiple scattering in the thicker scatterer, using the method of Alikhanian and co-workers [18]; this

fraction is about 30%. Since azimuthal asymmetry in scattering of polarized electrons depends strongly on the scattering angle and drops sharply for angles less than 90°, the asymmetry effect is small for electrons undergoing multiple scattering. This means that the results of I and II must be corrected, and that this correction is of the order of 30%; this leads to an asymmetry in good agreement with the longitudinal-neutrino theory.

For an electron energy of 1000 kev (E = 20 kv/cm, H = 71 oersteds) the measurements were performed with a source thickness of about 4 mg/cm^2, a gold foil thickness of about 1.9 mg/cm^2, and an absorber between the counters made of aluminum (0.08 g/cm^2) and copper (0.08 g/cm^2) (this absorber stopped electrons with energies less than 600 kev). The experimentally observed degree of polarization for these electrons was (0.8 ± 0.17) v/c. The measured correction due to multiple scattering is 6%.

Since in the electron energy region about 1000 kev the energy resolving power of the apparatus is small, the number of particles scattered into the counter is practically independent of the applied fields. This made it possible to perform a control experiment in the absence of an electric or magnetic field, and this experiment showed that the asymmetry in this case is not observed.

In the experiment of Frauenfelder and others [15], the longitudinal electron polarization was rotated to the transverse direction by passing the electrons through a cylindrical condenser. The measurements were performed with a Co^{60} source (allowed β-transition, $\Delta I = 1$). The electron energies investigated were 50, 68 and 77 kev. No corrections were used for depolarization of the electrons in the source, or for the thickness of the scatterer (the gold foil thickness was 0.15 mg/cm^2 for all energies and 0.05 mg/cm^2 at 77 kev). The results obtained are in qualitative agreement with the longitudinal-neutrino theory.

The source used in the experiment of Nikitin and co-workers [17] was Cu^{64} (allowed β-decay, $\Delta I = 1$). The source thickness was no greater than 2 mg/cm^2. The longitudinal polarization was transformed to transverse polarization by passing the electrons through a cylindrical condenser. A gold scatterer 0.12 mg/cm^2 thick was used. Electrons scattered through an angle of 90° were observed (both passing through the foil and reflected). The electron energy was 145 kev (v/c = 0.63). The measurements were performed on two instruments: in the first the electrons were rotated by an electric field through 108°, and in the second through 90°. For the electrons that passed through the foil, the calculations from the measured asymmetry give a degree of polarization equal to: for the first apparatus (1 ± 0.15) v/c, and for the second apparatus (0.77 ±0.15) v/c. Depolarization of the electrons in the source and multiple scattering in the foil were not accounted for. The asymmetry was much smaller for the "reflected" electrons, which indicates the important role of multiple scattering.

All the above experiments indicate uniquely that parity and charge conjugation are not conserved in weak interaction involving the neutrino, and make it reasonable to assume that the neutrino is a longitudinal particle.

LITERATURE CITED

[1] T.D. Lee and C.N. Yang, Phys. Rev. 104, 256 (1956).

[2] B.L. Ioffe, L.B. Okun' and A.P. Rudik, On the Question of Parity Nonconservation in Weak Interactions, J. Exptl.-Theoret. Phys. (in press).

[3] T.D. Lee, R.O. Ohme and C.N. Yang, Remarks on Possible Noninvariance under Time Reversal and Charge Conjugation, Phys. Rev. (in press).

[4] W. Pauli, Niels Bohr and the Development of Physics. Pergamon Press, London, 1955; G. Lüders, Dan. Mat. Fys. Medd. 28, No. 5 (1954).

[5] M. Gell-Mann and A. Pais, Phys. Rev. 97, 1387 (1955).

[6] R. Lande, E.T. Booth, J. Impeduglia, L.M. Lederman and W. Chinowsky, Phys. Rev. 103, 1900 (1956); W.F. Fry, J. Schneps and M.S. Swami, Phys. Rev. 103, 1904 (1956).

[7] B.L. Ioffe, On Two Possible Methods of Parity Nonconservation in Weak Interactions, J. Exptl.-Theoret. Phys. (in press).

[8] L.D. Landau, On the Conservation Laws for Weak Interactions, J. Exptl.-Theoret. Phys. (in press); Nuclear Physics 3, 127 (1957).

[9] L.D. Landau, Concerning a Possible Polarizing Property of the Neutrino, J. Exptl.-Theoret Phys. (in press); Nuclear Physics 3, 129 (1957).

[10] T.D. Lee and C.N. Yang, Possible Parity Nonconservation and Two Component Theory of the Neutrino, Phys. Rev. (in press).

[11] A. Salam, Nuovo Cimento (in press).

[12] C.S. Wu, E. Ambler, R.W. Hayward, D.D. Hoppes and R.P. Hudson, An Experimental Test of Parity Conservation in Beta Decay, Phys. Rev. (in press).

[13] R.L. Garwin, L.M. Lederman and M. Weinrich, Observation of the Failures of Conservation of Parity and Charge Conjugation in Meson Decays, the Magnetic Moment of the Free Muon, Phys. Rev. (in press).

[14] A.O. Vaisenberg and V.A. Smirtinskii, An Investigation of Correlation in π-μ-e Decays, J. Exptl.-Theoret. Phys. (in press).

[15] H. Frauenfelder et al., Phys. Rev. (in press).

[16] A.I. Alikhanov, G.P. Eleseev, V.A. Liubimov and B.V. Ershler, Polarization of Electrons in β-Decay, J. Exptl.-Theoret. Phys. (in press).

[17] M.E. Vishnevskii, V.K. Grigor'ev, V.A. Ergakov, S.Ia. Nikitin, E.V. Pushkin and Iu.V. Trebukhovskii, On the Polarization of Electrons in β-Decay, Nuclear Physics (in press).

[18] A.I. Alikhanian, A.I. Alikhanov and A.O. Vaisenberg, J. of Phys. 9, 280 (1945).

Received April 8, 1957

CERTAIN FEATURES OF THE VISCOSITY AND HEAT CONDUCTIVITY OF LIQUIDS AND GASEOUS MATERIALS

I. I. Novikov

In studies of the viscosity and heat conductivity of liquids and gaseous materials, particularly those which find application in nuclear reactors, we have noticed an interesting feature of the values of the viscosity and heat -conduction coefficients of liquids and the gaseous phase. This effect has apparently not been noticed up to this time and may be of some practical interest.

It is well known that in the liquid state the viscosity coefficient falls off with increasing temperature; on the other hand in the gaseous state, including the saturation point, this parameter increases with temperature, that is the temperature dependence of the viscosity is exactly opposite in the liquid and vapor phases. We may note that the density of the liquid and vapor phases changes in a similar way.

Temperature	Reference to literature		Value of $\frac{1}{\mu'}+\frac{1}{\mu''}$	
	liquid phase	vapor phase	computed from the experimental data	computed from Equation (2)
—15	0.001155	0.000165	6960	6930
—10	0.001112	0.000167	6880	6860
0	0.001007	0.000174	6740	6730
10	0.000869	0.000183	6620	6600
20	0.000701	0.000203	6350	6470
30	0.000475	0.000235	6360	6340
31	0.000316	0.000316	6330	6330

Since the equilibrium phase curve is symmetrical in the region of the critical point it is to be expected that the viscosity coefficient of the liquid phase μ' in equilibrium with its saturated vapor and the viscosity coefficient of a saturated vapor or vapor phase μ'' close to the critical point, i.e., at temperatures close to the critical temperature t_{cr}, will satisfy the relation

$$\frac{1}{\mu'}+\frac{1}{\mu''}=\frac{2}{\mu}+a\,(t_{cr}-t), \qquad (1)$$

where μ is a constant which is numerically equal to the value of the viscosity coefficient at the critical point. This relation is analogous to the well-known equation for the densities of a saturated vapor and a liquid in equilibrium with it in the region of the critical point.

From a comparison with the experimental data it is found that the sum $\frac{1}{\mu'}+\frac{1}{\mu''}$, remainsmore or less constant at temperatures not very different from t_{cr}, falling off slightly with increasing temperature and more or less following a linear relation.

It is apparent from the table that in CO_2 the following relation is obeyed with reasonable accuracy

$$\frac{1}{\mu'}+\frac{1}{\mu''}=6330+13\,(t_{cr}-t). \qquad (2)$$

The heat conductivity coefficients for the liquid and vapor phases display a similar dependence, the heat conductivity coefficient λ' of the vapor phase increases with increasing temperature while that of the liquid phase λ'' falls off. Hence the heat conductivity coefficient of a saturated vapor in equilibrium with its liquid also obeys a relation similar to (2) i.e.,

$$\frac{1}{\lambda'}+\frac{1}{\lambda''}=\frac{2}{\lambda}+b\,(t_{cr}-t). \qquad (3)$$

Received February 22, 1957

THE MASS OF He^3

R.A. Demirkhanov, T.I. Gutkin and V.V. Dorokhov

The mass of He^3 was determined by the mass spectrograph which was described in Reference [1]. A mixture of helium isotopes was used enriched to 99.5% of He^3.

For a check of their "internal consistency" the masses were measured in the doublets

$$H^3 - He^3 \text{ and } HD - He^3.$$

The results were also controlled by the $HD - H^3$ doublet in the same spectrum as the He^3, (see the figure). The mass scale was calibrated by the spectrum of $N^{14}H - N^{14}H_2 - N^{14}H_3$. The experimental data were utilized as described in [1].

The value of M_{av} from ΔM for the doublets $H^3 - He^3$ and $HD - He^3$ was 3.0207 and 3.0199 mass units, respectively.

TABLE 1

Reaction	Reference to literature	Q in Mev	Q calculated from the present work in Mev
He^3 (d, p) He^4	[2] (1949)	18.45 ±0.17	18.336±0.005
D (d, n) He^3	[3] (1949) and [4] (1951)	3.265±0.009	3.275±0.004
D (d, n) He^3	[5] (1952)	3.24 ±0.04	3.275±0.004
D (d, n) He^3	[6] (1953)	3.25 ±0.06	3.275±0.004
D (p, γ) He^3	[7] (1953)	5.50 ±0.03	5.501±0.003

TABLE 2*

Reaction	Reference to literature	Mass of He^3 by comparison with other masses	Mass of He^3 in mass units
He^3 (d, p) He^4	[2] (1949)	He^4—0.986781±170	3.017092±170
D (d, n) He^3	[3] (1949) and [4] (1951)	D+1.002248±9	3.016988±10
D (d, n) He^3	[4] (1952)	D+1.002274±13	3.017014±13
D (d, n) He^3	[6] (1953)	D+1.002273±60	3.017013±60
D (p, γ) He^3	[7] (1953)	D+1.002235±30	3.016975±30
	Present work (1956)	D+1.002234±2	3.016970±2
	[8] (1955)	D+1.002246±5	3.016986±5

*Errors are given in mass units · 10^{-6}.

Table 1 gives the values of Q measured directly in nuclear reactions and calculated from the results of the present work. The table shows best agreement of the values of Q for the D(p, γ)He^3 reaction. In this case best agreement was also found for the mass of He^3 (Table 2).

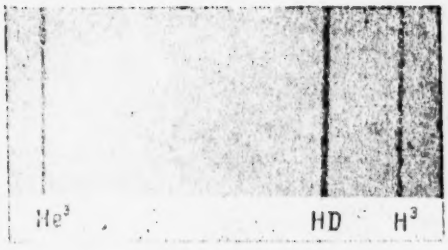

Photograph of the mass-spectrographic triplet $He^3 - HD - H^3$ (x 50).

Thus our value for the mass of He^3 is in good agreement with the most recent results obtained in nuclear reactions.

LITERATURE CITED

[1] R.A. Demirkhanov, T.I. Gutkin, V.V. Dorokhov and A.D. Rudenko, Atomic Energy 2, 21 (1956) (T.p. 163).*

[2] L. Wyly, V. Sailor and D. Ott, Phys. Rev. 76, 1532 (1949).

[3] A. Tollestrup, F. Jenkins, W. Fowler and C. Lauritsen, Phys. Rev. 75, 1947 (1949).

[4] C. Li, W. Whaling, W. Fowler and C. Lauritsen, Phys. Rev. 83, 512 (1951).

[5] H. Bichsel, W. Halg, P. Huber and A. Stebler, Helv. Phys. Acta 25, 119 (1952).

[6] A. Dyer and J. Bird, Austr. J. Phys. 6, 45 (1953).

[7] G. Griffiths and J. Warren, Phys. Rev. 92, 1084 (1953).

[8] A. Wapstra, Physika 21, 367 (1955).

Received December 29, 1956

*T.p. = C.B. Translation pagination.

SCIENCE CHRONICLE

SEVENTH ANNUAL CONFERENCE ON NUCLEAR SPECTROSCOPY AT LENINGRAD

The 7th Annual Conference on Nuclear Spectroscopy was held in Leningrad from January 25th to 31st of the present year. About 500 scientists from various research institutes and universities participated as well as foreign scientists from the Chinese People's Republic, France, Poland, Czechoslovakia, Rumania, Bulgaria, the German Democratic Republic and Yugoslavia. There were 10 sessions at which 3 reviews and about 90 brief original reports and communications were heard. We shall discuss only the most important papers. The proceedings of the conference will be published in detail in the "Izvestia Akademiie Nauk SSSR" (Physical Series).

Nuclear Shells, α- and β-Decay

In the review by L.A. Sliv (LPTI – Leningrad Physico-Technical Institute) of progress made with the collective model of the nucleus it was noted that new important advances during the past year confirm the value of this model for the understanding of low-lying excited nuclear states. Recently rotational levels of light nuclei have been observed ($23 < A < 28$). In heavy nuclei, vibrational levels of two types have been found, which correspond to different kinds of nuclear deformations. The extensive experimental data available at present are in good agreement with theory. The collective model will undoubtedly continue to be useful for the explanation of nuclear structure.

L.K. Peker (BAN – Belorusskaia Academy of Sciences) reported on work which he did in conjunction with L.A. Sliv on the characteristics of the transition from an elliptical to a spherical nuclear shape for $A = 190$. From an analysis of the levels of ${}_{76}Os^{190}_{114}$, ${}_{76}Os^{192}_{116}$, ${}_{78}Pt^{192}_{114}$, ${}_{76}Os^{191}_{115}$, ${}_{77}Ir^{191}_{114}$ it was shown that this transition occurs abruptly in a narrow range of Z (from 76 to 78) and N (from 114 to 116) and is manifested in a change of the character of the collective and single-particle levels.

In another paper L.K. Peker considered the spins and parities of deformed odd-odd nuclei. The ground states of such nuclei in all of the known 35 cases are well described by the relation $I = (\Omega_p + \Omega_n)$ derived from the Bohr-Mottelson model. Analysis of more than 70 nuclei showed that in all deformed nuclei, provided that the deformations of neighboring nuclei (of the periodic table) are close in magnitude, the levels are filled with nucleons in exactly the same way. It is therefore possible to tabulate the values of Ω_p and Ω_n for each Z and N, which enables us in many instances to predict the spins and parities of both odd-odd nuclei and nuclei with odd A. Similar considerations make it possible in the majority of cases to determine the spins and parities of the first excited states of odd-odd nuclei.

L.V. Grosnev of the IAE (Atomic Energy Institute) discussed the interesting question of the appearance of multiplets close to the ground states of odd-odd nuclei ($A < 60$), which is associated with the different interactions of odd nucleons with different spin orientations. When high-order multiplets exist in nuclei a new type of isomerism is possible – transitions with spin changes of 3 to 5 units and parity conservation.

P.E. Nemirovskii of the Atomic Energy Institute reported an interesting attempt to obtain the scheme of one-particle levels for nuclei with $A < 50$ from a potential well model.

The alpha decay of heavy nuclei was the subject of three theoretical reports. K.A. Ter-Martirosian and L.L. Gol'din (TTL)* reported on the alpha decay of nonspherical nuclei. A theoretical calculation was made of alpha decay to different levels belonging to the same rotational band. It was assumed that the alpha particle penetrates a potential barrier that results from a uniformly charged elliptical nucleus. The fine structure of alpha decay of even-even nuclei was reported on by V.G. Nosov of the Atomic Energy Institute. He suggested a method

of calculating the relative probability of excitation of rotational states as a function of the deformation of the daughter nucleus. V.M. Strutinskii (IAE) reported on a calculation of the probability of excitation of the second rotational level in even-even nuclei during alpha decay assuming small deformation of the daughter nucleus.

The values obtained for the relative intensities of fine structure lines are in most cases in good agreement with experiment. An experimental study of the alpha spectra fine structure of Pu^{238} and Pu^{239} was discussed by L.N. Kondrat'ev and G.I. Novikova (TTL). G.E. Kocharov (LPTI) reported an investigation of the alpha spectra of U^{234} and U^{238} using a gridded pulse ionization chamber. A similar method for the study of the alpha spectra of Th^{230} and Pu^{238} was reported by A.G. Zelenkov (IAE).

I.S. Shapiro (PIAN – Physics Institute of the Academy of Sciences) reviewed the question of parity-nonconservation in beta decay. For the purpose of explaining the results obtained from the study of K-mesons it has been suggested that parity is not conserved in weak interactions. Since the interaction in beta decay is weak it is assumed that in this case the parity is not an integral of the motion. Theoretical investigations of Soviet and foreign physicists have shown that rejection of the customary concept of parity leads to the possible existence of several very interesting effects which can be checked experimentally.

The "combined parity" theory recently proposed by L.D. Landau is worthy of special attention. When this theory is applied to beta decay it yields an angular asymmetry of the beta particles and longitudinal polarization of the neutrinos. This theory also requires a physical distinction between neutrinos and antineutrinos.

One of the facts supporting the existence of antineutrinos may be the result of an investigation of double beta decay of Ca^{148} by E.I. Dobrokhotov, V.R. Lazarenko and S.Iu. Luk'ianov (IAE). Measurements with a greatly reduced background showed that the halflife for this process assuming the absence of angular correlation of decay electrons is greater than 10^{18} years. If the neutrino and antineutrino are identical the theory gives a halflife of 10^{16} years.

Decay Schemes

Decay schemes were discussed at three sessions. Many short reports were heard concerning work done principally in the Leningrad Institutes. Much new data had been obtained on the structure of nuclear levels. The experiments discussed had been performed mainly with radioactive isotopes produced by reactors or accelerators. Measurements were made with magnetic and scintillation spectrometers. Radiospectroscopy was used by A.A. Manenkov, A.M. Prokhorov, P.S. Trukhlaiev and G.N. Iakovlev (PIAN) to measure the spin and magnetic moment of Eu^{152}. Note should be made of the extremely small number of experiments for the determination of nuclear levels from the angular and energy distributions of particles and quanta produced in nuclear reactions. There is great interest in a number of experiments by Leningrad physicists to determine the beta and gamma spectra of neutron-deficient isotopes of the rare earths, about which little is now known. The isotopes were produced by irradiating tantalum, uranium and hafnium with 600-Mev protons and were separated chromatographically. In a study of the spectra of gadolinium G.M. Gorodinskii, A.N. Murin and V.N. Pokrovskii (RIAN – Radium Institute of the Academy of Sciences USSR) discovered two new isotopes Gd^{147} and Gd^{145} (the latter mass number being hypothetical), with halflives of 1.5 and 60 days; the gamma spectra were also measured. The other experiments improved the radiation measurements for other rare earth isotopes.

An interesting report on the nuclear isomerism of Hf^{187m} was presented by V.S. Gvozdev (LPTI). He has detected two parallel isomeric transitions of 51.7 kev (El) and 501.2 kev (Es). The experimental lifetimes differ from those calculated by formulas for one-particle transitions by factors of 10^{16} and 10^{9}. The extremely long lives are explained by the higher-order forbiddenness (K forbiddenness) of these transitions in Hf^{187m}.

There were some reports from foreign scientists. Kouchka of Yugoslavia spoke of his study of the level structure of Tu^{169} and Tu^{171}. The 0-0-transition in $_{40}Zn^{90}$ from the beta decay of Y^{90} was discussed by Laberigue-Frolova of France. Conversion positrons and electrons were detected corresponding to a 1.74 Mev transition (E0). It was shown that to the 1.74 Mev level less than $3 \cdot 10^{-6}$ of the total number of beta decays in Y^{90} occur. Mladenovich of Yugoslavia reported on a nuclear spectroscopy laboratory established in Belgrade. The laboratory equipment includes a magnetic spectrometer with uniform field which records on photographic plates, a longitudinal coincidence spectrometer and a double-focusing spectrometer not containing iron.

Nuclear Gamma Radiation

Nuclear gamma rays were discussed in two sessions. In reviews B.S. Dznelepov (RIAN), E.E. Berlovich (L TI), I.Kh. Lemberg (L TI), Iu.A. Nemilov (RIAN) and L.K. Pekar (BAN) discussed the determination of lifetimes and widths of nuclear levels from gamma-ray measurements in Coulomb excitation of nuclei, (p, γ) and (n, γ) reactions and resonance scattering.

N.A. Burgov and Iu.V. Terekhov (TTL) reported on a study of the resonance scattering of gamma rays from Mg^{24}. They estimated the width of the 1.38 Mev level at 3×10^{-4} ev. Similar work was reported by N.N. Deliagin (2 NIFI-MGU – 2nd Physics Research Institute of the Moscow State University). D.G. Alkhazov (L TI) and his collaborators studied the Coulomb excitation of unseparated tin isotopes. This work was done with an extracted cyclotron beam of 13.1-Mev alpha particles. Previously unknown first excited levels of Sn^{112}, Sn^{118} and Sn^{124} were observed.

The E0-transition was discussed in theoretical papers of L.A. Sliv (LPTI), L.K. Peker (BAN) and D.P. Grechukhin (IAE). In the first paper for the purpose of determining the relative number of E0-transitions it was proposed to investigate nuclei with odd A and with two successive spin 1/2 levels. Between these only E0 and M1-transitions are possible. By measuring the internal conversion coefficient it is easily possible to calculate the fraction of E0-transitions. Such conditions apparently exist in In^{115}, Hg^{199} and Au^{197}. In the second paper a detailed account was given of processes arising through E0-transitions and matrix elements for a number of nuclear models were evaluated.

I.V. Estulin (2 NIFI-MGU) reported on measurements of soft gamma rays resulting from nuclear capture of thermal neutrons.

Spectroscopic Techniques

At two sessions reports were heard of newly-developed methods in alpha, beta and gamma spectroscopy. All of the work on magnetic spectrometers shares an attempt to increase the luminosity of the instruments and to eliminate all aberrations in order to increase the resolving power. Special mention must be made of a report by V.N. Lukashev (2 NIFI-MGU) on the calculation of a magnetic spectrometer using large solid angles with good resolution, as well as one by Iu.V. Vandakurov (LFTI) on the design of a magnetic spectrometer whose axial trajectory is a spiral of slowly varying radius. This instrument should possess dispersion several times greater than that of a spectrometer with $\pi\sqrt{2}$ focusing.

A.F. Malov (IAE) reported that such increase of dispersion is also possible in a spectrometer with a fixed-radius orbit for given focusing angles. He spoke of a combination of axially symmetrical electric and magnetic fields for the energetic analysis of charged particles.

Several reports were devoted to the measurement and stabilization of magnetic fields in magnetic spectrometers.

The gamma spectroscopy of weak sources has been limited principally by the quality of photomultipliers and scintillators. Therefore in addition to papers on new devices and methods of measurements the program of the sessions included talks by representatives of factories and research institutes which are concerned with the development and production of photomultipliers. Mention must be made of the report by A.N. Pisarevskii on a new multiplier developed under the supervision of G.S. Vil'drub, with louvered dynodes and combining small time spread with good spectrometric characteristics. The participants in the discussion commented on the clearly unsatisfactory rate of development of the new photomultipliers. Impatience is caused especially by the fact that multipliers which have been tested in many laboratories and have been approved have not yet been put into large scale production.

The final session heard reports on the polarization of the vacuum in mesic atoms, the angular distribution of annihilation gamma rays in germanium and the detection of the beta rays from natural C^{14} by scintillation methods. It was announced that American physicists have experimentally established the nonconservation of parity by observation of asymmetry in the beta decay of muons and polarized cobalt nuclei.

In a final talk B.S. Dzhelepov (RIAN), while commenting on the favorable aspects of the present conference, expressed the hope that there will be an increase in the number of investigations of fundamental problems of nuclear physics. The conference was conducted in a competent and friendly manner.

R.M. Polevoi and I.N. Serikov

WITHIN THE SOVIET UNION

AT THE ATOMIC PAVILION OF THE ALL-UNION INDUSTRIAL CONFERENCE (SAFETY METHODS SECTION)

The displays of this division showed various methods of protecting human beings from external radiation and from radioactive substances in the form of gases and aerosols which enter the organism or make contact with the skin. There was a varied display of monitoring devices for controlling the level of radiation and producing danger signals when a safe level is exceeded, as well as of tables and charts for determining safe conditions of work with radioactive sources.

In the Soviet Union in work connected with the use of radioactive isotopes special precautionary and shielding measures are used to prevent harm from ionizing radiation.

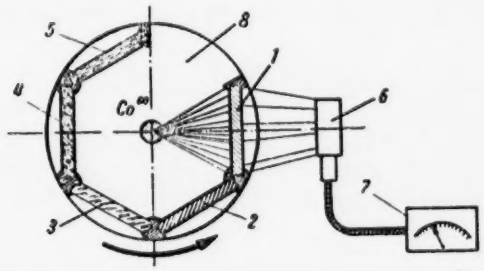

Fig. 1. Diagram of apparatus for demonstrating shielding capacity of materials: 1) lead; 2) iron; 3) lead glass; 4) concrete; 5) water; 6) ionization chamber; 7) microroentgenometer; 8) rotating platform.

The section showed tables of tolerance levels of ionizing radiation (approved by the VGSI, January 14, 1957, No. 233-57) which guarantee that protracted periods of work with radioactive isotopes will not injure the health.

The exhibit presented different methods of shielding from penetrating radiation. The shielding properties of such materials as lead, iron, lead glass, concrete and water are demonstrated by the apparatus shown in Figure 1. Samples of shielding materials (lead, iron, lead glass and concrete) were made in the form of blocks measuring 240 x 195 x 50 mm; the water was poured into a plexiglass tank of the same dimensions. The radiation source and the recording instrument are fixed while the shield blocks are rotated on a platform. This arrangement determines the size of the dose from a point source of radioactive cobalt (Co^{60}) placed behind the shielding material. The attenuation factor of each material of a given thickness is automatically indicated on an illuminated chart.

Work with highly active materials is performed in so-called "hot cells." In these rooms work is done behind lead or concrete shields by means of remote-control manipulators.*

Special tongs, grips and pincers with long arms are demonstrated for safe work with beta emitters because of the great distance from the source.

The exhibit shows the methods of designing and equipping laboratories which use radioactive materials.

There is an exhibit of sealed boxes with protective gloves fixed into their walls and manipulating blades for work with open radioactive materials.

There is an extensive display of methods of personnel protection during work with open radioactive substances:

Coveralls of white cotton for work with radioactive materials up to 10 microcuries;

*Atomic Energy No. 1, 102 (1956).

Aprons, sleeves, jackets and overalls made of polyvinylchloride over a cotton coverall for work above 10 microcuries;

The ShB-1 "Lepestok" valveless antidust mask. This mask is 99.9% effective under a respiratory pressure of 2-3 mm of water. This mask is designed for work during one shift;

Helmets with forced air supply;

LG-2 protective suits with force air supply (Figure 2). This suit is designed for repair and emergency work. The separate pieces of the masticated rubber coverall are joined by a high-frequency process. This insures uniformity of the material and permits the use of efficient acids and alkalis for deactivation;

Fig. 2. LG-2 breathing suit.

Various kinds of footwear: galoshes, slippers and shoes made of polyvinylchloride and rubber, from which radioactive contamination is easily washed.

In practice, extensive use has been made of a filtering material made of perchlorvinyl for ventilator filters, masks, etc.

There is a large display of radiation monitoring and measuring devices. A portable battery roentgenometer covering the range from 0.5 to 5000 microcuries per second is worthy of mention.

Mention must be made of a universal radiation meter for measuring the contamination of hands and working surfaces with alpha and beta emitters. This instrument is equipped with both gas discharge and luminescence counters, a dial and a signal lamp.

Extensive use is being made of a fixed monitoring devices with light and sound signals for controlling the radiation level in industrial establishments. This type of instrument is represented by a stationary dosimeter which measures from 0.2 to 20,000 microroentgens per second with an automatic signal (1 microroentgen per second threshold), and a signaling and measuring dosimeter, for simultaneous control of 12 rooms.

Methods of personnel monitoring are represented by sets including pocket condenser-type air-filled ionization chambers with air-equivalent walls, which are designed for integral dosage measurements. Two types are demonstrated:

1. The KID-1 paired ionization chambers with the ranges 0-0.2 roentgens and 0-2 roentgens. The set includes a charging and measuring device.

2. The DK-0.2 with a range of 0 to 200 milliroentgens. The dose is read directly from a scale mounted together with a microscope in the chamber wall. A charging unit is included.

Instruments for the measurement of fast neutron flux are also exhibited.

The exhibits demonstrate safe methods of working with radioactive isotopes and methods of general and individual protection.

The Safety Methods Section has attracted considerable attention among visitors to the exposition and will be considerably enlarged in 1957.

Z. Chetverikova and L. Kimel'

DESIGN OF A NEW LABORATORY FOR THE STUDY OF RADIOISOTOPES AND THEIR APPLICATIONS IN METALLURGY AND PHYSICS OF METALS

The State Planning Institute for Metallurgical Plants ("GIPROSTAL") of the Ministry of Heavy Metallurgy of the Ukrainian SSR has worked out the design of a research laboratory for the study of radioactive isotopes and their industrial applications to processes such as detection of defects by use of γ rays, investigation and control of smelting processes, scale formation, improvement of the composition of blast furnace mixtures, investigation of the structure of alloys, stability of brick linings, etc.

The laboratory will be located in a separate one-story building occupying an area of approximately 800 square meters. The building will be divided into three zones: a "dirty," a "semi-clean," and a "clean," in order to insure maximum safety for the laboratory workers.

The "dirty" zone is designed for direct handling of radioactive isotopes; it includes storage space for radioactive material, a room for preparing the isotopes, a corridor divided into compartments for repairs, "dirty" parts of the safety compartments (boxes), a chamber for decontamination of instruments and a space for the air purification filters. This zone will be hermetically sealed from the rest of the laboratory building.

During repairs and in cases of accident the radioactive isotopes would be admitted into the "semi-clean" zone. This zone will have space for work with radioactive isotopes (on the "clean" side of the safety compartments), detection of defects by γ radiation, high-frequency generator for the smelting furnaces, and also rooms for x-ray photography, microscopy and dosimetry, a storage room for instruments and a repair shop.

The "semi-clean"zone will be connected with the "dirty" zone by hermetically sealing safety compartments and a floodgate, and with the "clean" zone by a special sanitary passageway.

The "clean" zone (free from radioactivity) will include a room for precision instruments, a dark room, an office for the laboratory director, a hall and a space for clean clothes.

Concrete wells and steel safes will be provided for the storage of radioactive isotopes. The isotopes will be prepared in a special "hot" room equipped with a manipulator and other necessary installations. The protective compartments will be equipped with hot and cold water, plumbing for drainage, outlets for compressed air, gas, and vacuum, daylight electric light, etc. The transfer of isotopes from the preparation room into the compartments and between compartments will be accomplished by a conveyor belt mounted on hermetic casings.

The safety compartments are designed to house balances, laboratory glassware and instruments, hand and mechanical mortars, mixers, manipulators, various electric ovens and a portable machine tool for mechanical working of the metal. The air in the compartments will be maintained below atmospheric pressure; the air leaving the safety compartments will be filtered and drawn into the general exhaust system.

General air conditioning is planned, with an exchange capacity 10 times the total air volume.

A special room protected from radiations will be provided for the instruments of the detection of defects by γ rays. The instruments and doors will be provided with electromechanical blocking devices preventing the possibility of accidental radiation escape. The transportation of the objects to be submitted to radiation will be mechanized.

The floors in the "dirty" and "semi-clean" rooms will be covered with polyvinyl-chloride plastic, linoleum, or mat-lock plates; the walls and floors of these rooms are to be painted with an oil paint. Entry and exit from the "dirty" and "semi-clean" rooms will be possible only through the sanitary passages. The cleaning of radio-

actively contaminated dishes, instruments, and filter containers will be performed in a washer and in a decontaminating chamber.

The laboratories for work with radioactive materials are planned to be equipped with dosimetric control.

In order to control the activity of waste water and to dilute it to a safe concentration an ordinary household plumbing system and a special plumbing system are planned; the special plumbing will include an intermediate reservoir. Solid radioactive waste will be removed from the laboratory on conveyors and buried.

The new laboratory will have a number of advantages with respect to those existing; it will satisfy all the fundamental requirements for laboratories where work with radioactive materials is being performed.

V.S. and N.L.

POWERFUL GAMMA RAY EMITTERS FOR INVESTIGATIONS IN PETROLEUM CHEMISTRY

The All-Union Research Institute for Oil and Gas Processing and the Production of Artificial Liquid Fuel in the Petroleum Industry Ministry of the USSR has designed a laboratory to use radiation from cobalt.

The laboratory consists of three powerful gamma ray emitters in separate compartments with concrete shielding and will be housed in a separate one-story building. One of the radiators which is equivalent to 16,000 grams of radium can give doses up to 500 r/sec; the other two radiators are each equivalent to 800 grams of radium and can supply 80 to 90 r/sec.

Operating personnel will be protected by blocking and signal devices. The apparatus will be remote-controlled.

The apparatus is intended for research in petroleum processing and petroleum chemistry, especially for the study of the polymerization of unsaturated hydrocarbons, the oxidation of paraffin, aromatic and unsaturated hydrocarbons, etc.

V.S. and N.L.

DETERMINATION OF THE MOISTURE CONTENT OF STRUCTURAL MATERIALS BY MEANS OF GAMMA RAYS

The lack of reliable external methods of determining the moisture content of materials without interruption of an experiment and the destruction of the specimen under investigation has been a serious handicap in the study of moisture transfer, which is of great importance in the theory of drying, structural physics and some other branches of science.

Electrical methods have not been successful with all materials and only above the minimum temperature. Some moisture gauges which show a large time lag are not reliable. Weighing methods of determining moisture content require interruption of experiments and damage to the specimen, so that they are unsuited for the study of moisture migration. In their search for a method which is free of the shortcomings that have been mentioned the authors have constructed apparatus for measuring moisture content in structural materials by transillumination with a beam of gamma rays from radioactive isotopes.

The principle of this method, which is extensively used in the study of metal defects, is the attenuation of the gamma ray beam as a function of the density and thickness of the material.

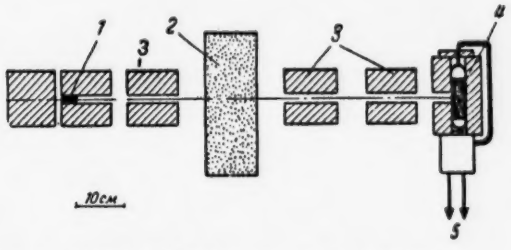

Fig. 1. Diagram of the apparatus: 1) gamma ray source; 2) sample of material; 3) lead diaphragms; 4) gamma ray counter; 5) to type B apparatus.

In gamma ray studies of moisture content it is assumed that the attenuation of the gamma ray beam in a moisture-containing material is equal to the combined attenuation of the same beam by the dry material and a layer of moisture whose combined weight is that of the moist material. This hypothesis has been confirmed experimentally with an accuracy which is suitable for practical purposes.

Figure 1 is a diagram of the apparatus. A radioactive sample of Co_{27}^{60} or Cs_{55}^{137} with an activity of 7-10 microcuries is placed in a lead gun (of 50 mm wall thickness) with a narrow cylindrical passage (of 8-10 mm diameter). The gamma ray beam which emerges from the gun passes through the specimen and after attenuation enters a gamma ray counter (AMM-4, STS-5) in a lead housing. The gamma count is obtained from a standard type B scaler.

For accuracy, the gamma ray beam must be well collimated by the three lead diaphragms, each of which is 100 mm thick.

The moisture of materials is determined as follows: The pulse count per unit time is determined:

1. For the natural background (in the absence of the gamma ray source).

2. During passage of the gamma ray beam:
a) in the absence of the specimen (J_0);
b) through the dry specimen (J_1);
c) through the moist specimen (J_2).

For the calculations we used the expression

$$\ln\left(\frac{J_1}{J_0}\right)-\ln\left(\frac{J_2}{J_0}\right)=\mu_{water}d_{water}$$

where μ is the absorption coefficient and d is the thickness of the layer.

For the investigation of moisture migration the measurement can be performed at the end of the experiment on a dried specimen or on parallel specimens.

Against a natural background of 10-15 pulses per minute and for a count of 300-500 pulses per minute accuracy was achieved by continuing the count for 30 to 40 minutes for a total count of 15,000 to 16,000 pulses.

In experiments on porous concrete (100 mm thick with volumetric weight 900-1100 kg/m^3) the discrepancy between moisture determinations by means of gamma rays and by weighing did not exceed 2% of the weighed moisture, which is very satisfactory.

The above-described method was successfully used by the authors for a year in the study of moisture migration in structural materials.

This work was done in 1955 and 1956 at the Institute of Construction and Structural Materials of the Esthonian Academy of Sciences.

L. Polozova and R. Reizman

FOREIGN SCIENTIFIC AND TECHNICAL NEWS

CONCERNING THE DISCOVERY OF THE ANTINEUTRON

After the discovery of the antiproton [1], there remained no doubt as to the existence of the antineutron, that is, of a neutral particle with the mass of the neutron and with its magnetic moment directed along its direction of spin (as opposed to the neutron, whose magnetic moment is antiparallel to its spin).

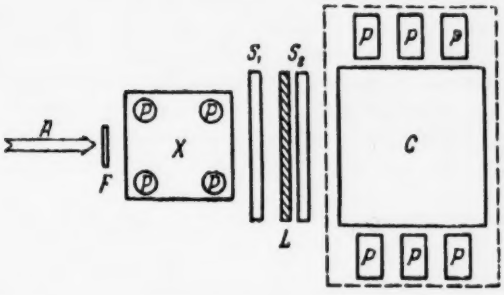

Fig. 1. Diagram of the experiment. A – antiproton beam; F – scintillation counter; X – liquid scintillation counter filled with a toluene-terphenyl solution; S_1 and S_2 – plastic scintillators; L – lead plate; C – lead glass Cerenkov counter; P – photomultipliers.

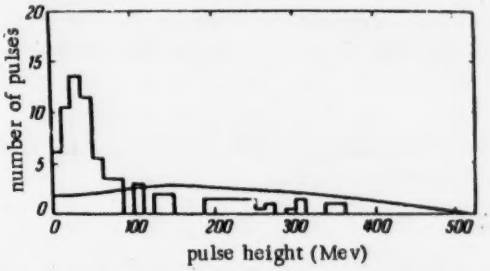

Fig. 2. Pulse-height spectrum in X for 74 pulses due to neutral particles in C. The smooth solid curve gives the pulse spectrum for antiprotons annihilating in X.

The experimental proof, however, of the existence of the antineutron was quite difficult, and has been given only recently by Cork, Lambertson, Piccioni and Wenzel [2].

The experiment was performed on the same accelerator as the one with which the antiproton was first observed, namely the Berkeley (USA) Bevatron.

Antineutrons were produced as a result of charge exchange in proton-antiproton collisions. The antiprotons were recorded by means of their annihilation in matter. A 1.4 Bev/c proton beam was formed with the aid of a system of deflecting magnets, magnetic focusing lenses, and scintillation counters (the last of which, F of Figure 1, counted 300-600 antiprotons per hour). The antiprotons then entered a charge-exchange converter X, which was a liquid scintillation counter filled with a toluene-terphenyl solution. As a result of charge-exchange collision in X, a part of the antiprotons were converted into antineutrons whose annihilation with nucleons was recorded by the Cerenkov counter C.

The scintillation counters S_1 and S_2 placed between X and C, and connected in anticoincidence with them, were used to indicate the passage of a neutral particle. The lead plate L between S_1 and S_2 was intended to convert high-energy γ-rays which give events similar to antineutrons.

The greatest difficulty arose in discriminating between the production of antineutrons and the annihilation of antiprotons in X, since in antiproton annihilation neutral particles are emitted in the direction of $S_1 - S_2 - C$. Neutral particles (neutrons and heavy mesons) can cause counts in counter C, thus imitating an antineutron passing through the counters S_1, S_2 and C. In order to eliminate errors due to such events, the pulse spectra were measured both in X and C (Figures 2 and 3). This can be done because antiproton annihilation in X gives large pulses in this converter (greater than 100 Mev), whereas antineutron creation gives small pulses. Therefore the pulse spectrum in counter C was analyzed on the basis only of those events which gave pulses of less than 100 Mev

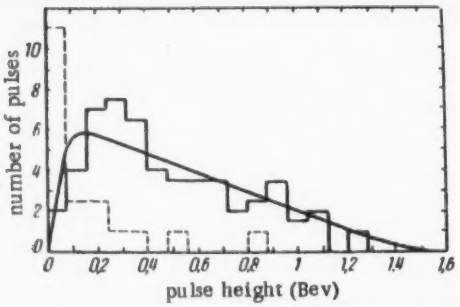

Fig. 3. Pulse-height spectrum in counter C. The solid histogram is for 54 antineutron events (the pulse in counter X is less than 100 Mev). The smooth curve gives the antiproton pulse spectrum. The dashed histogram is for 20 neutral particle events for which the pulse in counter X is greater than 100 Mev.

in the converter X. A pulse-height spectrum was drawn for counter C (Figure 3), corresponding to the creation of antineutrons in X and their annihilation in C. A separate experiment was performed to measure the pulse-height spectrum due to the annihilation of antiprotons in C. This was done by removing the counters S_1 and S_2, as well as the lead plate L, and by admitting the antiproton beam into counter C. The two spectra were found to be quite similar (Figure 3). This verifies the fact that the particles selected by the system are actually antiprotons.

Similar experiments were performed with the Cerenkov counter C replaced by a liquid scintillation counter, and these experiments gave similar results.

The antineutron yield was about 0.3% per antiproton for a thickness of the converter X of about 20 g/cm^2. Assuming that the cross section for interaction of antiprotons with the matter in counter C is equal to the cross section for antiprotons, the authors found that the cross section for charge exchange for 1.4 Bev/c protons in toluene is about 2% of the annihilation cross section, which corresponds to a charge-exchange cross section of 8 mbarns in carbon.

P.K.

LITERATURE CITED

[1] O. Chamberlain, E. Segre, C. Wiegand and T. Ypsilantis, Phys. Rev. 100, 947 (1955); see also J. Atomic Energy No. 1, 119 (1956).*

[2] B. Cork, G. Lambertson, O. Piccioni and W. Wenzel, Phys. Rev. 104, 1193 (1956).

*[Original Russian pagination. See translation pagination.]

ATOMIC LOCOMOTIVES

During the past three years there has been wide discussion of the feasibility of locomotives with atomic power plants, which in addition to possible economic advantages may allow an increase of mileage between refueling to 80,000 km and over.

An atomic locomotive must meet the following basic requirements: 1) economic fuel utilization; 2) minimum first cost and minimum operating costs; 3) dimensions and weight of the locomotive must allow its use on existing railroads, both singly and in coupling with single control; 4) complete safety in use, even under possible errors by the operating personnel.

TABLE 1

Comparative Data on Cost and Consumption of Fuel for Diesel Locomotive and the Planned Gas Turbine Locomotive with Air Cooling [8, 9]

	Diesel locomotive	Atomic gas turbine locomotive
Efficiency, %	28	16
Fuel consumption per km, in kg	8	7×10^{-6}
Full fuel load, kg	6350	15
Fuel burnup fraction	1.0	0.2
Mileage per year, km	228,000	
Annual fuel consumption, kg	1,825,000	1.6
Number of refuelings per year	288	0.535
Cost of one loading, dollars	200	240,000
Annual fuel cost, dollars	57,600	128,000
Fuel cost per 1 km, dollars	25	55

Not long ago it was the general opinion that the last requirement would lead to excessive weight and dimensions in an atomic locomotive. However, at present it is thought that with suitable materials for the biological shield around the reactor, its diameter including shielding can be lowered to 3.6 m, with total reactor and shield weight of 115 tons [18].

In principle, three types of atomic locomotives are feasible; with common piston engine, with steam turbine drive, and with gas turbine drive.

The first type is not desirable because of its low over-all efficiency. A locomotive of the second type has a somewhat greater efficiency but requires a large water storage capacity and also bulky condensers. The last locomotive type is more attractive by virtue of its greater efficiency and no requirement for a water supply.

One of the first foreign atomic steam turbine projects [1-3] was developed under the direction of Borst (Figure 1) at the University of Utah, USA. As the source of steam it uses a homogeneous reactor of 30 Mw thermal power. Working design of the reactor was done by the Babcock and Wilcox Co.

The reactor [4, 5] itself is a vessel having the form of a hexagonal plate 305 x 915 x 915 mm in size. The core contains 176 kg of uranylsulfate solution, containing 9 kg of U^{235}. The choice of uranylsulfate was made because of its high solubility in water and the resistance of the sulfate ions to the action of radiation. For good

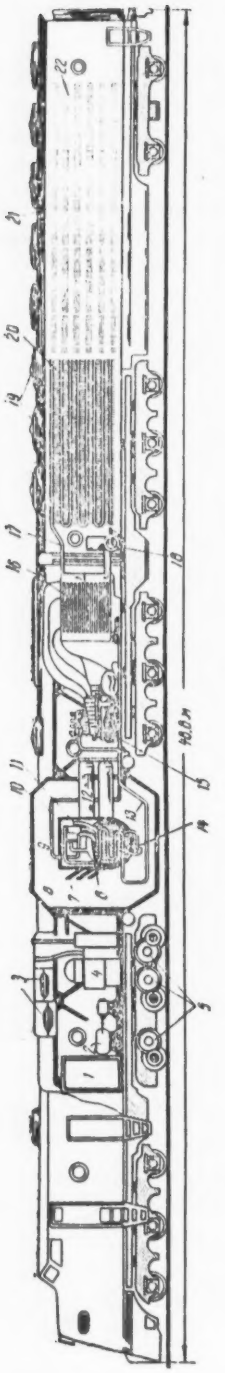

Fig. 1. Atomic steam turbine locomotive. 1) Switchboard; 2, 4) accessory equipment; 3) ventilators; 5) traction motors; 6) reactor shield; 7) control rods; 8) uranylsulfate solution; 9) water of the primary loop; 10) recombiner; 11) steam from reactor; 12) main generator; 13) steam line; 14) circulating pump; 15) turbine; 16) condenser-heat exchanger; 17) hot water from the heat exchanger-condenser; 18) cold water for the condenser-heat exchanger; 19) ventilators; 20) air cooling of water; 21) cooling installation; 22) air outlet.

heat transfer this solution is agitated by a special circulating pump, which is located under the vessel bottom. Water which surrounds the core and passes through 10,000. stainless steel tubes of total surface area 75 m^2 in the core, fulfills simultaneously the functions of reflector, moderator and coolant.

It is proposed to provide a special recombining chamber in which, during full power operation of the reactor, is given off about 500 kw of heat by the recombination of oxygen and hydrogen, which form by decomposition of water. It is also proposed to remove xenon and other gaseous products of fission. Particular attention is given to the corrosion resistance of the materials used in the reactor.

The reactor is controlled by cadmium rods, which automatically shut down the chain reaction when the locomotive is braked sharply, or in collisions, etc. A special separator is planned for the removal of steam from the circulating water. The slightly radioactive steam that emerges from the separator at a temperature of 204°C and 17.5 atmospheres pressure is introduced directly into an eight stage steam turbine of 8000 hp (6000 rpm). The reactor and the separator and recombiner are surrounded by a biological shield having external dimensions of 3.05 x 4.57 x 4.57 m and a thickness of 1.22 m. The weight of reactor and shielding is 181 tons. The shielding consists of alternate layers of steel and hydrogen bearing material of specific gravity near to unity. In order to reduce to a minimum the dangers resulting from a possible accident, it is proposed to make the shielding of steel containers placed one inside the other, each of which can securely contain the uranylsulfate within the reactor.

The steam turbine, through a reducer, drives 4 electrogenerators which feed direct current to 12 electric railway motors located on the wheel trucks. The turbine utilizes only 25-30% of the steam energy. The remaining heat is given up to cooling water in a tube condenser-heat exchanger with cooling area of 56 m^2, from which the condensate water is pumped back to the reactor. The coolant water used to condense the steam is in turn cooled by air in radiators which are carried in an attached section.

Start up of a cold locomotive requires 30 min. It is calculated that consumption of U^{235} will be 37 g per day. It is assumed that refueling of the locomotive's reactor will take place 4-6 times a year. Twice a year a complete recharging of the reactor will be required, at a special depot possessing the necessary equipment to safeguard the maintenance personnel. The approximate cost of such a locomotive is about 1.2 million dollars [6]. Its operation will be more profitable than the operation of a diesel locomotive if the cost of uranium does not exceed \$7/g for average operating conditions, and \$25/g for ideal operating conditions.

In the atomic locomotive with gas turbine installation, the heat carrier and working fluid can be either gas, circulating in a closed loop, or air drawn directly from the surrounding atmosphere, which obviates the necessity for special coolers in the locomotive. A plan for a locomotive of the second type was proposed in the USA by Gunnel [8, 10, 11]. The plan proposes discharging radioactive air to the atmosphere, which constitutes a considerable hazard to the operating personnel, passengers, and inhabitants, and therefore it is doubtful that this plan can be considered as satisfactory.

This locomotive has a heterogeneous reactor of 11 Mw thermal power, with enriched uranium, surrounded by shielding weighing 38.5 tons. The design of the reactor as well as the design and material of so light a shield are not reported. The air, heated in the reactor to 700°C, enters a gas turbine of 3000 hp which is connected to a direct current generator feeding 6 motors of 500 hp each, which are installed on two three-axle trucks.

In Table 1 are given comparative figures of fuel consumption and cost for the planned atomic gas turbine locomotive and a diesel locomotive used on the Southern Railroad of the USA. As is apparent in the table, supplying the atomic locomotive with fuel is 2.2 times as expensive as the diesel locomotive (with U^{235} cost of $16000/kg). The cost of the first atomic locomotive is estimated at 20 million dollars [9], but in mass production about 1 million dollars. If the amortization period of the atomic locomotive is taken at 15 years, as in the diesel locomotive, then including the additional costs of storing and handling the nuclear fuel, the special safety measures, the construction of special charging depots, etc., the cost of a 1 km run of the atomic locomotive will be 2.58 times as great as that of the conventional locomotive.

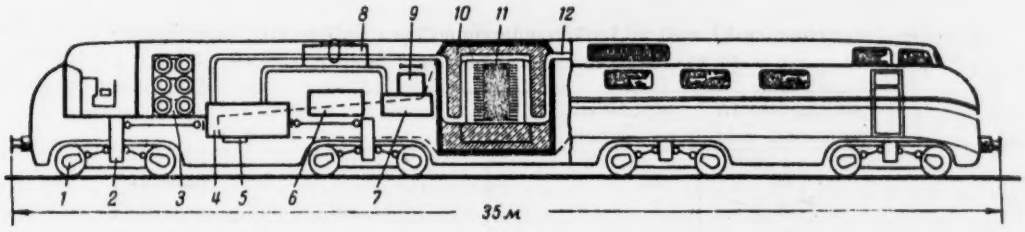

Fig. 2. Atomic gas turbine locomotive with helium cooling. 1) Driving axle (total of 8); 2) drive transmission; 3) cylinders with He; 4) low pressure turbine; 5) reactor supports; 6) high and low pressure compressors; 7) high pressure turbine; 8) cooler with ventilator; 9) heater; 10) reactor shield; 11) uranium rods in moderator; 12) helium line.

In Figure 2 is depicted the plan of another atomic gas turbine locomotive, also developed by Borst [13, 14], in which the heat carrier and working fluid is helium. The design of this locomotive is more complex than the previous one, since a secondary loop for cooling the helium is essential; however, it is much safer.

In Table 2 are shown the characteristics of several atomic locomotives and for comparison the characteristics of a steam locomotive, turbine locomotive, and diesel locomotive in use on the railroads of the USA, which are intended for greater loadings than the European counterparts.

Another type of atomic energy installation for locomotives is proposed in the USA by a group of engineers [19]. It is in the form of a cylinder filled with gaseous uranium hexafluoride (UF_6), with a piston in the cylinder. One end of the cylinder is immersed in reflector, which simultaneously performs the function of a regulator. Control is effected through the change of position of the reflector along the cylinder axis. When the piston is in the extreme position and the uranium hexafluoride is compressed, in the presence of reflector it reaches criticality, a chain reaction is initiated, as a result of which the gas is heated, expands, and the piston is thrown back to the opposite end of the cylinder, which can also be filled with hexafluoride of uranium and immersed in reflector; thus a reciprocating motion of the piston is obtained. To achieve complete sealing of the cylinder, direct conversion of motion into electrical energy is proposed by means of electromagnetic induction. No detailed descriptions of the design are given. The difficulties involved in executing this type of atomic prime mover are primarily in start up of such a system, and in the highly corrosive properties of uranium hexafluoride. The atomic energy commission of the USA awarded a contract in March 1955 [12] for the study of the requirements of design, technology and economics of this proposal.

TABLE 2

Comparative Characteristics of Locomotives Operating on Conventional and Nuclear Fuel

Type of locomotive	Efficiency %	Length, m	Number of axles	Horsepower	Gross weight, tons	Weight per axle, tons	Maximum sustained traction, tons
Conventional fuels							
Diesel locomotive	28	60.9	16	6000	450	28	72
Steam locomot	7	40.2	8	6670	245	30.6	58.3
Turbine locomotive	18	25.9	8	4500	250	31.3	47.3
Nuclear fuel							
Steam turbine locomotive	—	48.8	12	7000	326	27.2	71
Gas turbine locomotive with air cooling	16	21	6	3000	174	29	44.5
Gas turbine locomotive with helium cooling	~15	35	8	6000	187	23.4	—

An analysis of the proposals indicates that under the existing state of development of reactor technology, and under existing prices of uranium, the atomic powered locomotive has no economic advantages over the diesel locomotive.

If conventional locomotives were to be replaced with atomic powered ones the cost of the locomotive inventory replacement would be 10 million dollars. An important problem of their utilization is the requirement for maximum automatization of operations [17], compatible with utilization of present rail transport, to assure complete safety of operation of the atomic locomotives.

There exists the opinion that initially atomic locomotives will find application in military service [9]. Their use would be just as feasible in desert areas, for instance the central regions of Australia [11], where adaptation of rail transport powered by conventional fuels is difficult, and where radioactive contamination as the result of an accident would not present a very great danger because of the low population density.

V.A.

LITERATURE CITED

[1] Borst, Forum report (May, 1954).

[2] Railway Age 136, 8, 15 (1954).

[3] Railway Loco and Cars 128, 5, 51 (1954).

[4] Nucleonics 12, 3, 78 (1954).

[5] Arch. f. Energiewirtschaft 22, 968 (1954).

[6] Rosekilly, Model Engineering 113, 2833, 300 (1955).

[7] Kehoe, Trains 15, 9, 21 (1955).

[8] Gunnel, Forum report (August, 1955).

[9] Railway Loco and Cars 129, 7, 37 (1955).

[10] Doprani tech. 3, 11, 306 (1955).

[11] Commonwealth Engineering 43, 1, 7 (1955).

[12] Railway Age 138, 14, 7 (1955).

[13] Gössl, Bundesbahn 29, 22, 946 (1955).

[14] Reishaus, Elektro-technik 38, 16, 144 (1956).

[15] Railway Gaz. 104, 21, 400 (1956).

[16] Railway Age 140, 7, 10 (1956).

[17] Railway Age 140, 18, 14 (1956).

[18] Cockroft, Atomics 7, 7, 241 (1956).

[19] Railway Age 141, 16, 20 (1956).

[20] Electr. Engineering and Merchandiser 32, 10, 328 (1956).

ATOMIC ENGINES IN SHIPS OF THE USA

To date two atomic submarines have been launched in the USA, the "Nautilus" [1] and the "Sea Wolf" [2]. During the recently completed test cruises the Nautilus covered about 80,000 km, 60% of the time in a submerged state [3]. Despite the fact that the supply of excess reactivity of the reactor would have sufficed for some time, it was decided to replace the fuel loading in the reactor.

The depleted fuel has been sent to the National Reactor Testing Station in Idaho for examination [4].

The first atomic ship of the USA, the submarine Nautilus, although worthy of its name, still has many faults, which will be eliminated in the future in the design of additional ships of this class [5]. In regard to the second atomic submarine – Sea Wolf, during dock side trials of its reactor, sodium leaks were observed in the primary reactor loop. Serious technical difficulties in the operation of a sodium cooled reactor may force its replacement with a pressurized water reactor [6].

According to the American admiral John Wright almost all ships presently under design in the USA will have atomic power plants installed. Apparently, in the near future changes will be made in American laws, that will allow transfer to England of experience accumulated in construction of atomic submarines [7].

Besides the Nautilus and Sea Wolf there are 15 atomic submarines under design or construction in the USA. As part of this program, the Westinghouse Co. has been given orders to build six atomic submarine reactors and their accessory equipment [7]. These reactors are assigned to three submarines of medium size (displacement ~2500 tons) "Sea Dragon," "Sargo" and "Skipjack," to one large submarine ("Triton") of 5500 tons displacement, which has two reactors, and to one submarine of 2900 tons displacement. In the building docks are the two submarines "Skate" and "Swordfish." All orthodox submarines at present under construction in the USA will eventually be equipped with nuclear engines [6, 10].

Apparently in the course of the next ten years, the number of ships in the USA possessing atomic power plants will rise to 75 [7].

The first surface ship to be atomic powered in the USA – a cruiser – is in the building docks. The cruiser's displacement is 14,000 tons, its length is 210 m. The reactor for the cruiser's power plant is also being made by the Westinghouse Co. [8].

In 1958 it is planned to begin construction of the aircraft carrier "Forrestal" with 8 nuclear reactors. The displacement of the carrier is 85,000 tons, the speed 33 knots [6].

The Atomic Energy Commission of the USA is pressing work for creation of a cargo-passenger ship with atomic power plant. Shaft horsepower of the ship will be 20000 hp, the speed 21 knots. The cargo capacity of the ship will be 12000 tons. Its length will be about 180 m and it will carry 100 passengers.

The source of power on the ship will be a pressurized water nuclear reactor. The development of the reactor has been allowed about three years time. It is proposed to eventually declassify the design of the reactor and the technology of its construction. The construction of the power plant will be done by the Babcock and Wilcox Co. [6, 9].

Ya.K.

LITERATURE CITED

[1] Atomic Energy No. 1, 111 (1956).

[2] Atomic Energy No. 2, 109 (1956).

[3] Interavia Air Letter No. 3599, 5 (1956).

[4] New York Times

[5] Nucl. Power 2, 9, 4 (1957).

[6] Engineering 4739, 29 (1957).

[7] Nucl. Engineering 1, 8, 348 (1956).

[8] Engineering 4732, 29 (1957).

[9] Engineer 202, 5262, 791 (1956).

[10] Nucleonics 14, 11, R-9 (1956).

PRODUCTION OF URANIUM AND THORIUM TETRAFLUORIDES

Uranium tetrafluoride is usually prepared by fluorination of the dioxide by hydrofluoric acid, ammonium difluoride, or hydrogen fluoride. A disadvantage of these processes is that an additional operation, the reduction of a higher uranium oxide to the dioxide, is required, while the fluoride formed contains moisture. This lowers the yield of the metal in thermal reduction by calcium.

A process has been developed in the C.I.S.E. Laboratories for the production of the tetrafluoride by fluorination of UO_3 by Freon-12 (difluorodichloromethane) according to the equation [2]

$$UO_3 + 2CF_2Cl_2 \xrightarrow{400^\circ C} UF_4 + CO_2 + COCl_2 + Cl_2,$$

which does not have the disadvantages of the usual process.

Many materials, including quartz, are suitable for the equipment, which also distinguishes this process favorably from processes involving hydrofluoric acid.

The high cost of Freon-12 is balanced, in the authors' view [3], by the low running costs of the fluorination equipment. They believe that this process can compete with other dry processes (fluorination by HF or NH_4HF_2).

Investigation of the process showed that at 400°C a chlorination reaction

$$UO_3 + 3COCl_2 \rightarrow UCl_4 + Cl_2 + 3CO,$$

partially occurs (on 10% of the charge), and to decrease the amount of chlorine in UF_4 below 0.05% it is in practice necessary to use a 30% excess of CF_2Cl_2 for fluorination of the chloride according to the equation

$$UCl_4 + 2CF_2Cl_2 \rightarrow UF_4 + 2CCl_4.$$

The excess of Freon-12 should be recovered. If the reaction is carried out at 350°C it is incomplete, and UO_2F_2 is formed. At fluorination temperatures above 400°C the amount of chlorine in the fluoride increases and local temperature increases owing to heat of reaction may cause sintering of the reaction products, hindering further fluorination.

After several years of work and the conversion of hundreds of kilograms of oxides, an installation with a continuous rotating reactor has been designed. The products obtained in this installation have the following characteristics:

UF_4 — 99,5 — 99,65%; UO_2F_2 — 0,15 — 0,25%;
UCl_4 — 0,15 — 0,20%; UO_2 — 0,05%.

Bulk density 3.7-3.8 g/cc.

Experiments showed that at 300-400°C anhydrous thorium tetrafluoride can be obtained by the reaction

$$ThO_2 + 2CF_2Cl_2 \rightarrow ThF_4 + 2COCl_2$$

with 20% excess of Freon-12. In these experiments a specially reactive form of ThO_2 was used, obtained by decomposition of thorium oxalate at low temperatures. However, for production of cheaper thorium tetrafluoride it is recommended to make the aqueous fluoride by a wet process (for example, by precipitation of pure thorium

nitrate with ammonium difluoride) and then to heat the $ThF_4 \cdot nH_2O$ (or NH_4ThF_5) in a Freon atmosphere at 350-500°C (about 3 hours at 450°C). The oxidation of fluoride when heated in Freon-12 is very slight (less than 0.05% ThO_2) while the loss of Freon-12 is negligible.

G.Z.

LITERATURE CITED

[1] A. Cacciari, R. De-Leone, C. Fizzotti and M. Gabaglio, Energia Nucleare 3, 462 (1956).

[2] H. Booth, W. Krasny-Ergen and R. Heath, J. Am. Chem. Soc. 68, 1969 (1946).

[3] A. Cacciari, R. De-Leone, C. Fizzotti and M. Gabaglio, Energia Nucleare 3, 164 (1956).

INVESTIGATION OF RADIATION DAMAGE BY PARAMAGNETIC RESONANCE TECHNIQUES

In an attempt to study the paramagnetic resonance spectra of the ions Am^{3+} and Pm^{3+} it was found [1] that the radiation of these nuclei (α-particles from Am^{241} with an energy of 5.5 Mev and β-particles from Pm^{147} with an energy of 0.22 Mev) had a disturbing effect on the spectra on the host-crystals $La_2Mg_3(NO_3)_{12} \cdot 24H_2O$, containing respectively 3 mc of Am^{241} or Pm^{147}. From the nature and anisotropy of the hyperfine structure of the affected spectrum it was established that the magnetic electron is located at the nitrogen radical ion NO_3, a product of decay under the influence of radiation. Similar effects were noticed in the colorless transparent single crystal of $(La, 0.1\ Ce)_2Mg_3(NO_3)_{12} \cdot 24H_2O$ which was irradiated by γ-rays (dose 110 mega roentgens) from Co^{60}, which after irradiation became opaque with a yellow color. From the intensity of the disturbance it was established that it contained approximately 10^{17} magnetic centers (defects). A strong disturbance of the spectrum of the crystals with americium was noted a day after it was grown, this process taking 2-3 hours. From the intensity of the spectrum it was established that immediately after growth there were approximately $2 \cdot 10^{18}$ defects in the crystal. After three months of exposure of the crystal at room temperature the number of defects was approximately doubled, but in the succeeding eighteen months no significant increase was observed. As a consequence of the radiation damage there was also produced an increase in the intensity of the new lines, which hindered further observation.

In the crystal with promethium the damage was noticed after approximately three weeks following removal from the solution in which it was grown for about a week. From the intensity of the lines it was found that after six months the crystal contained only approximately $5 \cdot 10^{15}$ defects; three months later no significant increase in this number was observed. It is obvious that the β-particles produce these defects at a smaller rate than the α-particles. However, even α-particles of high energy produce in different nitrates (as was found in Ref. [2] $[(U, Np, Pu)O_2]Rb(NO_3)_3$) different damage effects in the spectra.

Thus, the paramagnetic resonance technique is convenient for studying radiation damage, especially if the hyperfine structure can be observed.

Further work is planned with materials in which all or the majority of the nuclei have spins different from zero.

G.Z.

LITERATURE CITED

[1] B. Bleaney, W. Hayes and P.M. Llewellyn, Nature 179, 4551, 140 (1957).

[2] P.M. Llewellyn, Thesis, Oxford Univ. (1956).

BRIEF COMMUNICATIONS

USA. A new type of experimental nuclear reactor has been developed at the Argonne National Laboratory; this reactor is a combination of a fast-neutron reactor and a thermal-neutron reactor.

In this design the active zone of the fast-neutron reactor is located inside the active zone of the thermal-neutron reactor in which the moderator is water and the fuel, uranium. The outside reactor consists of several sections of sub-critical dimensions. The control of the inside reactor is accomplished by regulating the outer reactor. (Financial Times January 25, 1957.)

USA. On December 29, 1956 at the Argonne National Laboratory the design power level was reached in the experimental boiling water power reactor (EBWR). The total capacity of the reactor is 20 megawatts, the electrical capacity is 5 megawatts. The construction of the reactor was completed in November of 1956. Criticality was first achieved in the reactor on December 1.

The EBWR reactor is the first of five power reactors which have been undertaken under the "demonstration" program in the USA. (Nucl. Engineering 2, 11, 82, 1957.)

USA. During preliminary tests at the Oak Ridge National Laboratory on the experimental power reactor NRE-2 (J. Atomic Energy 11, 4, 174, 1956) microscopic cracks were discovered and in the leak-detection system. The possibility has not been excluded that there may also be such cracks in the high-pressure system. The Atomic Energy Commission has issued a statement indicating that the cracks occur as a result of corrosion under the action of the load; it is planned to replace the piping of the leak-detection and certain flanges of the high-pressure system and to test the reactor again with fuel. A delay in starting the reactor until the fall of 1957 may occur if the Commission decides to replace all flanges including those in the low-pressure system. (Atomic Industry Reporter No. 82, December 26, 1956.)

USA. A group of public power companies in the midwest and the Allis-Chalmers Manufacturing Company have announced a plan to construct an atomic electric power station in the midwest in the course of the next five years. It is assumed that the electric power produced at this station will compete in cost with the electric power produced by ordinary power stations.

The electrical capacity of the station will be 60,000 kw, and it will make use of a boiling water reactor. In the cylindrical active zone of the reactor (diameter and height approximately 1.5 m) there will be produced as much energy as is produced in combustion of 20 tons of coal per hour.

The atomic power station will make use of a supplementary system for superheating the steam coming from the reactor. The fuel in the reactor will be enriched uranium. The operating period of the reactor will be one year. (Report from the Associated Press, February 8, 1957.)

USA. According to a report from the Navy Department, experience with the atomic engine installed in the supply ship "Sea Bird" has shown that the use of a solium heat exchanger involves a number of inconveniences and difficulties in the auxiliary system (especially the steam superheating system). Hence, although in the "Sea Bird" it has been decided to use a reactor with a liquid metal heat exchanger, in other Navy vessels this type of reactor with a sodium heat exchanger will not be installed. (Nucleonics 14, 12, R-3, 1957.)

USA. In a paper delivered by K. Brown (Oak Ridge National Laboratory) at the second meeting of the American Nuclear Society, it was reported that at the present time there have been developed in the US new ex-

traction agents [di(2-ethylhexl] phosphoric acid and other organic phosphor acids, alkyl phosphenoxides and alkyl phosphenamides with long chains giving the possibility of extracting uranium from various water systems, including solutions of sulfates, phosphates, chlorides and their compounds. (Atomic Energy Clearing House m. 2, No. 20, 11, 1956.)

USA. Dr. Wheeler of Louisiana University has developed a so-called "atomic" ink. This ink gives off radiation which is sufficiently intense so that it causes a reaction on a photographic paper which is placed above a drawing made with this ink. As a result one obtains a reproduction which is an exact image of the original. This type of accuracy of image reproduction is almost impossible in ordinary lithographic methods. Furthermore, it is possible to obtain thousands of copies without affecting the accuracy of the image of the original drawing. (Atomics 7, 11, 388, 1956.)

England. The Pie Company (Cambridge) has developed a television camera with a diameter less than 7.5 cm and a length of 60 cm, with a built-in light source, for studying sections of a reactor which are inaccessible because of high radioactivity. The dimensions of the camera make it possible to lower it in the reactor channel by means of a mechanical hoisting device.

Work with an earlier model of the television camera has shown that it is an effective means for studying heat-exchange elements of the reactor. The camera was developed in accordance with the design requirements given by the engineers of the Calder Hall Power Station. The camera was developed for the Atomic Energy Board. (Financial Times, January 8, 1957, p. 9.)

England. The Atomic Energy Board has issued a color film devoted to a description of the first English atomic power station at Calder Hall. The demonstration film lasta for about twenty minutes. The text of the film has been translated into eight languages. (Atomics and Nucl. Energy, 8, 1, 32, 1957.)

Holland. It has been decided to build an atomic power station in Holland; use will be made of a reactor such as that installed at Calder Hall (England). The station will be built in Bugenum in the Province of Linburg and it will be put in operation in 1962. (Financial Times, January 22, 1957.)

Greece. The Greek government has announced a contract with the American company, American Machine and Foundry Atomics, for the design and construction of a research reactor. Construction of the reactor will be started in 1958 in the region of Athens. (Financial Times, January 18, 1957.)

FRG. The program for the development of atomic energy in Western Germany provides for the construction at Karlsruhe of a reactor using natural uranium which will be extracted from a deposit in the Fichtel Mountains. The moderator in the reactor will be either graphite or heavy water which will be manufactured at the site. The construction of the reactor will require three years. (Atomics and Nuclear Energy 8, 1, 32, 1957.)

France. The Atomic Energy Commisariat has published detailed information of the extraction of uranium and its deposits. In territorial France the uranium deposits which have been explored amount to 10,000 tons and in addition it is believed that there are 50,000 tons in deposits which have not been investigated. In Madagascar deposits of thorianite have been explored which contain 10 to 20% uranium and 60 to 70% thorium and amount to 1,000 tons.

In territorial France there are three refining installations in operation or under construction:

1. In Geinon (Dept. of Sonn Luarne) there is an installation with an annual refining capacity of 50,000 tons of ore producing 500 tons of concentrate containing 10% uranium.

2. In Ekarper (Dept. of Lower Luar) an installation with an annual production of 400 tons of concentrate.

3. In Bessin (Dept. of Upper Venn) an installation with an annual capacity of 450 tons of concentrate.

One of the main goals of the French AEC is the achievement,in 1975, of the production of 3,000 tons of metallic uranium per year (L'Echo des Mines et de la Metallurgie No. 3500, 37, 1957.)

Italy. The Edison-Volt Company (Milan) has acquired from the American company, Westinghouse Elec-

tric International, an atomic power station with a capacity of 134,000 kw at a price of 34 and a half million dollars. This station is an exact copy of the station built by the Westinghouse firm in Rauz (Massachusetts) for the Yankee Atomic Electric Corporation; a reactor with high pressure water will be used. It is believed that the station will be started shortly after the American station which is to be started up in 1959. (Atomic Energy Newsletter 16, 11, 2, 1957.)

Australia. The Australian Atomic Energy Commission is building a research reactor similar to the English Dido reactor (Atomic Energy No. 3, 141, 1956)* 20 miles to the northwest of Sydney (Lucas Mountain). Construction of the reactor was started in October 1955, and is expected to be completed in June of 1957.

The graphite for the reflector and the enriched uranium will be supplied by the Atomic Energy Board of Great Britain; the heavy water used in this reactor as the moderating element and heat exchanger will be supplied by the United States Atomic Energy Commission.

In the initial stages of the development of its atomic energy industry Australia will rely on imported equipment, particularly from Great Britain; however, at the present time in Australia there are a number of firms which can fill some of the orders for the fabrication of required equipment. (Nucl. Power 2, 10, 41, 1957.)

*[Original Russian pagination. See C.B. Translation pagination.]

REVIEWS AND BIBLIOGRAPHY

POPULAR SCIENTIFIC LITERATURE ON ATOMIC ENERGY

During recent years various publishing houses of the Soviet Union have issued a large number of popular scientific books and pamphlets dealing with atomic energy.

The value of popular scientific literature for the spreading of knowledge concerning atomic energy can hardly be overestimated. The wide audience for which this literature is intended requires a popular form of presentation on a high scientific level. The facts must be presented in a practical, concrete and interesting manner without superfluous flights of fantasy. The format of the books is also important.

However, only a very small number of the books on atomic energy for the public satisfy these requirements. Among these we can include the pamphlet "Atomic Energy for Peaceful Purposes" [1], A. Trifonov's pamphlet "Atomic Energy in the Service of Mankind" [2], P.T. Astashenkov's pamphlet "Atomic Industry" [3] and with some reservations D.I. Voskoboinik's book "Nuclear Power" [4].

The collection of articles issued by the Academy of Sciences USSR is devoted to various aspects of the utilization of atomic energy. The authors of the articles present their facts clearly and succinctly, emphasizing description and avoiding boring calculations. The illustrations are well chosen; these are either photographs of actual apparatus or concise clear drawings. The pamphlet as a whole reflects the contemporary state of the use of atomic energy and does not mislead the reader by fantastic speculations as is often done by other popular literature.

A. Trifonov's pamphlet follows a different plan and describes a trip. The reader accompanies the author on an interesting tour of physical laboratories where the staffs speak of their work in an interesting manner. The well-chosen language of the explanations, the clear drawings and photographs and the intriguing headings as well as the accurate treatment of scientific questions hold the attention of the reader.

Astashenkov's booklet shows the author's desire to avoid minor matters and to report on the most important subject, which is the operation and construction of nuclear reactors and their auxiliary equipment. In this he has been very successful. One feels that the author is well acquainted with the foreign literature and can view the achievements of nuclear technology abroad in an objective manner. The writing is smooth and matter-of-fact; the author makes little use of numbers; he diversifies his material with descriptions of interesting events and occurrences related to the development of nuclear technology. The book contains a few errors which are not of a serious nature, and the general impression is very good.

Finally, Voskoboinik's book has been included with reservations for the following reasons.

This book explains thoroughly with scientific accuracy the elements of atomic structure and the operation of nuclear reactors; it describes the materials and equipment which are used and the construction of nuclear power stations. The author introduces data and makes the calculations needed to explain the functioning of a reactor.

The book can hardly be included in the popular literature that is intended for unprepared readers; it can rather be recommended for a deeper study of atomic power by readers who have some knowledge of general physics, radio, electronics and materials. A few inaccuracies do not affect the value of the book as a whole.

Yet, such brochures and books are few in number. The majority of popular writings on atomic energy do not satisfy the requirements which must be made of them.

Such publications include the popular literature issued by the following publishing houses: Gostekhizdat, Znanie, DOSAAF, "The Moscow Worker," Voenizdat, Medgiz and a few additional local publishers.

Within the limitations of this article we shall attempt to point out their shortcomings in a few examples and present our views regarding methods of improving the literature on atomic energy for the general public.

The first and most serious fault of many brochures is the insufficiently informed and in some instances simply ignorant and inaccurate explanation of certain matters.

Let us consider Shcherbakov's "Atomic Energy in the Service of Mankind" [5]. In the section which describes the principles of the operation of nuclear reactors the author is guilty of some serious blunders. For example on page 27 he states that "the multiplication factor is changed by introducing into U^{235} or into plutonium some substances which can absorb neutrons."

Although, in principle, in heterogeneous nuclear reactors (the author does not state what type of reactor he is discussing, which is essential) the absorbing rods can be introduced into the fuel, it must be mentioned that in all of the heterogeneous reactors whose designs have been published, the rods are introduced into the moderator rather than into the nuclear fuel.

The author also states that "in a heterogeneous reactor the uranium blocks in the form of rods form a checkerboard pattern within the moderator, which is most often made of graphite." Here, it is not made clear why a checkerboard pattern is used when other arrangements of the fuel are possible and why in this instance graphite is used most often although other moderators are also in use.

In V.P. Romadin's booklet "Power from Atomic Energy" [6], we find on page 19: "Liquid sodium circulating in the first reactor loop when used directly to generate steam induces a high level of radioactivity in the steam." This is incorrect since the energy of the gamma rays that are emitted by radioactive sodium is insufficient to excite secondary radioactivity in steam. Farther on the author states that "the maximum fuel temperature in a reactor must not exceed 665° because at this temperature the crystal structure of uranium is changed thus hindering the subsequent chemical elimination of fission products." This is also false because in actuality at the temperature of the first phase transition of uranium its volume changes considerably, so that the fuel elements may be ruptured unless special precautions are taken. The change of structure does not at all affect the later chemical treatment of the nuclear fuel.

The author also states: "When natural uranium is used in reactors the consumption of 1% of it is allowed. In this case 0.56% of U^{235} is used (with a final content of 0.15%) and 0.44% of plutonium (with a final content of 0.44%)."* We cannot agree with this. In the first place it is not clear which uranium isotope, U^{238} or U^{235}, is burned up. Secondly, why is the consumption of uranium "allowed" when we know that the more the U^{235} is burned up the greater the utilization of the nuclear fuel? In this instance, the word "allowed" is used incorrectly. Thirdly, why is 0.56% of U^{235} used? In some reactors, using natural uranium (containing a little more than 7 kg of U^{235} per ton) the burn-up of this isotope reaches 1 kg per ton or more than 14%. Fourthly, what is the meaning of the statement that "0.44% of the plutonium is used"? Natural uranium contains no plutonium and if it is consumed as it is formed, then why the figure 0.44%?

On page 43 we find: "As the fuel is consumed the quantity of fission fragments increases, the reactor is "filled with slag," as it were, and its power level is reduced"! This statement simply shows that the author does not understand what goes on in a nuclear reactor. The author of a booklet on the functioning of a nuclear reactor should know that slag formation only limits the length of time during which a reactor can be operated at a given power level and with a given load of nuclear fuel; the power of the reactor during its run does not depend on the amount of slag formed.

In the already-mentioned book by D.I. Voskoboinik, "Nuclear Power," in the course of a description of the first Soviet atomic power plant it is stated that in the process channels water bathes the fuel elements "both externally and internally" (page 122). The author apparently has not carefully read the literature in which this reactor is described. In the process channels of the reactor in the first Soviet power plant water flows only inside of the annular fuel elements.

In G.A. Zisman's book "The World of the Atom" [7], the automatic regulation of a reactor is confused with the removal of heat (page 126). The author's discussion amounts to saying that first, every nuclear reactor possesses a negative temperature coefficient of reactivity (which is far from being true) and is thus self-regulatory, and, secondly, that automatic regulation of a reactor is associated only with the amount of heat removed from it, which is also incorrect.

*As in original.

A second serious fault of popular literature on atomic energy is sketchiness and over-inclusiveness. Here is the plan of such books. First something is said concerning the history of atomic physics; then modern concepts of the structure of the atom are reviewed; following this the fission of heavy atoms and the liberation of nuclear energy are described. Usually there is a discussion of thermonuclear reactions, atomic and hydrogen bombs and finally chain reactions, nuclear power and the future of atomic energy.

Each of these topics is an independent section of nuclear physics and can be the theme of a serious and interesting work. But some authors strive to cover as many questions as possible, so that their books are filled to excess with concepts, terms, figures, formulas, numbers and tables which exhaust the reader.

An example of such an attempt to include as much as possible is V.A. Mikhailov's "Physical Principles of Atomic Power Production" [8], in the "Soldiers' and Sailors' Popular Science Library." Although the author attempts to explain the fundamental concepts of nuclear physics he touches on so many subjects and the presentation is so complicated that this book can hardly be recommended to those for whom it was intended. It describes the properties of radioactive emission, the radioactive families, recording apparatus, atomic structure and nuclear models, the mass-energy relation, the binding energy of nucleons in nuclei, accelerators, nuclear fission, chain reactions, reactor technology and many other subjects. As a result the book is an accumulation of information concerning nuclear physics and it is not clear on what the author is laying emphasis. Even more typical in this respect is Zisman's "World of the Atom" in the same series. The last edition, which is the fifth revised and enlarged edition, includes so much that a mere enumeration would occupy a great deal of space. Instead of a direct presentation the author gives wordy expositions of minor matters so that the book becomes too extensive. For example, the author devoted 28 pages to a single section on light. The book is also very uneven in its treatment: the author explains decimals (!), which are studied in the fifth grade, along with positron decay and K capture, etc. The range is thus very broad. Finally, in a pseudopopular manner, the author misuses quotation marks, employing them either for well-established terms such as active zone, heavy water, moderator, tagged atoms, etc., or for words which could just as well be omitted ("exploding" nuclei, the "correct" ratio between the numbers of protons and neutrons, a "productive" reactor, etc.) and replaced with simple and comprehensible scientific terms. The quotation marks literally make one dizzy and the manner of presentation is seriously affected by their use.

Romadin's brochure also suffers from lack of directness. It is overloaded with calculations, numbers and coefficients. The author very accurately gives figures for the lattice spacings of reactors, the sizes of fuel elements, the thicknesses of tube walls and their diameters, the temperature drop in reactor cores, and at the same time does not attempt to give a logical reason for the choice of one design or another, why certain dimensions are used, the advantages and disadvantages of each type of reactor, etc., although this is essential for the popular understanding of reactor technology as of any other.

For example, it was hardly necessary to tell the reader the pressures developed by different pumps for coolants, or in a hasty and very sketchy description of one type of reactor to give in detail the figures on heat release, etc. Without comparison with familiar knowledge these figures mean nothing to the nonspecialist.

A third serious shortcoming of the literature on atomic energy is an insufficiently popular presentation of some topics and in some instances its complete absence.

We turn again to Romadin's brochure. The heating efficiency of nuclear fuel is explained in a confused manner and in a nonpopular style. The author attempts to explain the relation between mass and energy in a few sentences and uses terms which only a physicist can understand (for example, "nuclear energy levels").

The very important topic of nuclear instability, which must be explained in a consistent explanation of fission is limited to the comment that "the large number of positively charged protons make the uranium nucleus unstable."

E.M. Balabanov's brochure "Nuclear Reactors" [9] is also insufficiently popular in style. All of its 40 pages are filled with numbers and calculations, although these are admittedly elementary. For some unknown reason the author does not use a graphical representation of the dependence of one quantity on another but prefers to illustrate the relationship less clearly by means of tables.

One more defect of popular literature on atomic energy must be mentioned. The authors discuss only one aspect of the utilization of atomic energy by emphasizing that it gives mankind an unlimited power over nature,

increases productive capacity and the public wealth, etc. Such statements are onesided, orientate the Soviet reader incorrectly and do not permit the formation of a real idea of the economic and engineering difficulties which lie in the path of the development of atomic technology.

Atomic power, like any other form of power, possesses many advantages, but also serious fundamental shortcomings which must not be forgotten or intentionally overlooked. One of the disadvantages is the necessity for the massive shielding of nuclear reactors. Therefore, it is an error for authors to state that the reduction of the weight and size of the biological shields of reactors is only a question of time. Mankind is unable to change the laws of the passage of radiation through matter, so that the shields of nuclear reactors will never be reduced beyond a certain minimum of many tons. In popular pamphlets and articles mention is often made of an atomic automobile or locomotive which could travel thousands of miles on a few grams of fuel. But the authors "forget" to state that the cost of these few grams of fuel is immeasurably greater than the cost of many tons of the most expensive gasoline or coal and we can hardly foresee the improvement of the methods of producing atomic fuel which will bring its cost in line with that of ordinary fuels. A serious shortcoming of the utilization of atomic energy by means of reactors is the production of a large quantity of radioactive waste products which are injurious to health; the removal of such products from a large number of reactors can be a very serious problem.

It is also incorrect to imagine that in the future atomic power will replace such practically unlimited sources of energy as the sun, wind, tides and heat of the earth. We therefore cannot agree with A. Buianov, the author of the popular book "Atomic Energy" [10], who in describing the future of atomic power actually rejects all other forms of power.

We must finally point out that careless expressions are found in many books; for example, "an intermediate heat exchanger which transfers heat from the metal of the reactor to the metal of the steam generator" ([6], page 35), "concrete with an admixture of boron is a good absorber of neutrons and gamma rays" (page 19), "neutrons can easily escape from the reactor by passing through its walls" (page 44), "inert carbon atoms" ([10], page 121), "the device (that is, the reactor) consists of a core . . . ." ([7], p. 132), "dying stars" (page 92), etc.

What is the cause of such a low scientific level of many popular books and pamphlets on atomic energy? On the one hand, the publishers impose low standards on the authors of popular booklets on atomic energy so that many of them have been written by nonspecialists. This is clearly seen in the majority of such publications. So long as the authors give general information on atomic and nuclear physics which can be found in any textbook, all goes well. But as soon as they touch on nuclear reactors, or other phases of nuclear technology they are guilty of the kinds of errors which were indicated above.

On the other hand our periodical press, such as the journals "Priroda" (Nature) and "Nauka i Zhizn" (Science and Life) do not critically review the popular literature on atomic energy. The first result of such neglect is that certain publishing houses reissued a number of books and pamphlets during 1955 and 1956 in which the errors of the first editions were retained. For example, the Tula Press issued a second large printing of L.M. Shcherbakov's "Atomic Energy in the Service of Mankind" and the DOSAAF issued I.A. Naumenko's "Atomic Energy and its Utilization" without correcting the first editions.

The defects and errors in popular literature on atomic energy can be eliminated if more specialists write or at least edit the books and pamphlets, if higher standards are set and unceasing efforts are made to raise the scientific level and improve the popular style of such writings.

Iu.I. Koriakin and G.A. Bat'

LITERATURE CITED

[1] Atomic Energy for Peaceful Purposes, Collection of articles, Acad. Sci. USSR Press, 1956.

[2] A. Trifonov, Atomic Energy in the Service of Mankind, Pravda Press, Moscow, 1956.

[3] P.T. Astashenkov, Atomic Industry, Voenizdat, Moscow, 1956.

[4] D.I. Voskoboinik, Nuclear Power, Gostekhizdat, Moscow, 1956.

[5] L.M. Shcherbakov, Atomic Energy in the Service of Mankind, Tula Press, 1955.

[6] V.P. Romadin, Power from Atomic Energy, "Znanie" Press, 1955.

[7] G.A. Zisman, The World of the Atom, Voenizdat, Moscow, 1956.

[8] V.A. Mikhailov, Physical Principles of Atomic Power Production, Voenizdat, Moscow, 1955.

[9] E.M. Balabanov, Nuclear Reactors, "Znanie" Press, 1955.

[10] A. Buianov, Atomic Energy, "Moscow Worker" Press, 1955.

NEW LITERATURE

BOOKS AND REPORTS

Benson, M.I. Irradiation of Meat and Milk Products (Review) Min. Prod. Meat and Milk Products USSR, Tech. Board. Div. Tech. Inform. 1956, 26 pp., free.

Problems of Radiation Therapy. Collection of papers edited by E.A. Bazlova. Kiev, State Med. Press Uk. SSR Kharkov Sci. Research Medical Radiology 1956, 250 pp., 8 rubles, 40 kopecks.

Heitler, W. Quantum Theory of Radiation, Trans. from 3rd English Edition; Ed. and Foreword by N.N. Bogolyubova, IL, 1956, 491 pp., 22 rubles, 95 kopecks.

Getseva, R.V. and Saveleva, K.T. Handbook on Identification of Uranium Minerals, State Geo. Tech. Press, 1956, 260 pp., 15 rubles, 70 kopecks.

Grodzensky, D.E. Atomic Energy – Medicine, State Tech. Press, 1956, 72 pp., 1 ruble, 10 kopecks.

Kitaigorodsky, A.I. Order and Disorder in the Atomic World, 2nd ed. revised, State Tech. Press, 1956, 139 pp. 2 rubles.

Korsunsky, M.I. The Atomic Nucleus, 5th ed. revised, State Tech. Press, 1956, 428 pp., 6 rubles, 60 kopecks.

Review of Practical Work in Radiochemistry. Len. Univ. Press 1956, 211 pp., 6 rubles, 30 kopecks.

Severny, A.B. Physics of the Sun. Izv. AN SSSR (popular science series) 1956, 159 pp., 2 rubles, 40 kopecks.

Fermi, E. Lectures on π-mesons and Nucleons. Trans. from the English. Foreword by B.M. Pontecorvo IL 1956, 109 pp., 5 rubles.

Shlyk, A.A. Tracer Atom Methods in Studies of the Biosynthesis of Chlorophyl. Minsk Acad. Sci. BSSR, 1956, 299 pp., 10 rubles.

Shramenko, A.I. Shielding Against Radium and Radium Substitutes in Radiation Therapy Institutes, State Med. Press Uk SSR 1956, 32 pp., 75 kopecks.

Einstein and Contemporary Physics. Collection in Memory of A. Einstein. State Tech. Press 1956, 260 pp., 9 rubles, 25 kopecks.

Nuclear Reactors. Trans. from English (US Atomic Energy Commission) 1956, 398 pp., 31 rubles, 35 kopecks.

JOURNAL ARTICLES

Anisimov, B.I. Application of Radioisotopes in the Automobile and Tractor Industry, Auto. and Tract. Ind. No. 11 (1956).

Beridze, G.I. and Kurdgelashvili, M.V. Effect of Ionizing Gamma Rays on the Quality of Wine (with editorial notes). Vinodelie i Vinogradarstvo SSSR (Winemaking and Viticulture USSR) No. 7 (1956).

Blinov, N.I. Course of Damaged Soft Tissue and Bone Fractures in Radiation Sickness in Experiment. Khivurgiya (Surgery) No. 11 (1956).

Blokhin, N.N. et al. Carbohydrate Function of the Liver in the Development of Radiation Sickness.

Doklady Akad. Nauk Vol. 111, No. 3 (1956).

Borzyak, P.G. et al. Characteristics of the Photo Effect in Silver-Oxide Caesium Photocathodes (Proceedings of the All-Union Conference on Cathode Electronics and Appendix to Report, Nov. 1955) Izv. Akad. Nauk SSSR,Ser. Fiz. Vol. 20, No. 9 (1956).

Bykhovskaya, L.N. Effect of Electron Bombardment on Photoelectric Emission of Complex Cathodes, Izv. Akad. Nauk SSSR, Ser. Fiz. Vol. 20, No. 9 (1956).

Garbalyauskas, Ch.A. Results of an Investigation by the α-Radiographic Method of the Radioactive Properties of Air Masses, Proc. Acad. Sci. Lit. SSR, Ser. B., No. 4 (1956).

Goldshtein, M.I. and Prokhorova, L.G.

Gorlov, G.V. et al. Measurement of the Effective Cross Section of the Reaction $Li^6(n, t)He^4$ in the Neutron Energy Region from 9 to 700 kev. Doklady Akad. Nauk SSSR 111, No. 4 (1956).

Gulyakin, I.V. and Yudintseva, E.V. The Effect of Radioisotopes on Agricultural Plants. D_k Doklady Akad. Nauk SSSR 111, No. 2 (1956).

Gulyakin, I.V. and Yudintseva, E.V. Intakein Plants of Radioisotopes on Strontium, Caesium, Ruthenium, Zirconium and Serium, Doklady Akad. Nauk SSSR 111, No. 1 (1956).

Gulyakin, I.V. and Yudintseva, E.V. Intake of Radioisotopes in Plants Through Leaves, Doklady Akad. Nauk SSSR 111, No. 3 (1956).

Dontsova, E.I. The Problem of the Isotopic Composition of Exchange Equilibrium of Oxygen of the Lithosphere (Report presented to the XX Session of the International Geological Congress in Mexico) Geochem. No. 6 (1956).

Drukarev, G.F. Spatial Distribution of Charge and "Electric Radius" of Heavy Nuclei. Uspechi Fiz. Nauk 60, No. 3 (1956).

Eselson, B.N. et al. λ-Temperatures of Solutions of Helium Isotopes, Doklady Akad. Nauk SSSR 111, No. 3 (1956).

Zolotukhin, V.K. Tartrate Compounds of Beryllium, Journal of Inorganic Chemistry 1, No. 12 (1956).

Koltypin, E.A. and Morozov, V.M. Estimate of the Upper Limit for the Cross Section for Radiative Capture of Resonance-Energy Neutrons (275 kev) in Li^7, Doklady Akad. Nauk SSSR 111, No. 2 (1956).

Korolev, F.A. and Kulikov, O.F. Discovery of the Isotope He^3 in a Natural Mixture of Helium Isotopes by the Optical Method, Vest. Mos. University, Series Mathematics, Mechanics, Astronomy, Physics and Chemistry No. 1 (1956).

Kugushev, I.D. Application of Radioactive Elements in Studying the Flow Process and Paper Structure, Printing Industry No. 11 (1956).

Kudrin, L.P. and Nikolsky, B.A. Interaction of Fast π-Mesons with Nuclei, Doklady Akad. Nauk SSSR 111, No. 4 (1956).

Kuni, F.M. Dispersion Relations in Nucleon-Nucleon Scattering, Doklady Akad. Nauk SSSR, 111, No. 4 (1956).

Livshits, M.S. The Intermediate System Formed in the Scattering of Elementary Particles, Doklady Akad. Nauk SSSR 111, No. 4 (1956).

Murin, A.N. et al. Concentration of the Radioactive Isotopes of Iodine, Germanium, Arsenic and Antimony Obtained in the (γ, n) Reaction, Doklady Akad. Nauk SSSR 111, No. 4 (1956).

Natanson, G.L. Radioactive Aerosols, Progress of Chemistry 25, No. 12 (1956).

Nikolsky, S.I. et al. Investigation of the Nuclear-Active Component of Broad Atmospheric Showers

of Cosmic Radiation, Doklady Akad. Nauk SSSR 111, No. 1 (1956).

Nikulin, K.G. Certain Results of the Diagnostic Application of Radioactive Iodine in Internal Disease Clinics,Therapeutic Archives 28, No. 7 (1956).

Niselson, L.A. Separation of Zirconium and Hafnium by Rectification of Products of the Tetrachloride of these Elements with Phosphor Oxychloride, Journal of Inorganic Chemistry 1, No. 2 (1956).

Novitsky, Yu.I. Device for Studying Photosynthesis with C^{14} in Air Flow, Plant Physiology 3, No. 6 (1956).

Novoselova, A.V. et al. Investigation of Quartzitic Beryllium Fluoride, Journal of Inorganic Chemistry 1, No. 12, (1956).

Rozental, K.I. and Veselovsky, V.I. Study of the Mechanism for the Separation of Oxygen at a Platinum Electrode by Means of the Isotope O^{18}, Doklady Akad. Nauk SSSR 111, No. 3 (1956).

Rukman, G.I. et al. A Method for the Energy Utilization of Beta-Active Isotopes, Proc. of the Scientific Research Inst. Min. Radiation Tech. Industry USSR No. 6 (1956).

Ryabchikov, D.I. et al. Application of Phytic Acid in the Analytical Chemistry of Thorium, J. of Analytical Chem. 11, No. 6 (1956).

Savich, I.A. et al. Complex Compounds of Sextuply Valent Uranium in Certain Inorganic Materials, Journal of Inorganic Chemistry 1, 12 (1956).

Solovev, V.G. Nucleon Distribution Function in the Quadratic Approximation, Doklady Akad. Nauk SSSR 111, No. 3 (1956).

Spesivtseva, V.G. Rate and Duration of Precipitation and Purification Rate of Sodium 24 in Blood Plasma in Certain Diseases, Prelim. Report Therapeutic Archives 28, No. 7 (1956).

Starik, I.E. Role of Secondary Processes in Determining the Age of Rocks by Radioactivity Methods, Geochem. No. 5 (1956).

Striganov, A.R. and Korostylev, L.A. Atomic Spectrum of Plutonium, Optics and Spectroscopy 1, No.8 (1956).

Styro, B.I. and Garbalyauskas, Ch.A. Histograms of the Radioactivity of Atmospheric Precipitates, Proc. Acad. Sci. Lat. SSR, Series B, No. 5 (1956).

Sudakov, V.V. Meson-Meson Scattering in Quantum-Mesonic Field Theory, Doklady Akad. Nauk SSSR 111, No. 2 (1956).

Suslov, B. Shielding Costs (Utilization of Heavy Water in Nuclear Energy Installations), Science-Power No. 11 (1956).

Syromyatnikova, N.V. Certain Aspects of the Albumin Function of the Liver in the Development of Radiation Sickness, Doklady Akad. Nauk SSSR 111, No. 3 (1956).

Takibaev, Zh.S. et al. Production of π-Mesons by High-Energy Particles in Cosmic Rays, Doklady Akad. Nauk SSSR 111, No. 2 (1956).

Ushakov, N.V. Application of a Gamma-Ray Method for Control of Thin Parts, Factory Laboratory 22, No. 12 (1956).

Fomin, V.V. and Maiorova, E.P. Determination of the Stability Constant for the Ions $Th(NO_3)_j^{4-j}$, Journal of Inorganic Chemistry 1, No. 2 (1956).

Chernikov, Yu.A. and Kuchmistaya, G.I. Identification of Zirconium in Ores by an Iodate Method, Factory Lab. No. 1 (1957).

Chernyaev, I.I. et al. Carbonate Compounds of Uranium, Journal of Inorganic Chemistry 1, No. 12 (1956).

Chizhikov, A.I. and Boyarshinov, V.K. Experiment on the Application of Tritium for Investi-

gating the Effect of Water on Metals, Factory Lab. No. 1 (1957).

Sheka, I.A. and Pevzner, Ts.V. The Composition of Phtalates of Zirconium and Hafnium, J. of Inorganic Chemistry 1, No. 12 (1956).

Shteding, M.N. et al. The Problem of Using Materials with a Polyvinylchloride Base for Individual Shields Against Radiation, Chem. Industry No. 7 (1956).

Shchukarev, S.A. et al. On the Disproportionation of Uranium Trifluoride, Journal of Inorganic Chemistry 1, No. 12 (1956).

Yagodin, G.A. et al. Precipitation Coefficients for Carbon Isotopes in Equilibrium of Liquid-Vapor Equilibrium of Ethylene, Ethane and Methane, Doklady Akad. Nauk SSSR 111, No. 2 (1956).

SOVIET JOURNAL OF ATOMIC ENERGY VOLUME 2, NUMBER 5, 1957

CONTENTS

		Page	Russ. page
1.	The Measurement of the Resonance Absorption of Neutrons in an Atomic Power Station Reactor. Z.I. Gromova, B.G. Dubovsky, A.V. Kamaev and V.V. Orlov	507	411
2.	The Influence of Cavities on the Critical Mass of a "Basin-Type" Reactor. B.P. Rastogi	513	416
3.	A Turbogenerator Designed for Atomic Electro-Stations. M.M. Kogan	519	421
4.	The Principle of Coherent Acceleration of Charged Particles. V.I. Veksler	525	427
5.	Some Theoretical Questions Concerning the 10 Bev Proton Synchrotron of the Academy of Sciences USSR. M.S. Rabinovich	529	431
6.	Thermodynamics of the Extraction Equilibria for Uranyl Nitrate. A.M. Rozen	545	445
7.	Mechanism of Formation of Zirconium Sponge in Zirconium Production by the Magnesothermic Process. F.G. Reshetnikov and E.N. Oblomeev	561	459
	Letters to the Editor		
8.	Parity Nonconservation in Weak Interactions. (Review.) A.P. Rudik	565	463
9.	Certain Features of the Viscosity and Heat Conductivity of Liquids and Gaseous Materials. I.I. Novikov	573	468
10.	The Mass of He^3. R.A. Demirkhanov, T.I. Gutkin and V.V. Dorokhov	574	469
	Science Chronicle		
11.	Seventh Annual Conference on Nuclear Spectroscopy at Leningrad. R.M. Polevoi and I.N. Serikov	576	471
	Within the Soviet Union		
12.	At the Atomic Pavilion of the All-Union Industrial Conference (Safety Methods Section). Z. Chetverikova and L. Kimel'	579	474
13.	Design of a New Laboratory for the Study of Radioisotopes and their Applications in Metallurgy and Physics of Metals	581	475
14.	Powerful Gamma Ray Emitters for Investigations in Petroleum Chemistry	582	476
15.	Determination of the Moisture Content of Structural Materials by Means of Gamma Rays. L. Polozova and R. Reizman	583	476
	Foreign Scientific and Technical News	585	478
	Concerning the Discovery of the Antineutron (585). Atomic Locomotives (587). Atomic Engines in Ships of the USA (591). Production of Uranium and Thorium Tetrafluorides (593). Investigation of Radiation Damage by Paramagnetic Resonance Techniques (594). Brief Communications (595).		
	Reviews and Bibliography		
	Popular Scientific Literature on Atomic Energy. Iu.I. Koriakin and G.A. Bat'	598	487
	New Literature		
	Books and Reports	603	490